AN ANALYSIS OF THE PULSING CHARACTERISTICS OF THE KANSAS STATE UNIVERSITY TRIGA MARK II NUCLEAR REACTOR

by 503

JERRY W. STAUDER

B.S., Kansas State University, 1967

A MASTER'S THESIS

submitted in partial fulfillment of the

requirements for the degree

MASTER OF SCIENCE

Department of Nuclear Engineering

KANSAS STATE UNIVERSITY

Manhattan, Kansas

1969

Approved by:

M. John Robinson

Major Professor

CONTENTS

LIST OF FIGURES

NOMENCLATURE

a	reactivity insertion rate for the pulse rod going up ($\Delta k/k$ sec)
A_c	cross sectional area of the fuel (cm^2)
A_s	surface area of fueled length of a fuel element (cm^2)
$\underline{B}$	vector of the solution values
$\underline{b}$	minimum variance unbiased estimator vector of $\underline{B}$
$C_i(t)$	precursor density of the ith delayed neutron group at time t (cm^{-3})
$C(\bar{T}_f)$	fuel heat capacity at temperature $\bar{T}_f$ (watt sec/°C)
C_p	specific heat at constant pressure (watt sec/gm °C)
c	cladding thickness (cm)
$\underline{D}$	inverse matrix of $\underline{\tilde{T}}\ \underline{V}^{-1}\ \underline{T}$
$\underline{e}$	deviation vector
E_f	energy per fission that is released in the fuel (MeV)
$\underline{f}$	a deviation vector ($\underline{f} = \underline{s}^{-1}\ \underline{e}$)
g'	reactivity insertion rate for the pulse rod going down ($\Delta k/k$ °C)
g	acceleration of gravity (cm/sec^2)
G	gap thickness (cm)
Gr	Grashoff number
I	number of vertical positions per fuel-moderator element
$\underline{I}$	identity matrix
k_{eff}	effective multiplication constant
$K(\bar{T}_f)$	core thermal conductance at temperature $\bar{T}_f$ (watts/°C)
k_f	thermal conductivity of the fuel (watts/cm °C)

k_g	thermal conductivity of the gap (watts/cm °C)
k_c	thermal conductivity of the clad (watts/cm °C)
k	thermal conductivity of the water (watts/cm °C)
$\underline{K}$	core thermal conductance vector
ℓ	prompt neutron lifetime (sec)
L	fueled length of a fuel element (cm)
M	total number of fuel elements in the core
m_k	number of fuel elements in the kth ring
$\dot{m}$	mass flow rate per channel (gms/sec)
$n(t)$	neutron density at time t (cm^{-3})
N_5	U^{235} atom density (nuclei/cm^3)
Nu	Nusselt number
P	reactor power (watts)
Pr	Prandtl number
q'''	volumetric heat generation rate (watts/cm^3)
$\overline{q'''}$	average volumetric heat generation rate per fuel element (watts/cm^3)
r_f	radius of the fuel (cm)
R_G	gap resistance (cm °C/watt)
$R_i(t_j)$	remainder term of the Taylor series at time t_j.
$\underline{S}$	nonsingular symmetric matrix
t	time (sec)
$\bar{T}_f(t)$	average fuel temperature of the core at time t (°C)
$\bar{T}_{f0}$	average fuel temperature of the core at time zero (°C)
T_{fik}	average radial fuel temperature at the ith level of the kth fuel element (°C)
$\bar{T}_{fk}$	average temperature of the kth fuel moderator element (°C)

$T(r)$	fuel temperature at radius r (°C)
T_{fm}	fuel centerline temperature (°C)
T_{w1}	coolant temperature at channel inlet (°C)
T_{w2}	coolant temperature at channel outlet (°C)
$\bar{T}$	mixed mean temperature of the coolant (°C)
$\bar{T}_c$	average cladding temperature (°C)
$\bar{T}_w$	average coolant temperature (°C)
$\underline{T}$	temperature matrix
$T_T(t)$	measured fuel temperature at time t (°C)
$T_a(t)$	actual fuel temperature at time t (°C)
u	unit step function
$\underline{V}$	variance-covariance matrix of the deviations
$y_i(t_j)$	ith dependent variable at time t_j
$y_i^{(k)}(t_j)$	kth derivative of the ith dependent variable at time t_j
α	reactivity temperature coefficient ($\Delta k/k$ °C)
α_1	minimum variance unbiased estimator of the reactivity temperature coefficient
β_i	fraction of delayed neutrons of the ith delayed neutron group
β	total delayed neutron fraction
β	thermal coefficient of volume expansion ($°C^{-1}$)
γ_i	effectiveness of the ith delayed neutron group
$\bar{\gamma}$	average delayed neutron effectiveness
$\Delta\rho_i$	ith reactivity loss
ΔT	temperature difference between average clad and reactor tank bulk water temperature
ε	truncation error
λ_i	decay constant of the ith delayed neutron group (sec^{-1})

Λ	prompt neutron generation lifetime (sec)
μ	viscosity of water (gm/sec cm)
$\rho(t)$	reactivity at time t ($\Delta k/k$)
ρ_0	zero power reactivity insertion ($\Delta k/k$)
ρ	density of water (gms/cm^3)
σ_5	fission cross section of U^{235}
σ^2	variance
τ_1	time the pulse rod reaches the top of its travel (sec)
τ_2	time the pulse rod drops from its uppermost position (sec)
τ_3	time the pulse rod reaches its lowest position (sec)
τ	time constant (sec)
ϕ_{ik}	average neutron flux at the ith vertical level in the kth fuel element ($neutrons/cm^2$ sec)
ϕ_k	average flux in the kth fuel-moderator element ($neutrons/cm^2$ sec)

1.0 INTRODUCTION

The pulsing capability of the TRIGA reactor provides a mechanism for research in the areas of dose rate phenomena, short time domain studies, reactor safety and kinetics, and other applications (1,2,3). The development of an analytical model to predict the transient behavior of the TRIGA is necessary in support of pulsed reactor research.

A simplified, space independent approach, known as the Fuchs, or the Fuchs-Nordheim, or the Hansen-Fuchs model (4,5,6,7), which neglects the effects of delayed neutrons and heat transfer, will give a satisfactory description of the reactor power during the prompt burst. However, this model only applies to prompt critical transients where the assumptions of negligible heat transfer and delayed neutron effects will hold.

A more detailed model (4,23) couples the space independent kinetic equations to a space independent thermal model through the reactivity temperature coefficient. This model describes the time dependent behavior for the prompt burst and for later times, when the effects of the delayed neutrons and heat transfer become important. The thermal model is based on an average fuel heat capacity, an average core water heat capacity, a fuel core water resistance, and a core water-reactor tank water resistance.

It is the purpose of this paper to develop a digital code to predict the reactor power and the average fuel temperature of the TRIGA Mark II reactor as functions of time during a transient, and to compare the results with experimental data. A time dependent reactivity input function is developed which describes the net reactivity of the reactor for specific control rod motion and temperature effects. The time dependent position and associated reactivity of the pulse rod are experimentally measured in

this investigation. The thermal model is based on an average fuel heat capacity and a fuel-reactor tank water heat transfer conductance. The heat transfer conductance and the reactivity temperature coefficient needed to complete this model are determined from data obtained in steady state experiments.

The transient model is presented in Section 2.0. Section 4.0 contains the theoretical development, the experimental procedure, and the data from which the heat transfer conductance and the reactivity temperature coefficient were obtained. The comparison between the results of the transient model and the transient data are presented in Section 5.0.

2.0 THE TRANSIENT MODEL

The one energy group, space independent reactor kinetic equations will be used to describe the neutron density. In particular,

$$\frac{dn(t)}{dt} = \frac{\rho(t)-\beta}{\Lambda} n(t) + \sum_i \lambda_i C_i(t), \tag{1}$$

$$\frac{dC_i(t)}{dt} = \frac{\beta_i}{\Lambda} n(t) - \lambda_i C_i(t), \quad i = 1,2,\ldots,6 \tag{2}$$

where $n(t)$ = neutron density at time t,

$\rho(t)$ = reactivity at time t,

Λ = prompt neutron generation lifetime,

β = total delayed neutron fraction,

β_i = fraction of delayed neutrons of the ith delayed neutron group,

λ_i = decay constant of the ith delayed neutron group,

$C_i(t)$ = density of the ith delayed neutron group precursor at time t.

Since delayed neutrons have lower energies than prompt neutrons, they will escape less readily while slowing down, and hence are more effective. This increased effectiveness can be accounted for by substituting a β_{eff} for the experimental value of β (8). In particular,

$$\beta_{eff} = \bar{\gamma}\,\beta = \sum_i \gamma_i \beta_i, \tag{3}$$

where $\bar{\gamma}$ is the average delayed neutron effectiveness. A value of β_{eff} is given (9) for the TRIGA Mark II reactor; however, there are no values of γ_i available to correct the ith group fraction. Keepin (10) suggests

that for slow, bare systems,

$$\gamma_i = 1 \quad .$$

A value of the prompt neutron generation time, Λ, is not available for the TRIGA, but a value is given for the prompt neutron lifetime, ℓ (11). These two quantities are related through the effective multiplication constant, k_{eff}, i.e.,

$$\ell = \Lambda\, k_{eff} \quad .$$

For most kinetic problems the distinction between Λ and ℓ can be ignored (10). Thus in this work ℓ will be substituted for Λ.

In Eq. (1) the reactivity function must not only describe the initiation of the pulse but also the termination. Thus the following form is assumed,

$$\rho(t) = at - a(t-\tau_1)u(t-\tau_1) - g'(t-\tau_2)u(t-\tau_2) + g'(t-\tau_3)u(t-\tau_3) - \alpha[\bar{T}_f(t) - \bar{T}_{f0}] \quad , \qquad (4)$$

where a = ramp reactivity insertion rate (pulse rod up),

τ_1 = time the pulse rod reaches the top of its travel,

u = unit step function,

τ_2 = time the pulse rod drops from its uppermost position,

τ_3 = time the pulse rod reaches its lowest position,

g' = ramp reactivity insertion rate (pulse rod down),

α = reactivity temperature coefficient,

$\bar{T}_f(t)$ = average core fuel temperature at time t,

$\bar{T}_{f0}$ = average core fuel temperature at time zero.

The average fuel temperature can be expressed as

$$C(\bar{T}_f) \frac{d\,\bar{T}_f(t)}{dt} = P(t) - K(\bar{T}_f)[\bar{T}_f(t) - T_{wl}], \tag{5}$$

where $C(\bar{T}_f)$ = core heat capacity of fuel,

$P(t)$ = reactor power at time t,

$K(\bar{T}_f)$ = core thermal conductance at average fuel temperature $\bar{T}_f$,

T_{wl} = reactor tank bulk water temperature.

The core thermal conductance is the summation of all the conductances between the fuel and the bulk water temperature. Reactor power is proportional to the neutron flux and thus to the neutron density for a one group approximation, and it can be determined from Eq. (1).

Note in Eqs. (4) and (5) that the coefficients are functions of the average core fuel temperature. Much of the work in this investigation will be devoted to the determination of this average temperature. This is necessary for the calculation of the core thermal conductance and the reactivity temperature coefficient.

3.0 REACTOR DESCRIPTION

The TRIGA reactor core is near the bottom of a tank 20.5 feet deep (see Fig. 1). The tank contains light demineralized water which acts as a coolant, moderator, and radiation shield. The entire reactor assembly is supported by the 1 foot thick graphite reflector assembly which surrounds the core. Upper and lower grid plates bracketed to the reflector provide axial and lateral support for the fuel-moderator elements, the graphite dummy elements, and the control rods. The fuel-moderator elements are cooled by natural convection of the tank water passing down around the outside of the reflector and up through 36 cooling holes in the lower grid plate (see Fig. 2). Triangular-shaped spacers (Fig. 3) on the top-end fixtures of the elements allow the cooling water to pass through the top grid plate (11).

The TRIGA fuel-moderator elements are an alloy of zirconium hydrided to approximately one hydrogen atom for each zirconium atom, and uranium 20% enriched in U^{235} (12). The elements are solid cylinders approximately 1.5 inches in diameter with the fueled region being 14 inches in length. Graphite pieces 4 inches long on either end of the fuel act as upper and lower reflectors. The elements are clad with aluminum 0.030 inches thick. Figure 4 depicts the arrangement of the fuel-moderator elements. Note that the elements form 5 concentric rings, where the innermost ring is designated the B-ring, the next is called the C-ring, and so on out to the F-ring. There are 63 fuel-moderator elements with a total mass of 2291 grams of U^{235} (17).

The reactor is operated with 3 boron carbide control rods. The shim and regulating rods are motor driven and are used for controlling the

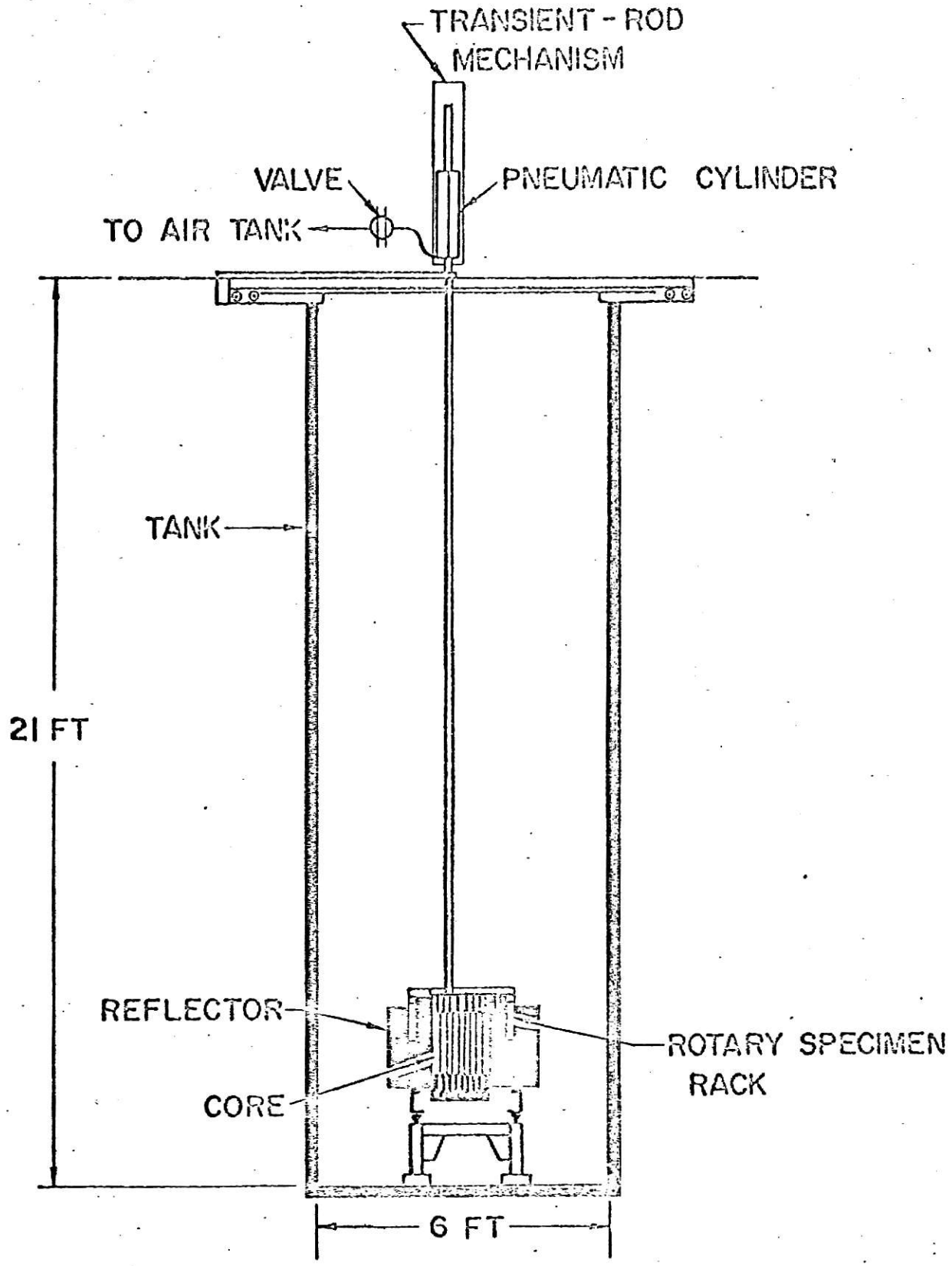

Fig. 1--Elevation view of TRIGA reactor.

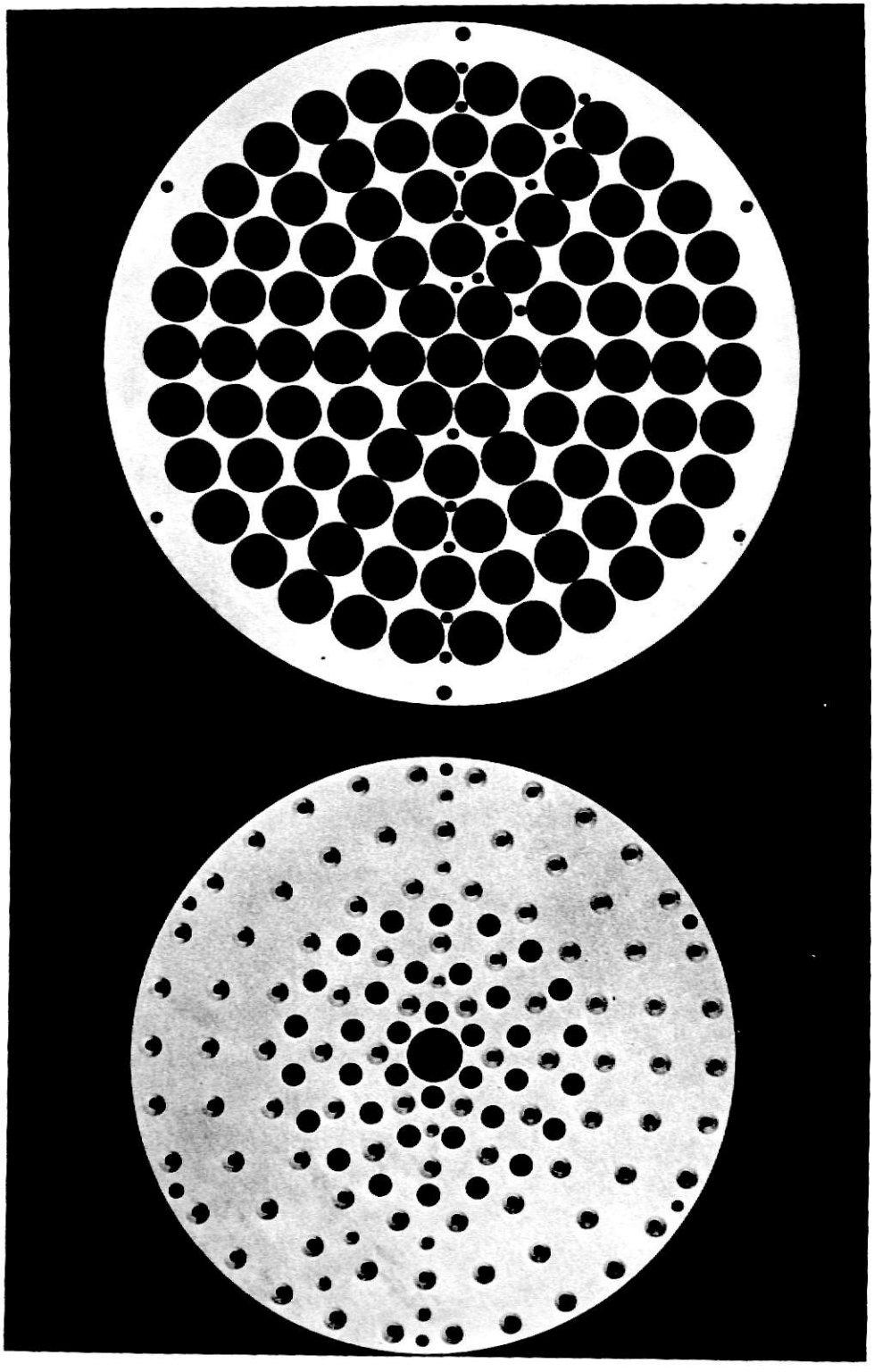

Fig. 2 Grid plates

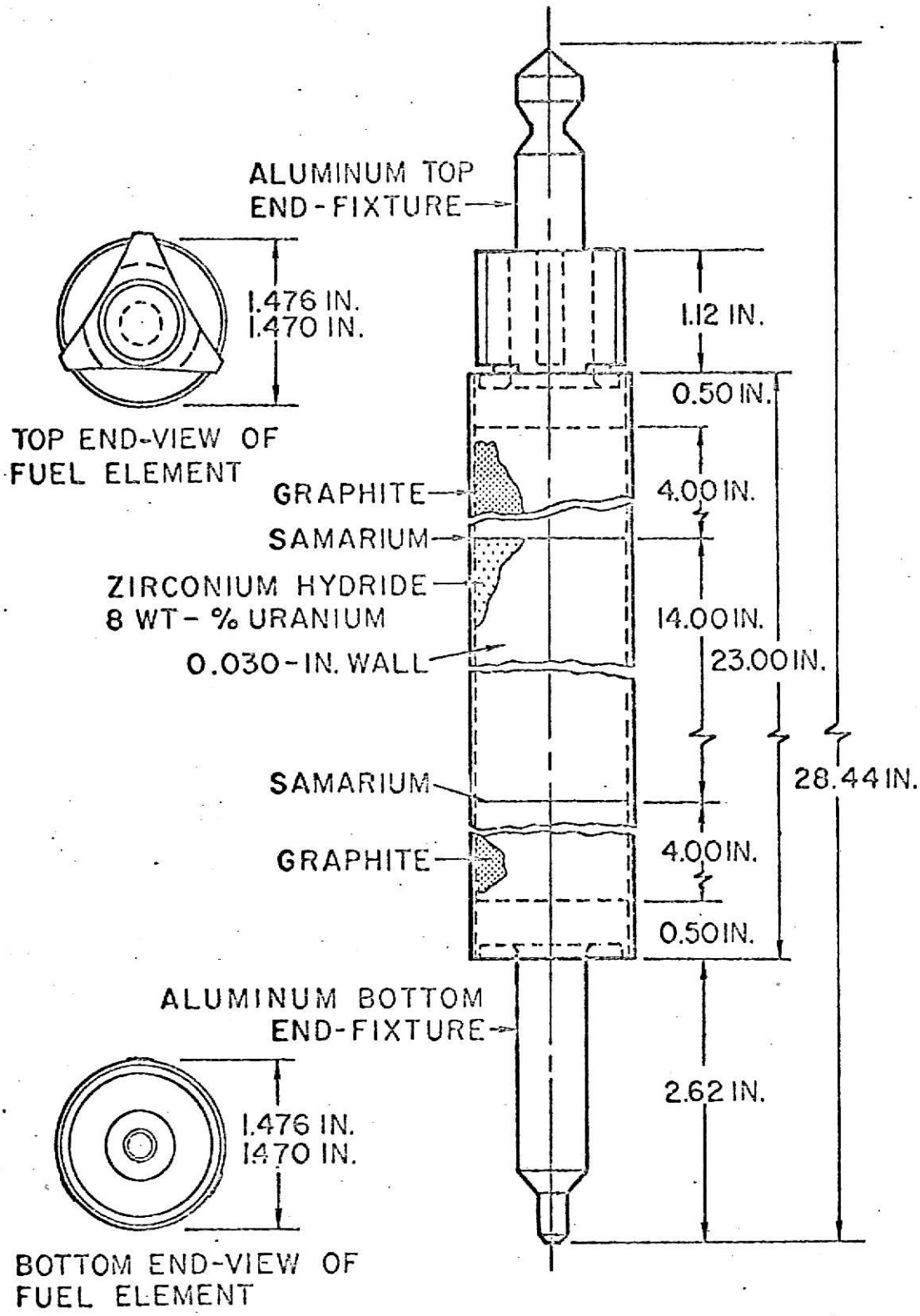

Fig. 3. TRIGA fuel-moderator element.

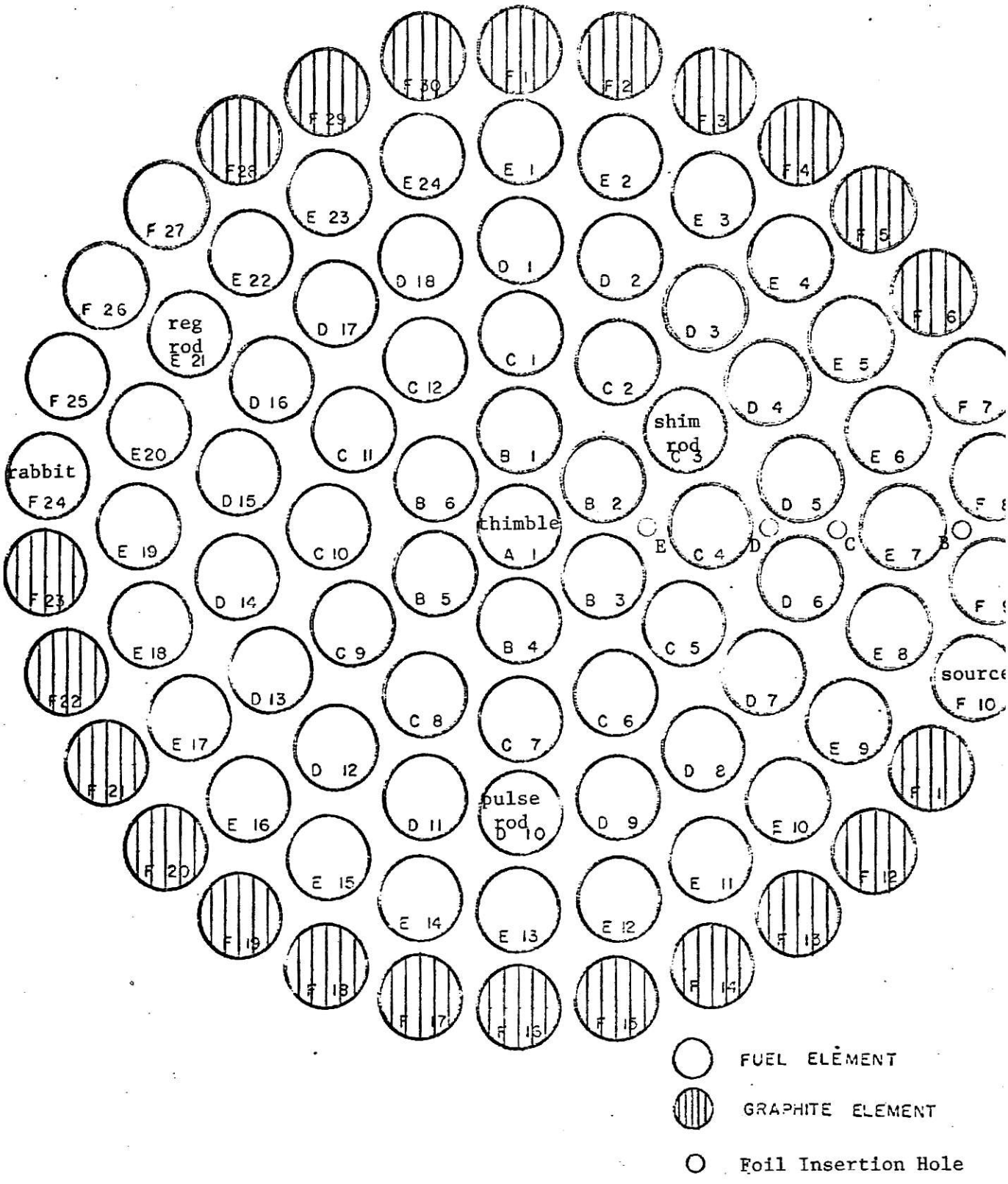

Figure 4. Core Loading Diagram

power of the reactor. The pulse rod is pneumatically operated and is used for pulsing operations. The pulse rod movement for the KSU TRIGA Mark II reactor is characterized by a finite time interval at the top of its travel. This time interval between the full up position and the start of the drop back into the core is approximately 3 seconds. Thus this time interval (τ_2) has been incorporated into the reactivity input function (Eq. (4)) in addition to the finite travel times (τ_1 and τ_3). Steady state operation is restricted to a reactor power below 250 kilowatts. Transient peak powers are to be held below 250 megawatts.

4.0 EXPERIMENTAL DETERMINATION OF THE PARAMETERS

4.1 Theory

With the reactor at steady state, Eq. (5) becomes

$$P = K(\bar{T}_f)\ [\bar{T}_f - T_{w1}]\ ,$$

or

$$K(\bar{T}_f) = \frac{P}{\bar{T}_f - T_{w1}}\ . \tag{6}$$

Since the power and the average fuel temperature are known, the core thermal conductance can be obtained. The amount of reactivity needed to bring the reactor to a steady state condition at some power is

$$\rho = \rho_0 + \alpha(\bar{T}_f - \bar{T}_{f0})\ , \tag{7}$$

where ρ_0 is the zero power reactivity insertion. Zero power is that power where there is negligible heat generation in the fuel. Thus the slope of a curve of ρ vs. $(\bar{T}_f - \bar{T}_{f0})$ will yield the value of the reactivity temperature coefficient.

4.1.1 Average Fuel Temperature

If T_{fik} is the average radial temperature at the ith level in the kth fuel element, then the average temperature of the kth fuel element is

$$\bar{T}_{fk} = \frac{1}{I} \sum_{i=1}^{I} T_{fik}\ , \tag{8}$$

where I is the number of vertical positions or levels. The average temperature of the fuel across the core is then

$$\bar{T}_f = \frac{1}{M} \sum_{k=1}^{5} m_k\ \bar{T}_{fk}\ , \tag{9}$$

where m_k is the number of fuel elements in the kth ring and M is the total number of fuel elements in the core.

4.1.2 Average Radial Temperature

The solution of Poisson's equation for the temperature of the fuel in a long cylindrical fuel element with constant thermal conductivity is

$$T_f(r) = T_{fm} - \frac{q'''r^2}{4\,k_f} \quad , \tag{10}$$

where $T_f(r)$ = fuel temperature at radius r,

T_{fm} = fuel centerline temperature,

q''' = average heat generation rate per unit volume,

k_f = thermal conductivity of the fuel.

The average radial temperature is then

$$T_f = \frac{2}{r_f^2} \int_0^{r_f} T_f(r) r dr = T_{fm} - \frac{q'''r_f^2}{8\,k_f} \quad , \tag{11}$$

where r_f is the fuel radius. Thus by measuring the centerline temperature and the heat generation rate, the average radial temperature can be determined.

4.1.3 Heat Generation Rate

In a thermal reactor it may be assumed that 90% of the fission energy is deposited in the fuel elements and that this heat source is distributed in a manner proportional to the neutron flux (8). This heat source is called the volumetric heat generation rate and is expressed in units of power per unit volume. In particular,

$$q''' = E_f N_5 \sigma_5 \bar{\phi} \quad , \tag{12}$$

where E_f = energy per fission that is released in the fuel,

$N_5 = U^{235}$ atom density,

σ_5 = fission cross section of U^{235},

$\bar{\phi}$ = average neutron flux.

For the average radial temperature at the ith vertical position of the kth fuel-moderator element (Eq. (11)), the average neutron flux is ϕ_{ik}.

4.1.4 Fuel Centerline Temperature

A TRIGA instrumented fuel-moderator element is presented in Fig. 5. Note that there are only 3 thermocouples and they are located near the middle of the element on its vertical centerline. Thus some estimate must be made of the fuel centerline temperatures at other positions.

The fuel centerline temperature at vertical level z can be expressed as

$$T_{fm}(z) = T_{wl} + \frac{A_c}{\dot{m}\, c_p}\int_0^z q'''(z)dz + \frac{q'''(z)r_f^2}{2}\left[\frac{1}{2k_f} + \frac{1}{k_G}\,\ell n\left(\frac{r_f+G}{r_f}\right) + \frac{1}{k_c}\,\ell n\left(\frac{r_f+G+c}{r_f+G}\right) + \frac{1}{h(r_f+G+c)}\right], \tag{13}$$

where A_c = cross sectional area of the fuel,

$\dot{m}$ = mass flow rate of coolant in channel surrounding the fuel-moderator element,

c_p = specific heat at constant pressure of coolant,

k_G = thermal conductivity of the gap,

G = gap thickness,

k_c = thermal conductivity of the cladding,

c = cladding thickness,

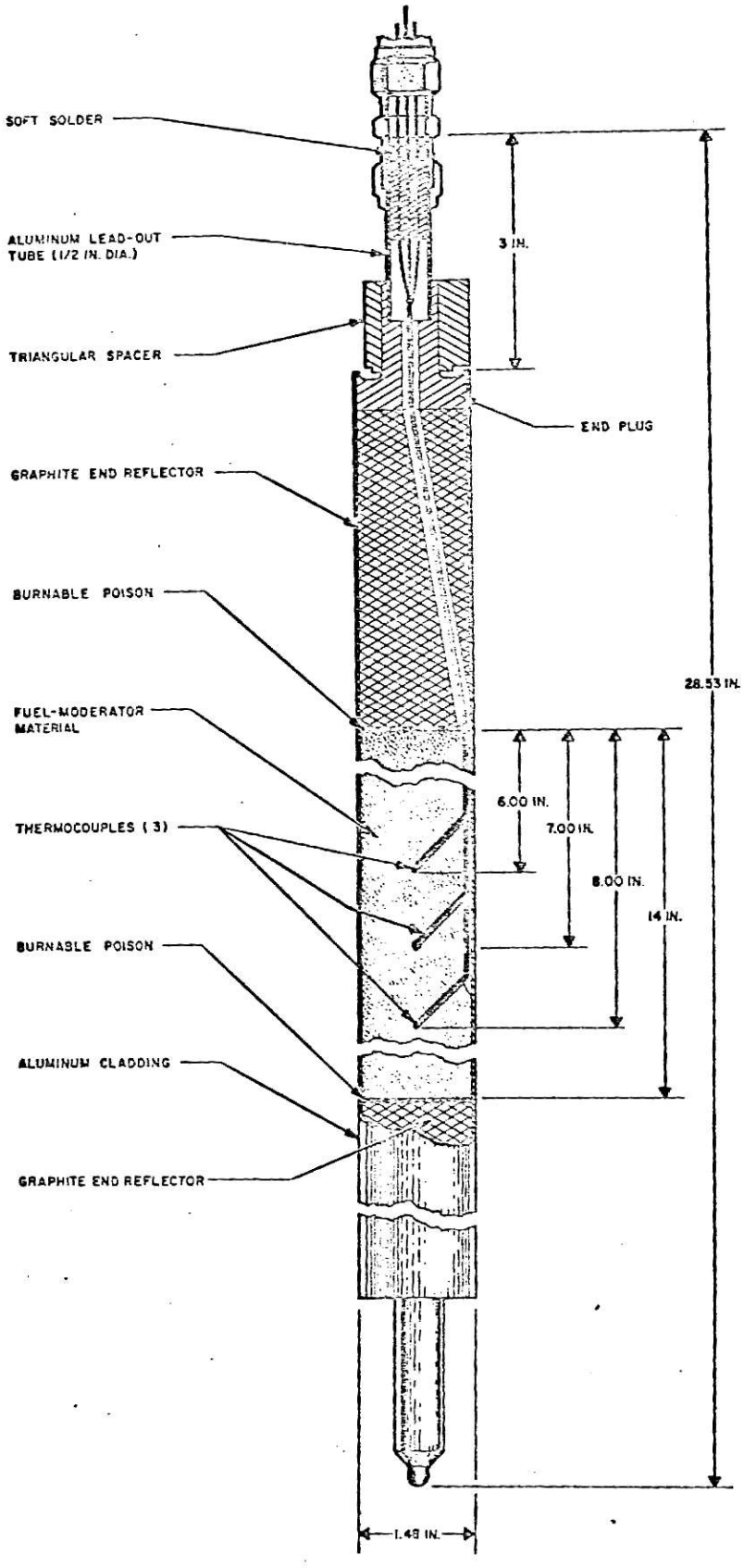

Figure 5. TRIGA instrumented fuel element

h = film coefficient of heat transfer between the fuel moderator element and the coolant,

T_{w1} = coolant temperature at channel inlet.

The lower limit on the integration of the heat generation rate starts at the bottom of the active region of the fuel element.

All of the above quantities are known or can be measured except the film coefficient h, the flow rate $\dot{m}$, the thermal conductivity of the gap k_G, and the thickness of the gap G. Bonilla (13) suggests the use of the following correlation for natural convection flow past vertical tubes,

$$Nu = 0.13\ (GrPr)^{1/3}\ , \tag{14}$$

where Nu, Gr, and Pr are the Nusselt, Grashoff, and Prandtl numbers respectively. Recall that

$$Nu = h\ L/k\ ,$$

where L is length of the active portion of the fuel-moderator element, and k is the thermal conductivity of the coolant. The Grashoff number is defined as

$$Gr = \rho^2 L^2\ g\ \beta\ \Delta T/\mu^2\ ,$$

where ρ, β, and μ are the density, thermal coefficient of volume expansion, and the viscosity of the coolant respectively. The temperature difference, ΔT, used was the difference between the average cladding and the reactor tank bulk water temperature, i.e., $\bar{T}_c - T_{w1}$. The Prandtl number is defined as

$$Pr = c_p\ \mu/k\ .$$

The physical properties of the coolant are evaluated at the mixed mean temperature, i.e.,

$$\bar{T} = (\bar{T}_c + \bar{T}_w)/2 \ , \tag{15}$$

where $\bar{T}_c$ = the average cladding temperature,

$\bar{T}_w$ = the average coolant temperature (the arithmetic mean of the channel inlet and outlet water temperatures).

The average cladding temperature is determined by

$$\bar{T}_c = \bar{T} + \frac{r_f^2 \, \bar{q}'''}{2(r_f+G+c)h} \tag{16}$$

where $\bar{q}'''$ is the average heat generation rate in the fuel-moderator element.

The mass flow rate of the coolant can be found by making a heat balance between the fuel element and the cooling water. In particular,

$$\dot{m} = \frac{A_c}{c_p(T_{w2}-T_{w1})} \int_0^L q'''(z)dz \ , \tag{17}$$

where T_{w2} is the channel outlet temperature.

Making the substitution,

$$R_G = \frac{1}{k_G} \ln \left(\frac{r_f+G}{r_f}\right) \ ,$$

into Eq. (13) and rearranging leads to

$$R_G = \frac{T_{fm}(z) - T_{w1} - \frac{A_c}{\dot{m} \, c_p} \int_0^z q'''(z)dz}{q'''(z) \, r_f^2} - \left(\frac{1}{4k_f} + \frac{1}{2k_c} \ln \left(\frac{r_f+c}{r_f}\right) + \frac{1}{2(r_f+c)h}\right) \ , \tag{18}$$

where the gap thickness has been assumed to be negligibly small.

The procedure to estimate the centerline temperature along the kth fuel-moderator element is as follows:

1. Assume an average cladding temperature and calculate the mixed mean temperature of the coolant using Eq. (15).
2. Estimate the film coefficient by Eq. (14).
3. Check the assumed $\bar{T}_c$ by Eq. (16) and if not within a specified accuracy, repeat steps 1, 2, and 3 with the new $\bar{T}_c$.
4. When the preceding steps have been completed satisfactorily, calculate the gap conductance by Eq. (18) for the three measured centerline temperatures and average linearly.
5. Estimates of the centerline temperatures can now be made at any vertical position with Eq. (13) using the average gap conductance and the film coefficient.

4.2 Experimental Equipment and Procedure

4.2.1 Absolute Flux Measurements

The spatial neutron flux distribution in the core was measured with a 0.025 inch outside diameter fission chamber made by Reuter-Stokes Electronics Components, Inc. of Cleveland, Ohio. The chamber was inserted into the core through the 0.314 inch foil insertion holes in the upper grid plate. See Fig. 4 for the location of these holes.

The thermal neutron operating range of the detector is from 1×10^{8} to 2×10^{14} neutrons/cm^2 sec. The active length of the detector is 1 inch and the sensitive volume is 0.1 cm^3 which contains He gas at 76 cm Hg.

The outer shell is 304 stainless steel, the inner electrode Titanium, and the neutron absorber is U_3O_8 enriched 93% in U^{235} and containing 3.34 milligrams of U^{235} (14). The U_3O_8 thickness is 1 milligram/cm^2 and the plated area is 4.08 cm^2. Twenty feet of coaxial cable is provided with the chamber.

Figure 6 shows the fission chamber and associated equipment as used to map the flux in the core. The chamber and cable were housed in a flexible aluminum tube filled with water, but the 26 11/16 inch aluminum probe at the bottom is rigid and it positioned the chamber in the core. All the equipment except the chamber was located on top of the reactor shield.

From its bottom-most position the chamber was withdrawn at a rate of 1 inch per minute and readings were taken at 0.5 inch intervals. Since its lowest position was fixed with respect to the upper grid plate, the position of the fission chamber was always known.

4.2.2 Fuel and Water Temperature Measurements

Figure 7 shows the instrumentation used to measure the fuel and water temperatures. The thermocouples are chromel-alumel and a Leeds-Northrup potentiometer was used to measure their emf.

The instrumented fuel element normally in B-3, number 2788 E-TC, was used to make all the fuel temperature measurements. With the series of measurements completed with the element in B-3, it was exchanged with the element in C-4 and the measurements repeated. This same procedure was followed for the elements in D-6, E-7, and F-8.

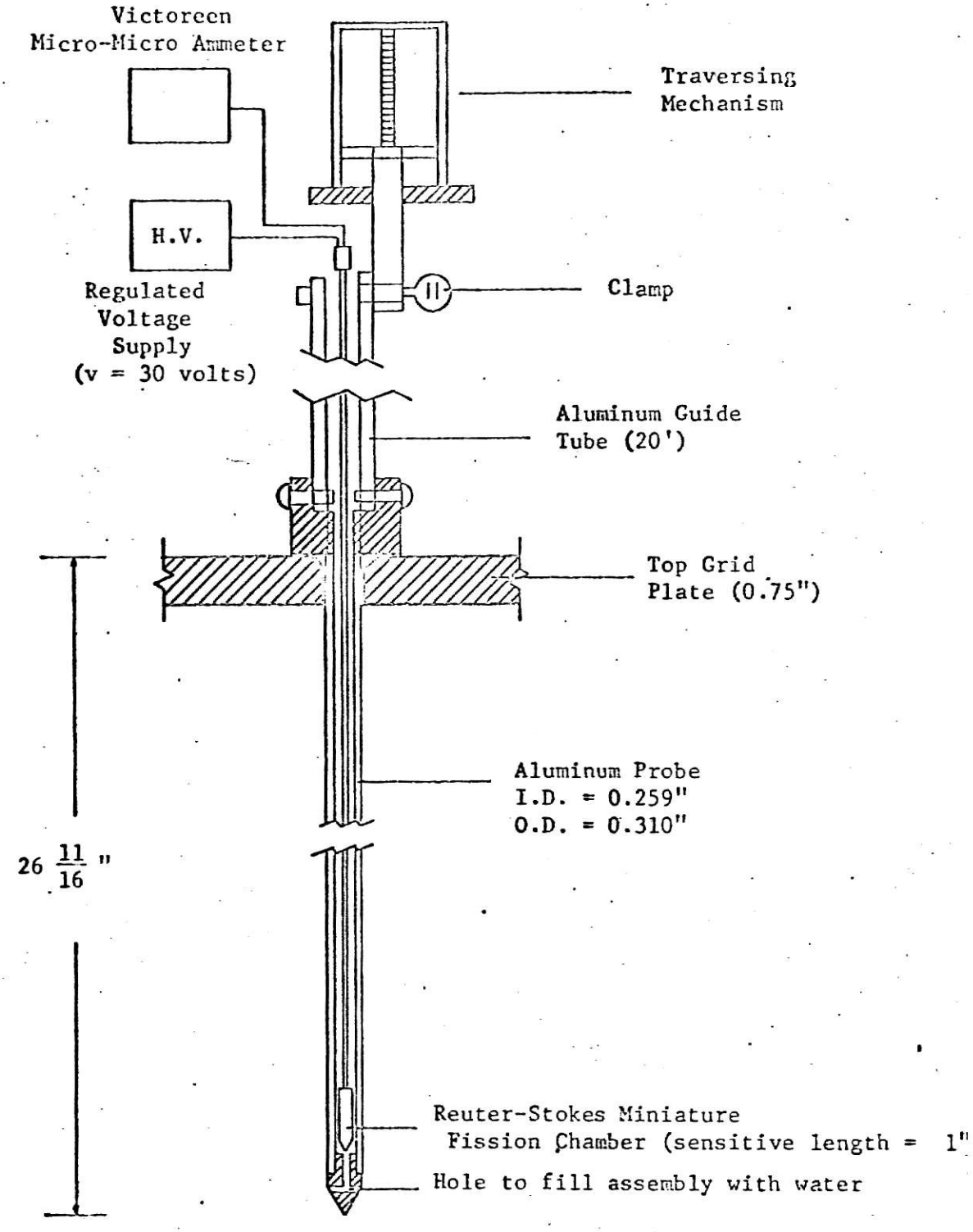

Figure 6. Positioning of the fission chamber in the core

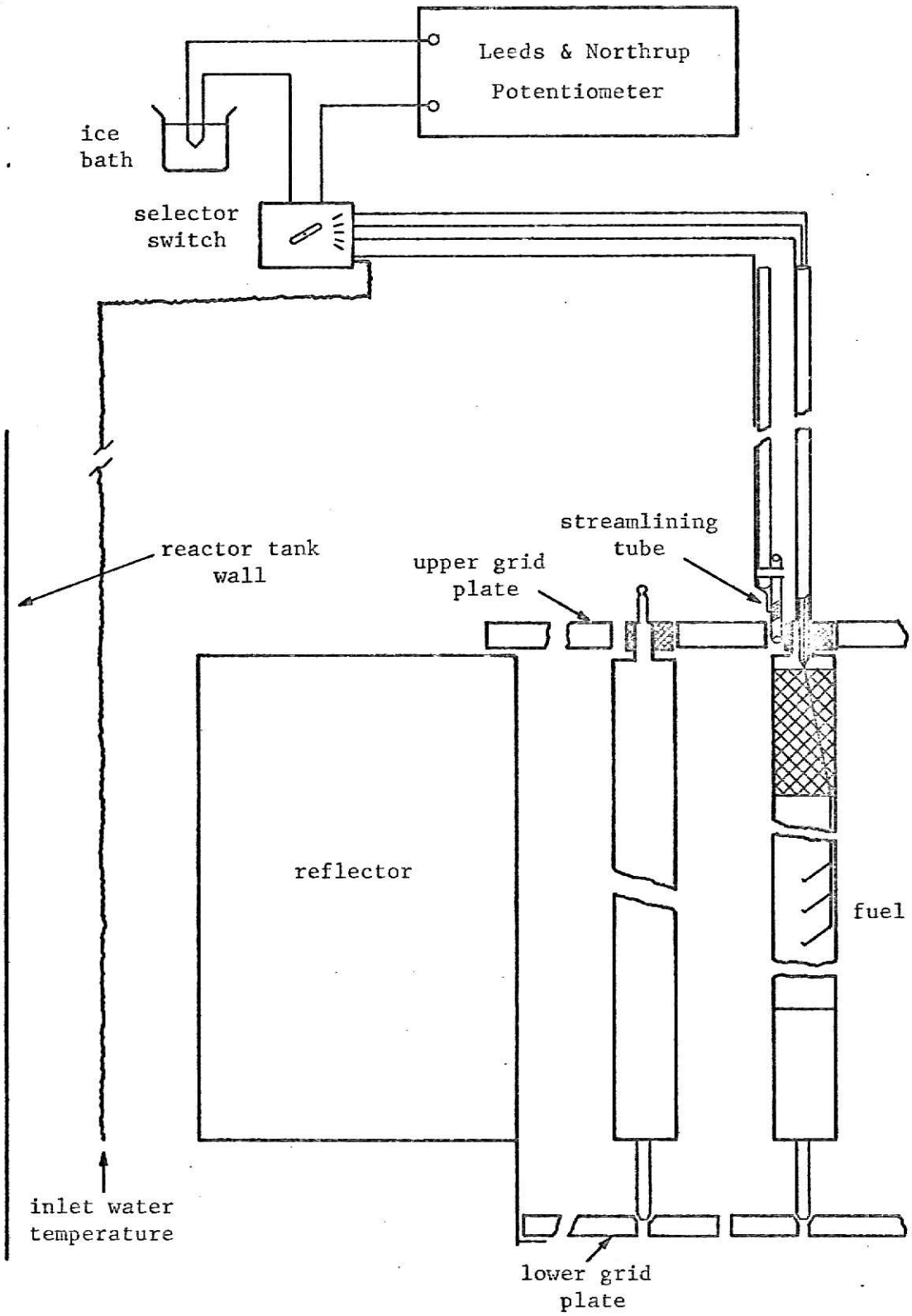

Figure 7. Fuel and water temperature instrumentation. (Note that this thermocouple circuit is not recommended for accurate measurements. See Leeds and Northrup recommended circuits.)

The thermocouple, which measured the exit water temperature from the channel which surrounds the instrumented fuel element, was placed in a streamlining tube to reduce the turbulence of the water. It was found through earlier measurements that without the streamlining tube it was very difficult to obtain a steady reading because of the turbulence of the water surrounding the thermocouple. The streamlining tube with the thermocouple was placed into the space between the triangular block and the grid plate with a long flexible aluminum tube.

A thermocouple was placed in the water about halfway between the reflector and the reactor tank wall and approximately level with the bottom of the reflector. This measurement was considered to be the inlet water temperature to the core.

The series of measurements with the instrumented fuel-moderator element in each ring consisted of the 3 fuel temperatures, and the inlet and outlet water temperatures across the fuel element, all taken at various steady state power levels from zero power to 250 kW.

4.2.3 Reactivity Measurements

For each steady state power level where the fuel and water temperatures were recorded, the critical position was also recorded, i.e., the shim and regulating rod positions. Prior to these measurements, the rods were calibrated by the procedure outlined in the KSU Hazards Summary Report (11).

4.3 Results and Discussion

4.3.1 Neutron Flux Distribution

The vertical flux distribution in foil insertion holes A, B, C, D, E, and the central thimble are presented in Fig. 8. These data were corrected for flux perturbations using the self-shielding factor for infinitely long hollow cylinders (15). The flux perturbation is due to the presence of the fission chamber itself because it is relatively black in terms of cross section when compared to the water it displaced. The measurements were taken at a reactor power of 500 watts.

The average flux in a particular fuel-moderator element at a given vertical level was obtained by averaging the measured flux values on both sides of the element at the given level, and then dividing by the ratio of the maximum flux in the water to the average flux in the fuel (Appendix A). This ratio can be approximated by the disadvantage factor which Bouchey (14) estimated to be the ratio of the absorbtion cross section in the moderator to the absorbtion cross section in the fuel, i.e., 1.37.

The average heat generation rate is calculated (Eq. (12)) from the average flux values in the fuel. The power generated in a fuel-moderator element is just the heat generation rate integrated axially over the length of the element times the cross sectional area of the fuel. In particular,

$$P = A_c \int_0^L q'''(z)dz \ ,$$

where $q'''(z)$ is the heat generation rate at vertical level z. The total reactor power is

$$P = A_c \sum_{k=1}^{5} m_k \int_0^L q_k'''(z)dz \ , \qquad (19)$$

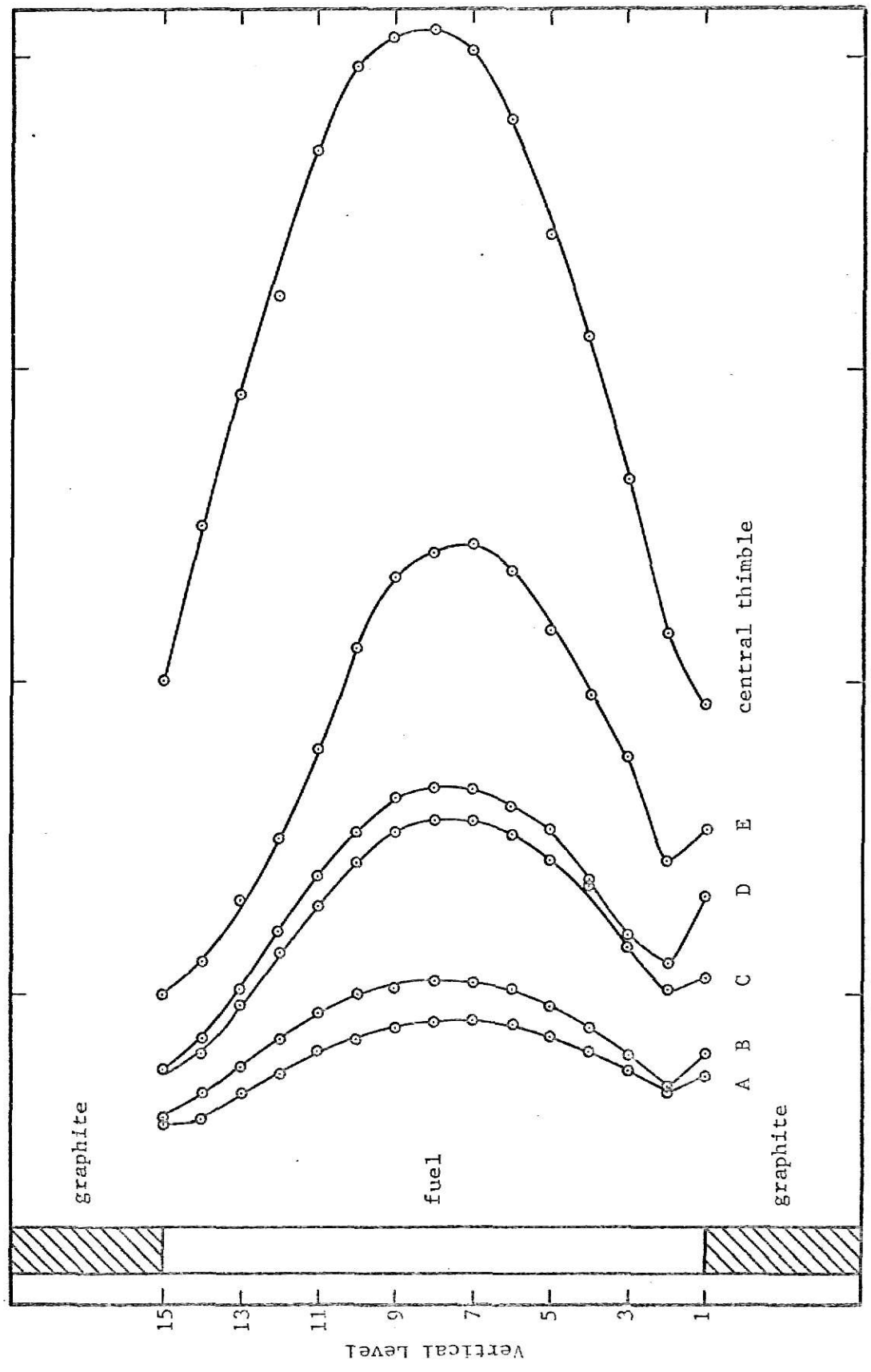

Figure 8. Vertical flux distribution in the central thimble and foil insertion holes A,B,C,D, and E.

where m_k is the number of fuel elements in the kth ring. Thus for 10 kilowatts, Eqs. (12) and (19) yield 9.6 kilowatts which is 4% low. This result is well within the limitations of the accuracy of the method.

4.3.2 Fuel Temperature Results

The fuel and water temperature data were processed as described in Section 4.1. The computer code with which the analysis was performed is discussed in Appendix A. The fuel centerline temperatures were all adjusted to an inlet water temperature of 25°C and then from each the average radial temperature was calculated at that vertical level. These radial averages were then used to calculate the average core fuel temperature by Eqs. (8) and (9). The maximum fuel temperature, the average core fuel temperature, and the average core outlet water temperature as functions of power are plotted in Fig. 9.

4.3.3 Core Thermal Conductance

Figure 10 presents the core thermal conductance as a function of average fuel temperature as determined by this investigation from Eq. (6). The data were fit to a straight line with a weighted least squares analysis (see Appendix C). The resultant equation is

$$K(\bar{T}_f) = (0.00424 \pm 0.00047)\bar{T}_f + (0.532 \pm 0.054)\ \text{kW/°C}$$

4.3.4 Reactivity Temperature Coefficient

Figure 11 presents the reactivity loss as a function of the power level. Use of Figs. 11 and 9 with Eq. (7) yields Fig. 12, the reactivity loss as a function of the average fuel temperature rise. The average fuel

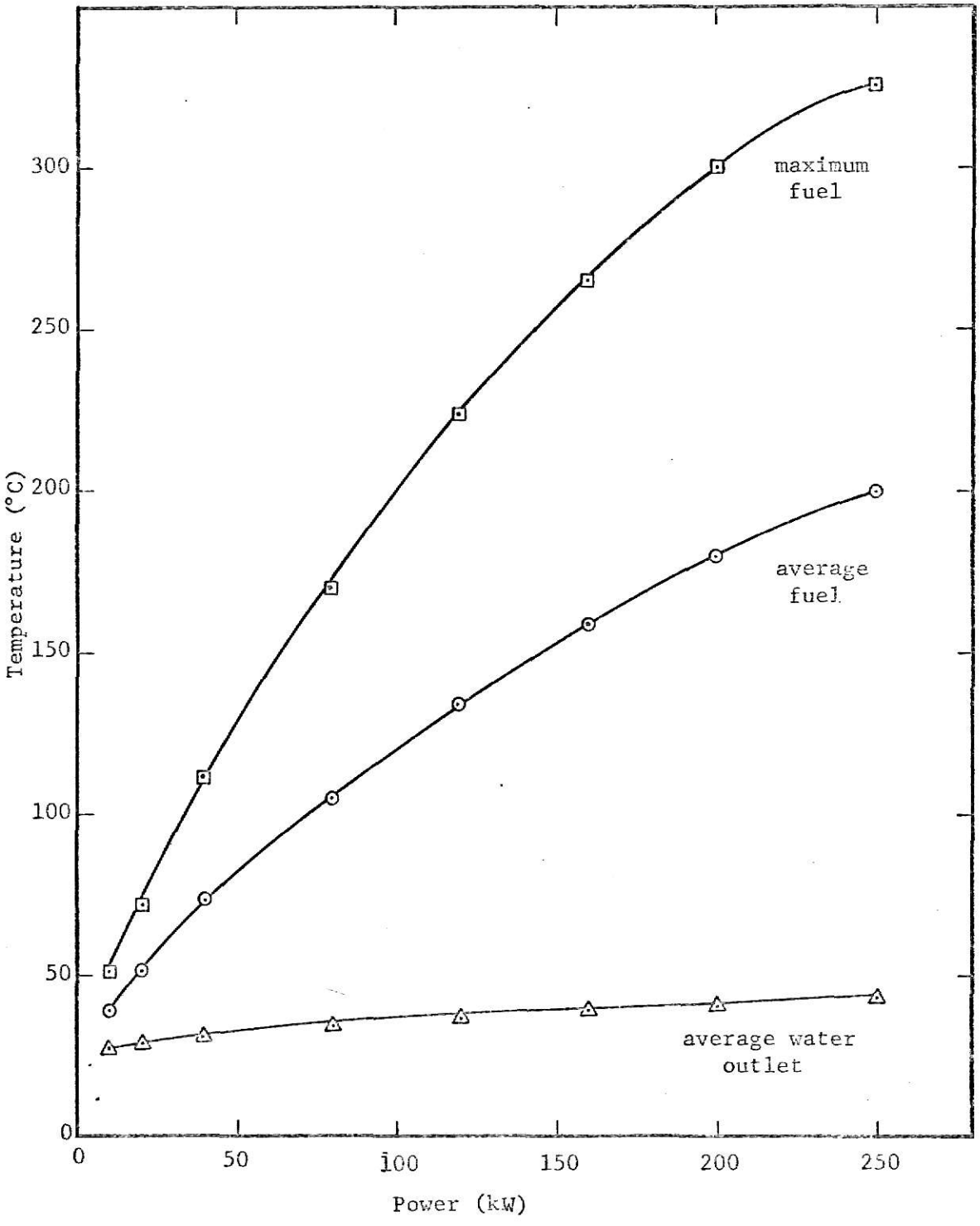

Figure 9. Reactor fuel and water temperatures.

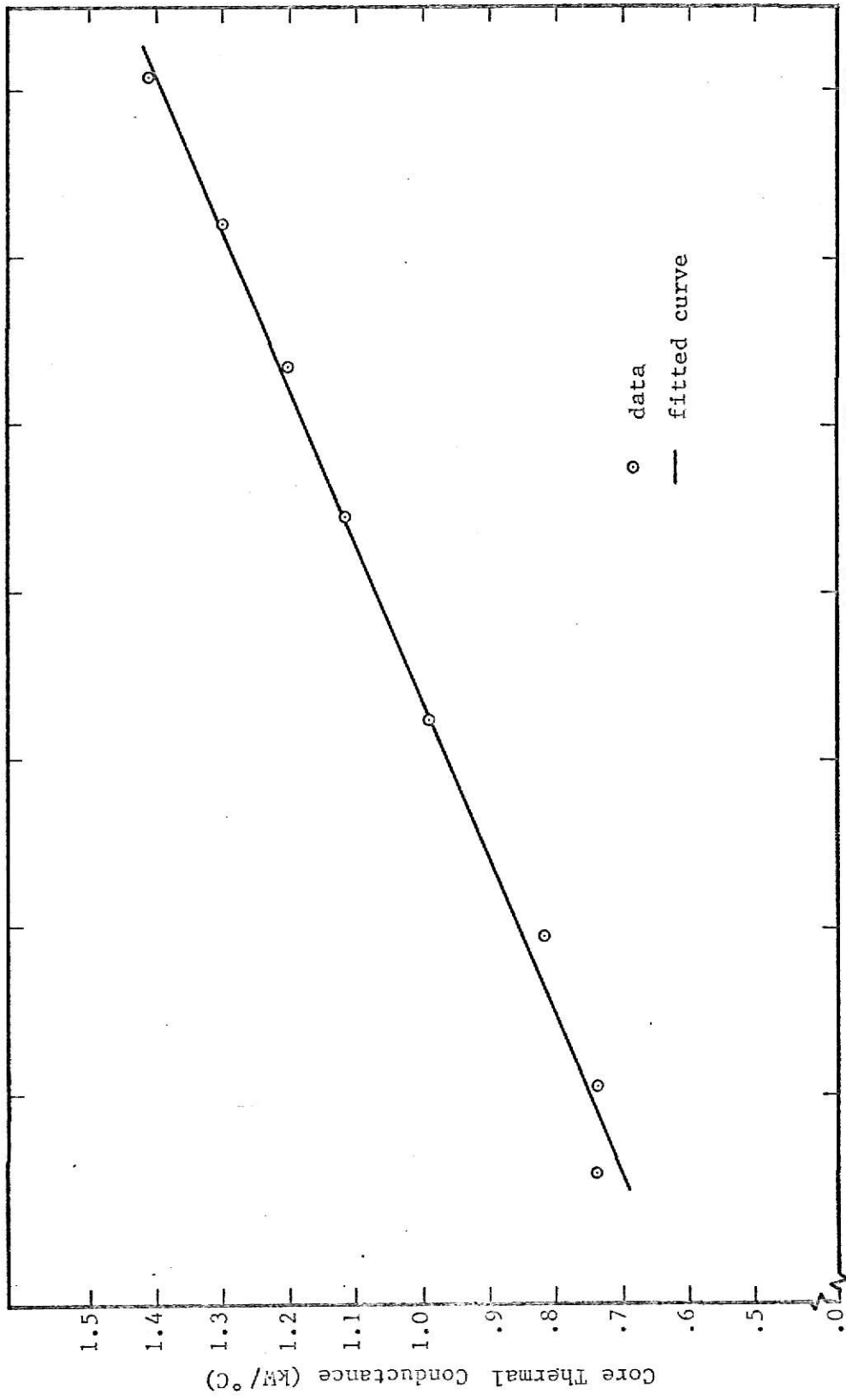

Figure 10. Core thermal conductance as a function of the average fuel temperature.

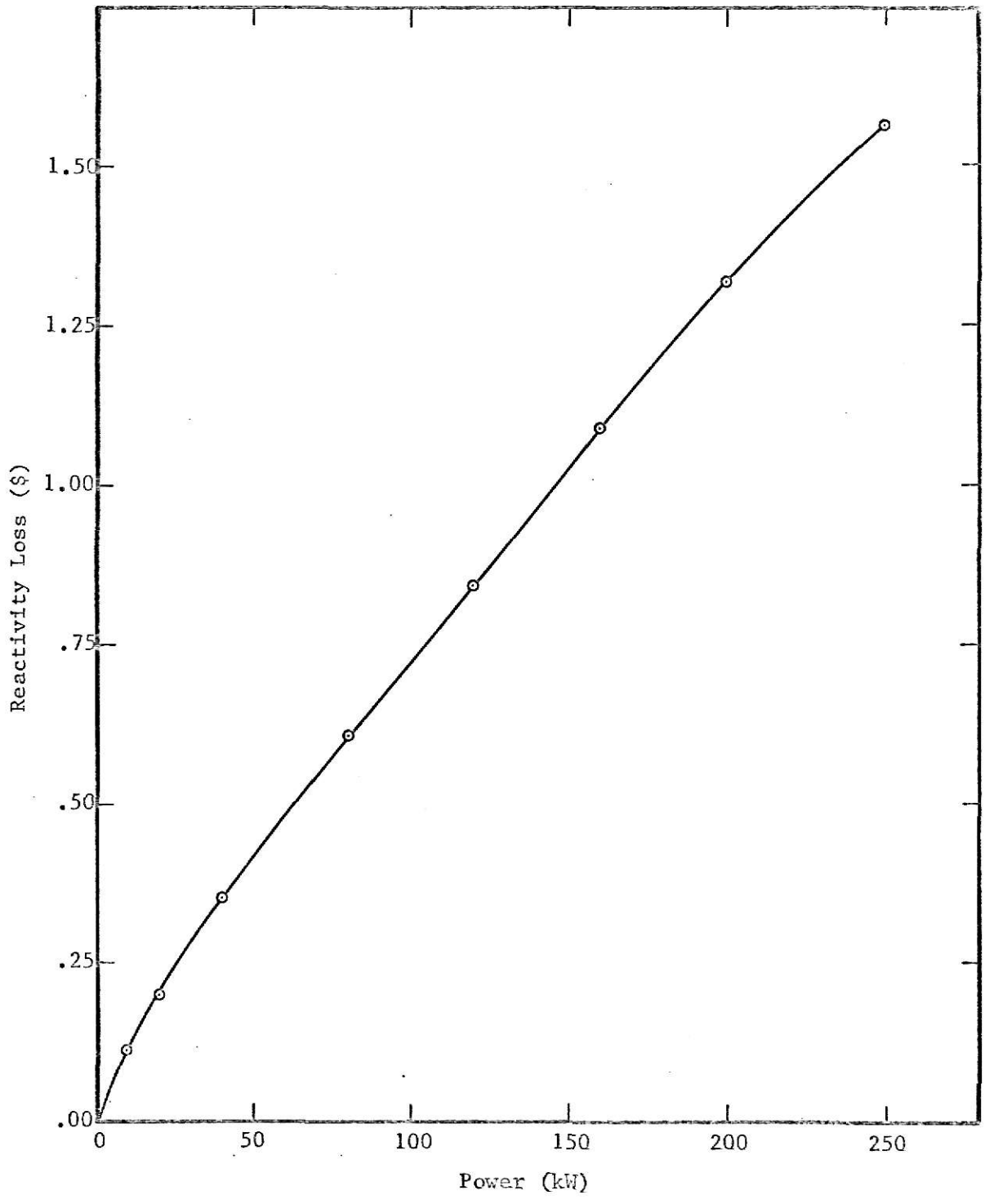

Figure 11. Reactivity loss as a function of reactor power.

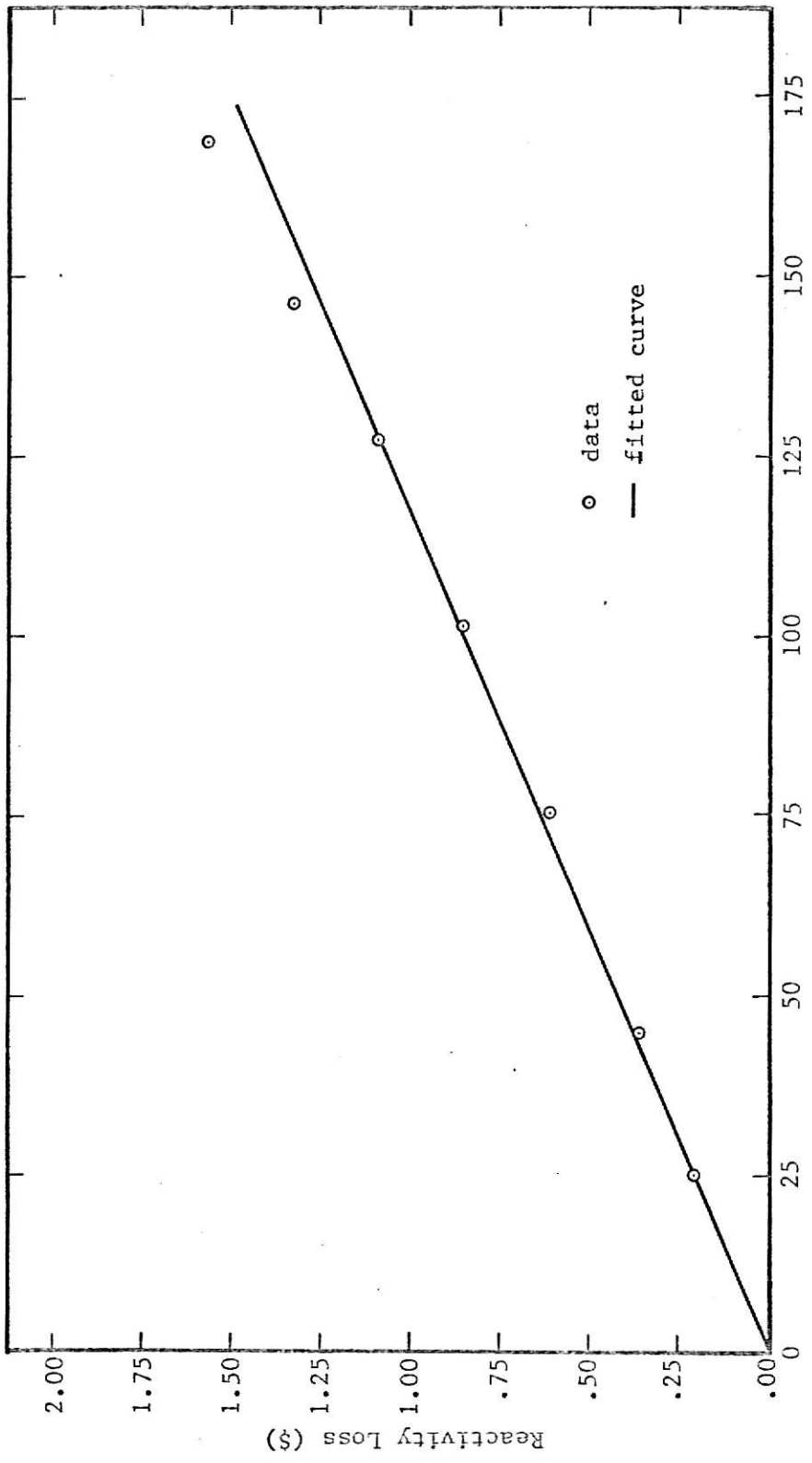

Figure 12. Reactivity loss as a function of the average fuel temperature rise.

temperature rise actually refers to the temperature difference between the fuel and the water. It has been observed for the TRIGA reactor (12) that a negligible reactivity loss would be obtained if the fuel and water temperatures were raised simultaneously to the same temperature. Thus the reactivity loss is presented as a function of the difference between the average fuel temperature, $\bar{T}_f$, and the average core water temperature, $\bar{T}_{f0} + \frac{\Delta T}{2}$, where $\bar{T}_{f0} = T_{w1}$ for zero reactor power.

The weighted least squares analysis was used to fit the data to a straight line and the slope is the temperature coefficient. The value obtained is

$$\alpha = 0.869 \pm .02 \text{ cents/°C} ,$$

or

$$\alpha = 0.686(10^{-4}) \text{ } \Delta k/k \text{ °C} .$$

Examination of the data in Fig. 12 suggests possible second order effects may be important. Theoretical work (6) has indeed predicted an increasing value of the reactivity temperature coefficient with temperature. However, in this work it was considered constant for two reasons: first, because of the basic assumption in the kinetic analysis of a constant reactivity coefficient, and second, because of license requirements no data could be obtained at temperatures greater than 200°C in order to accurately predict the coefficients behavior at these higher temperatures. It should be noted that this value differs by 50% from the value of $1.2(10^{-4})$ $\Delta k/k$ °C determined by Stone, et al. (12), using a similar analysis. No explanation can be offered for this discrepancy, but some confidence can be had in the value determined in this investigation since it predicts a reasonably good transient behavior (Section 5.2). Recent

theoretical work (6) yields a value of approximately $7(10^{-5})$ $\Delta k/k$ °C averaged over the same temperature range which further supports the value obtained herein.

5.0 COMPARISON OF TRANSIENT MODEL WITH TRANSIENT DATA

5.1 Experimental Equipment and Procedure

The reactor power during the transient was measured with a Reuter-Stokes neutron ionization chamber, a Keithley 410 micro-micro ammeter, and a Clevite Mark 260 Brush recorder (see Fig. 13). The ion chamber is 1 1/32 inches in diameter and 9 1/16 inches in length. The neutron sensitive material is Boron 10 and the fill gas is 95% Argon-5% Nitrogen at a pressure of 76 cm of Hg. The chamber was inserted into the central thimble and calibrated with the linear recorder on the reactor console at various power levels below 250 kilowatts. The chamber was positioned so that the 250 kW reading was on a scale 3 decades below the maximum scale on the Keithley micro-micro ammeter in order to allow for the predicted 250 MW reading at the peak of a $2.00 pulse.

The recorder has six channels and uses a pressurized inking system which produces smudge-proof traces. Input sensitivities are from 1 millivolt per division to 500 volts full scale with an input impedance of 10 megohms. Frequency response is flat from DC to 40 Hz full scale, and to 100 Hz at 10 divisions. Eight chart speeds from 1 millimeter per minute to 125 millimeters per second are available.

Just prior to a transient test, the range selector switch on the Keithley was set on the scale corresponding to the peak power of the pulse. In order to obtain sufficiently accurate and readable data after the peak of the pulse the switch had to be shifted to more sensitive ranges. The chart paper was operated at a speed of 125 mm/sec during the test.

Fuel temperature was measured with the center thermocouple of the instrumented fuel-moderator element in position B-3. The emf of the

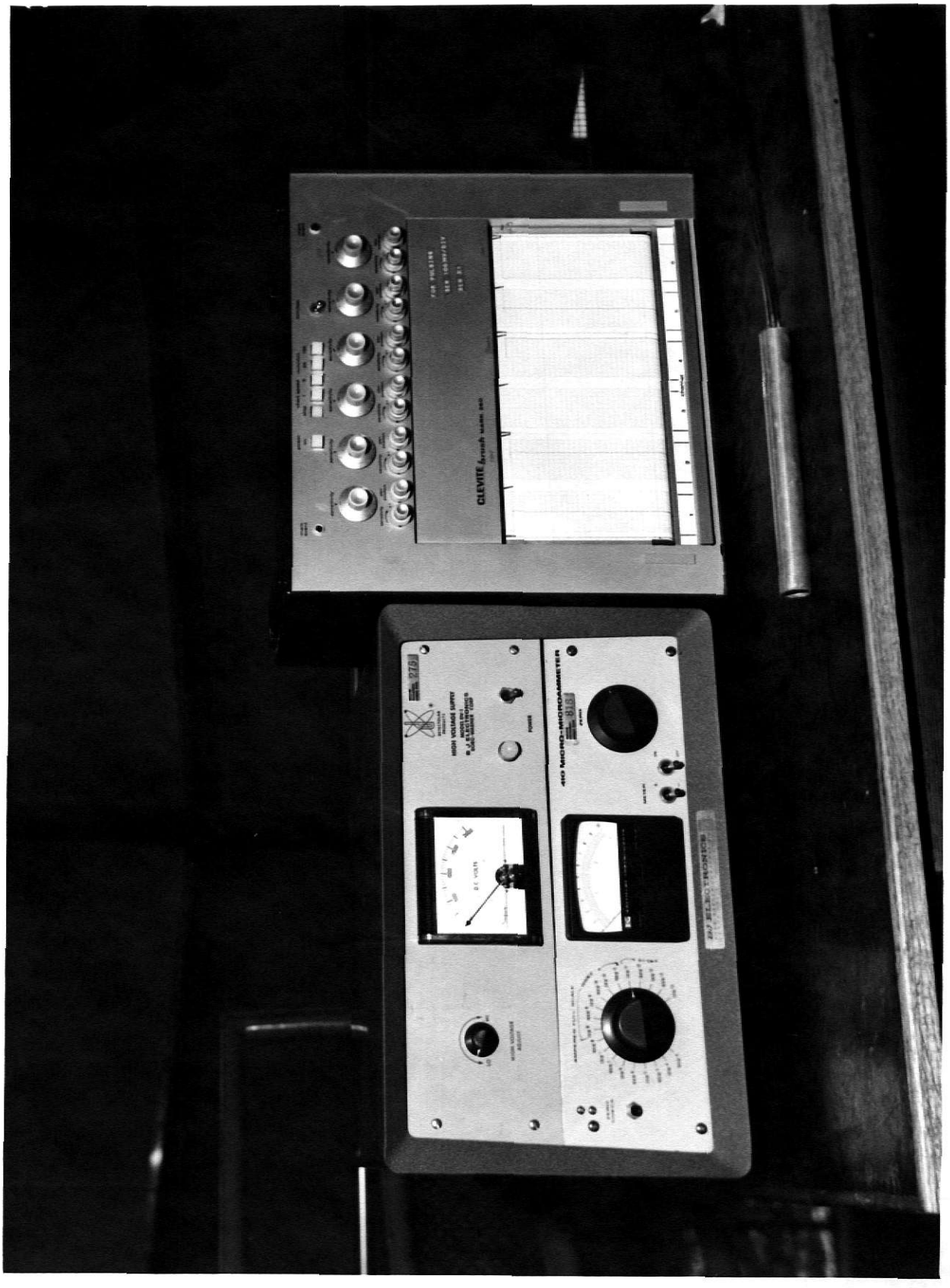
CLEVITE
HIGH VOLTAGE SUPPLY
400 MICRO-MICROAMMETER

thermocouple was read directly with the Brush recorder. Since the input impedance of the recorder is very large, it was assumed that the Peltier effect would be negligible.

The pulse rod movement was measured with the Brush recorder and two micro switches, one for its lowest position, and the other for its highest position. Thus the time the pulse rod left its lowest position, the time it reached its uppermost position, the time it started to drop, and the time it reached its lowest position were all known. These measurements were necessary for the reactivity insertion function, Eq. (4).

5.2 Results and Discussion

Figures 14 through 17 present the results of the transient power data and the transient power calculations for reactivity insertions of \$1.93, \$1.76, \$1.55, and \$1.25. The transient equations were solved by the method of analytic continuation (Appendix D). The results show the excellent agreement that was obtained using the point kinetic equations, the simplified reactivity function and the average thermal model. For the \$1.93 pulse the calculated peak power was 214 MW compared to the measured value of 222 MW, a difference of $\sim$ 4%. The full width at half maximum of the calculated pulse was within 11% of that measured. It is interesting to note that the analysis is valid for the pulse as well as the later times when heat transfer effects become important ($t > .4$ sec).

However, there are two regions that show a small disagreement between the data and the calculations in the \$1.25 pulse (Fig. 17). First, the calculated peak appears to be shifted to the right of the measured peak. This probably occurs because the upper micro switch, which marks the time the pulse rod reaches its uppermost position could not be installed for the

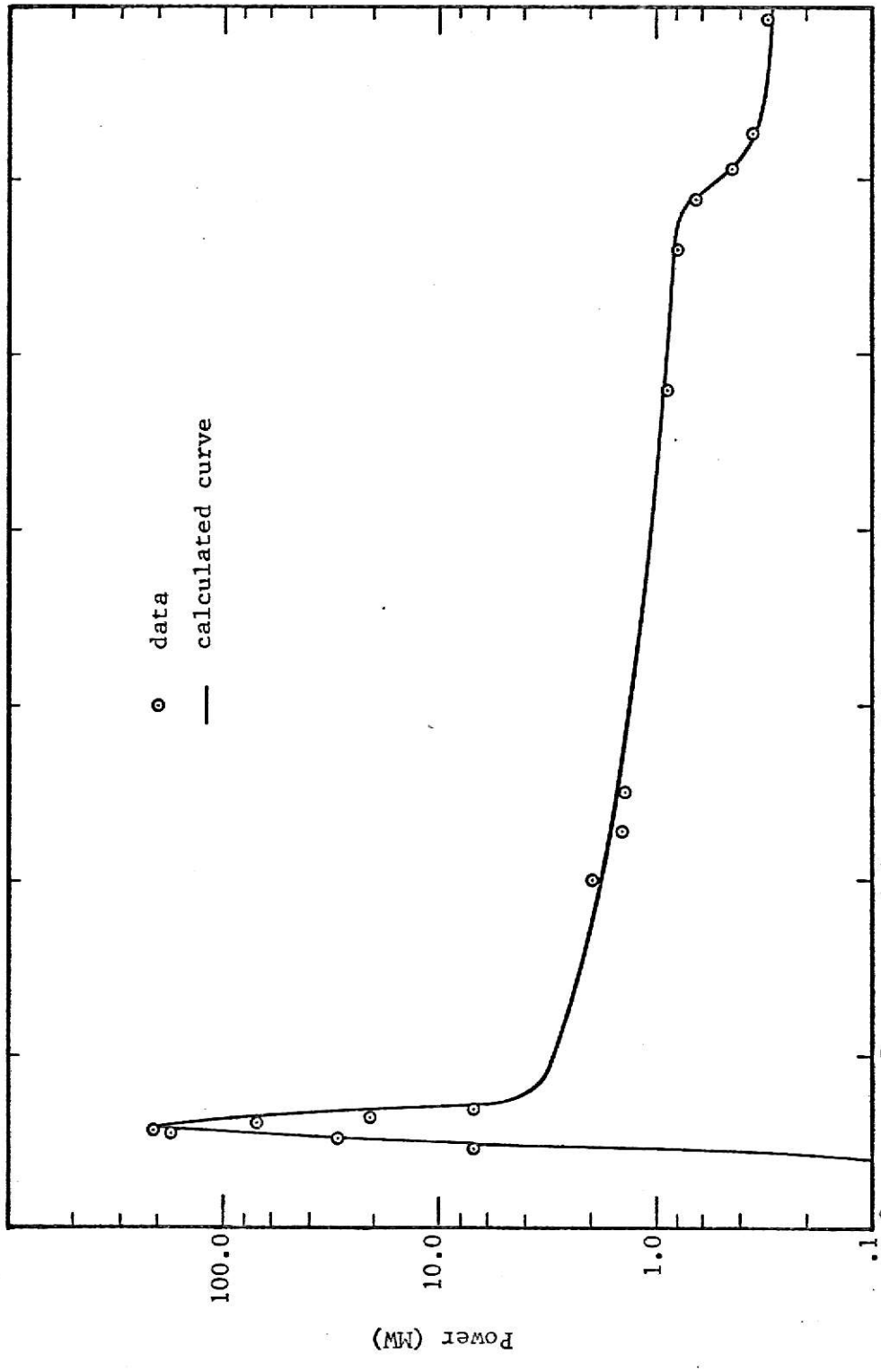

Figure 14. Transient power data and calculations for the $1.93 pulse.

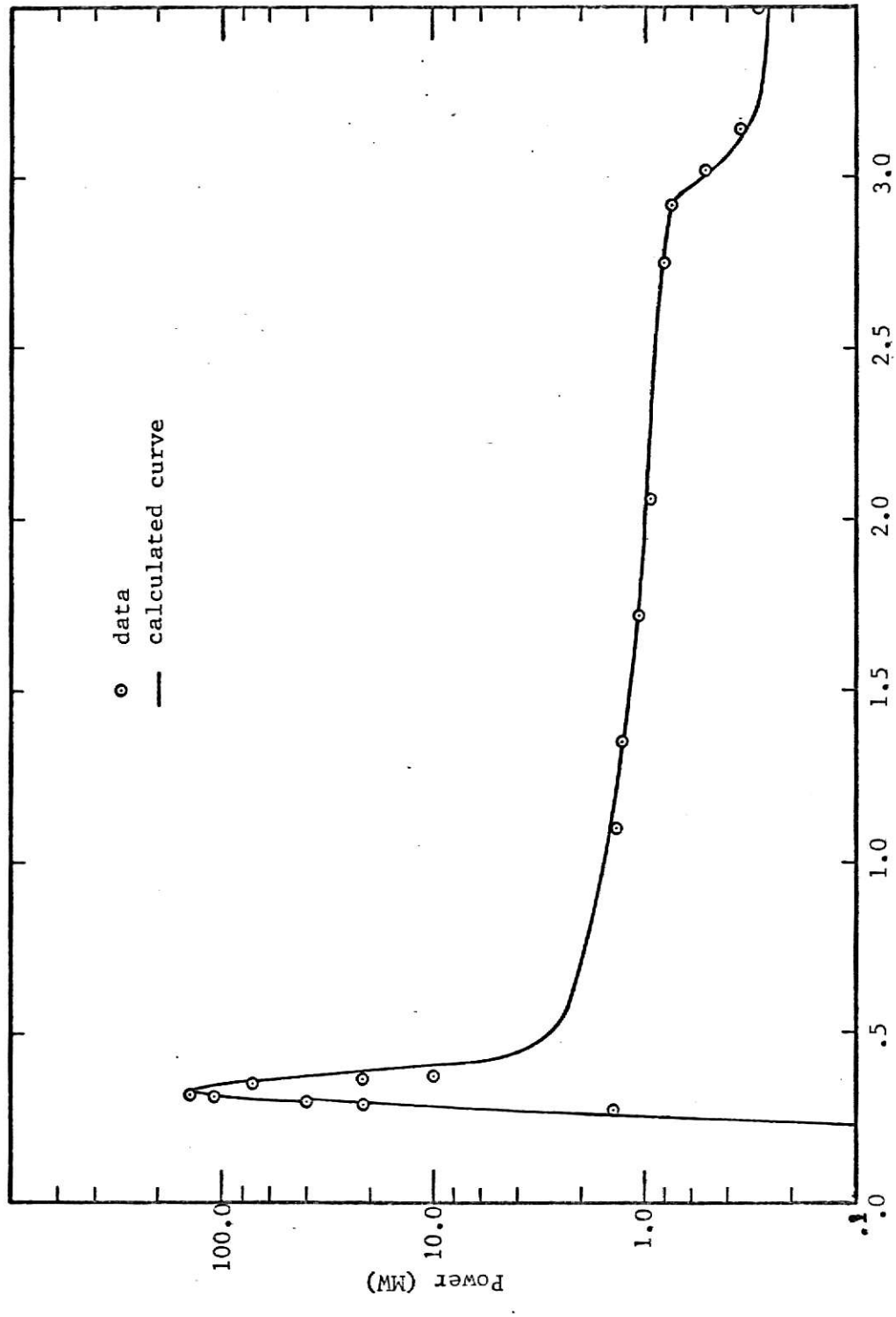

Figure 15. Transient power data and calculations for the $1.76 pulse.

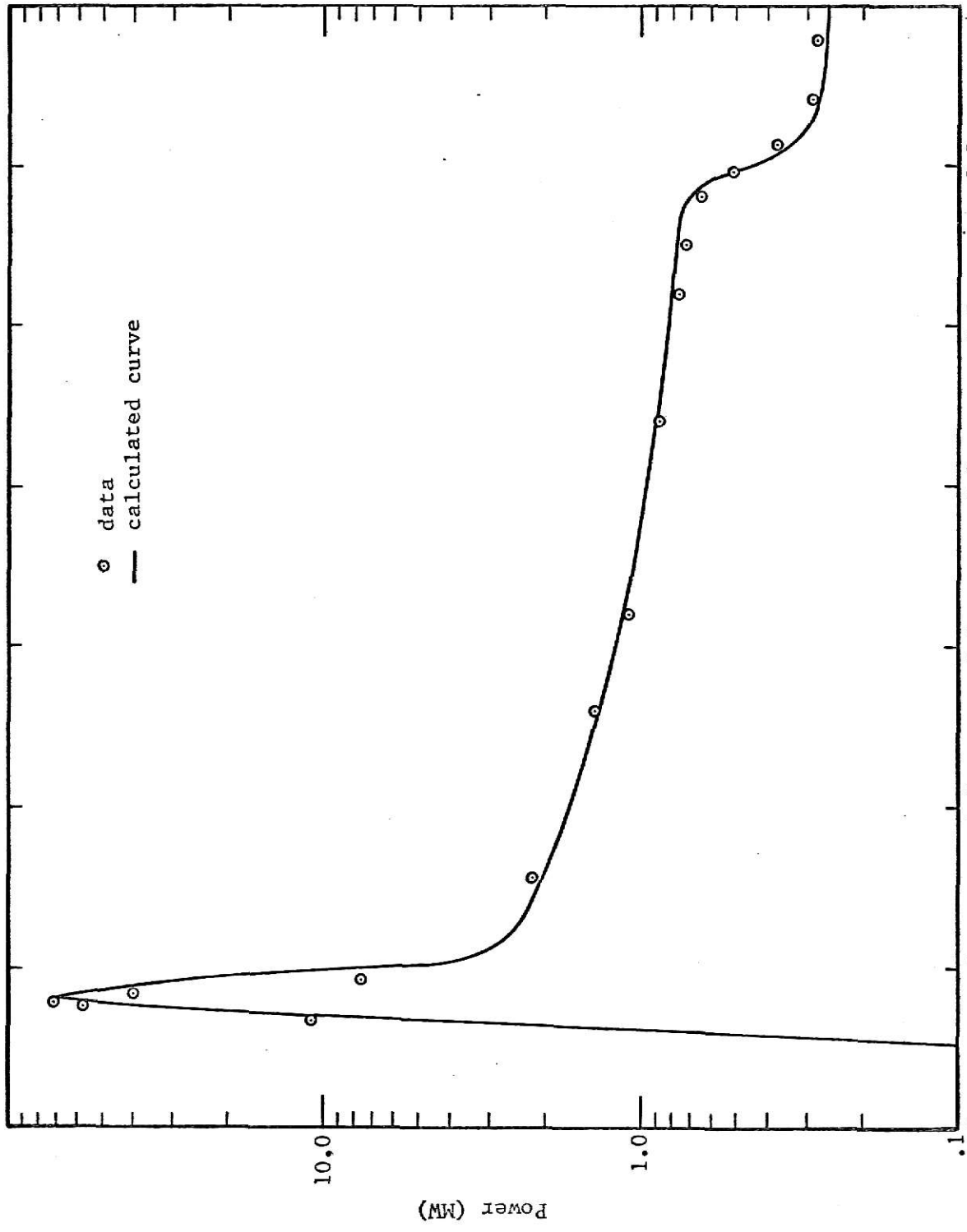

Figure 16. Transient power data and calculations for the $1.55 pulse.

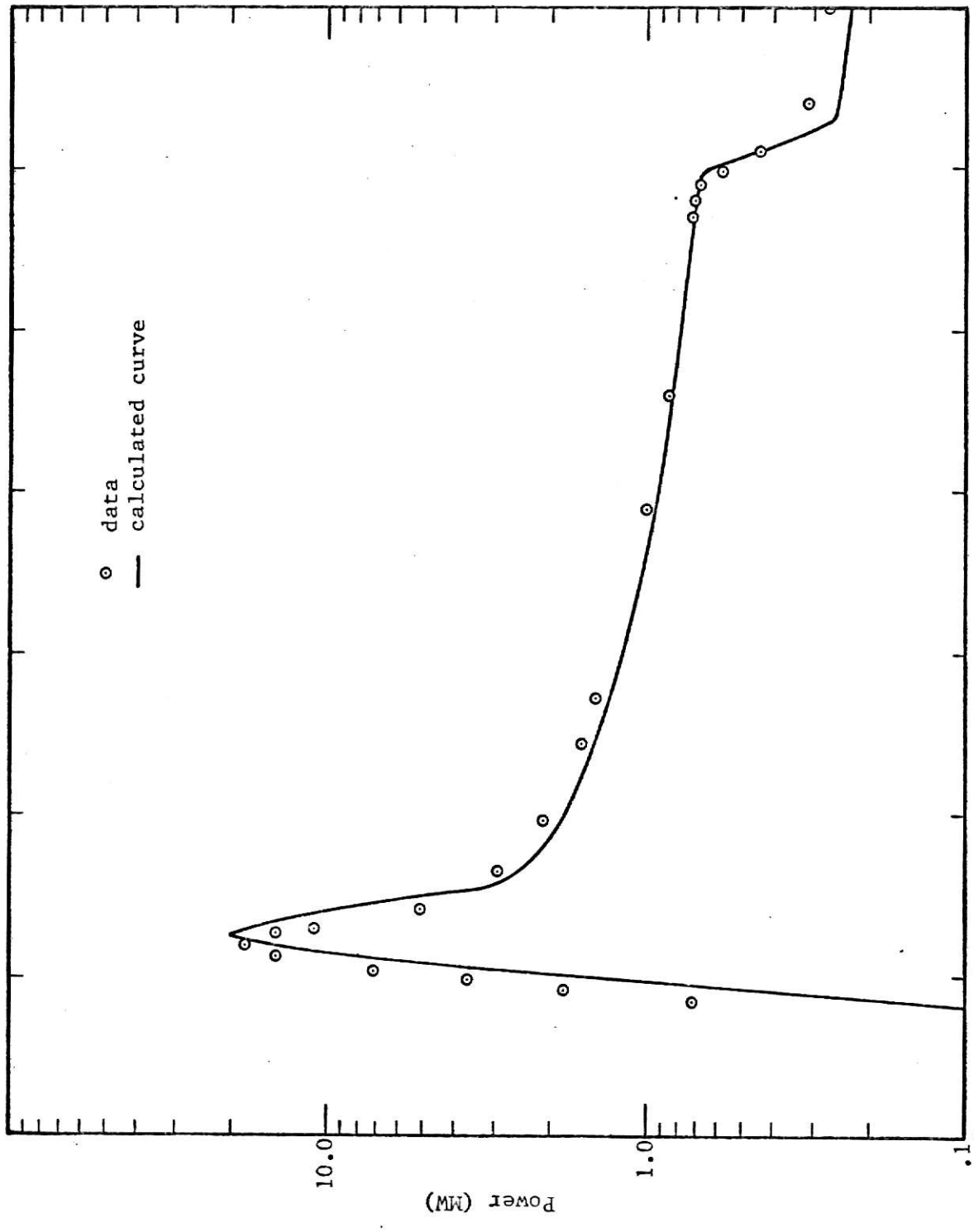

Figure 17. Transient power data and calculations for the $1.25 pulse.

$1.25 pulse because of the location with respect to the reactor bridge. Thus this time had to be estimated, and an overestimation of this time would explain the observed discrepancy.

The second region of disagreement occurs after the pulse rod falls back into the core ($\sim$ 3 seconds). Note that the calculated curve lies below the data. Again it is suspected that the discrepancy is due to the time measurement estimation of the $1.25 pulse.

The transient temperature data and calculations are illustrated in Figs. 18 through 21. The calculated values represent the average fuel temperature from Eq. (5), and the data points are the temperatures measured in the instrumented fuel-moderator element. The measured temperatures were corrected for the time lag (Appendix F) due to the time constant of the thermocouple. Comparison of the calculations with the data must necessarily be limited to a qualitative analysis because they represent different temperatures.

The general trend is that the measured centerline temperature lags behind the average calculated temperature during the transient, but later on surpasses it. This is reasonable because during a transient most of the heat is generated near the periphery of the element and negligible heat transfer occurs during this time. Thus the effect will be to make the average temperature greater than the centerline temperature. After the prompt burst, when the power is monotonically decreasing, the heat transfer will become significant, and the radial temperature distribution of an element will tend to maximize in the center. Calculations by West, et al. (6), and experiments by Wyman, et al. (16) have verified this behavior.

In conclusion, it has been shown that the transient model gives a satisfactory description of the transient behavior of the TRIGA.

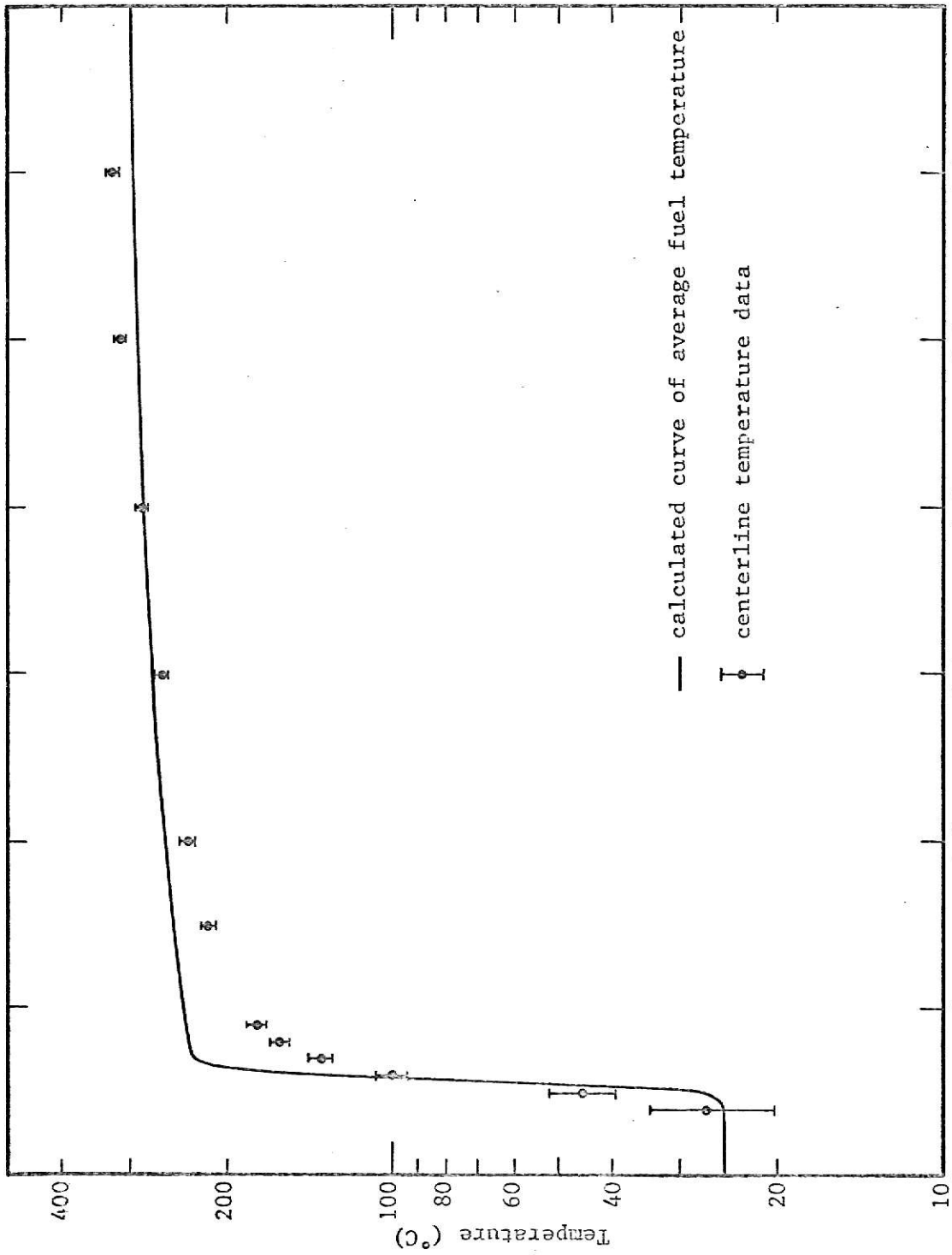

Figure 18. Transient temperature data and calculations for the $1.93 pulse.

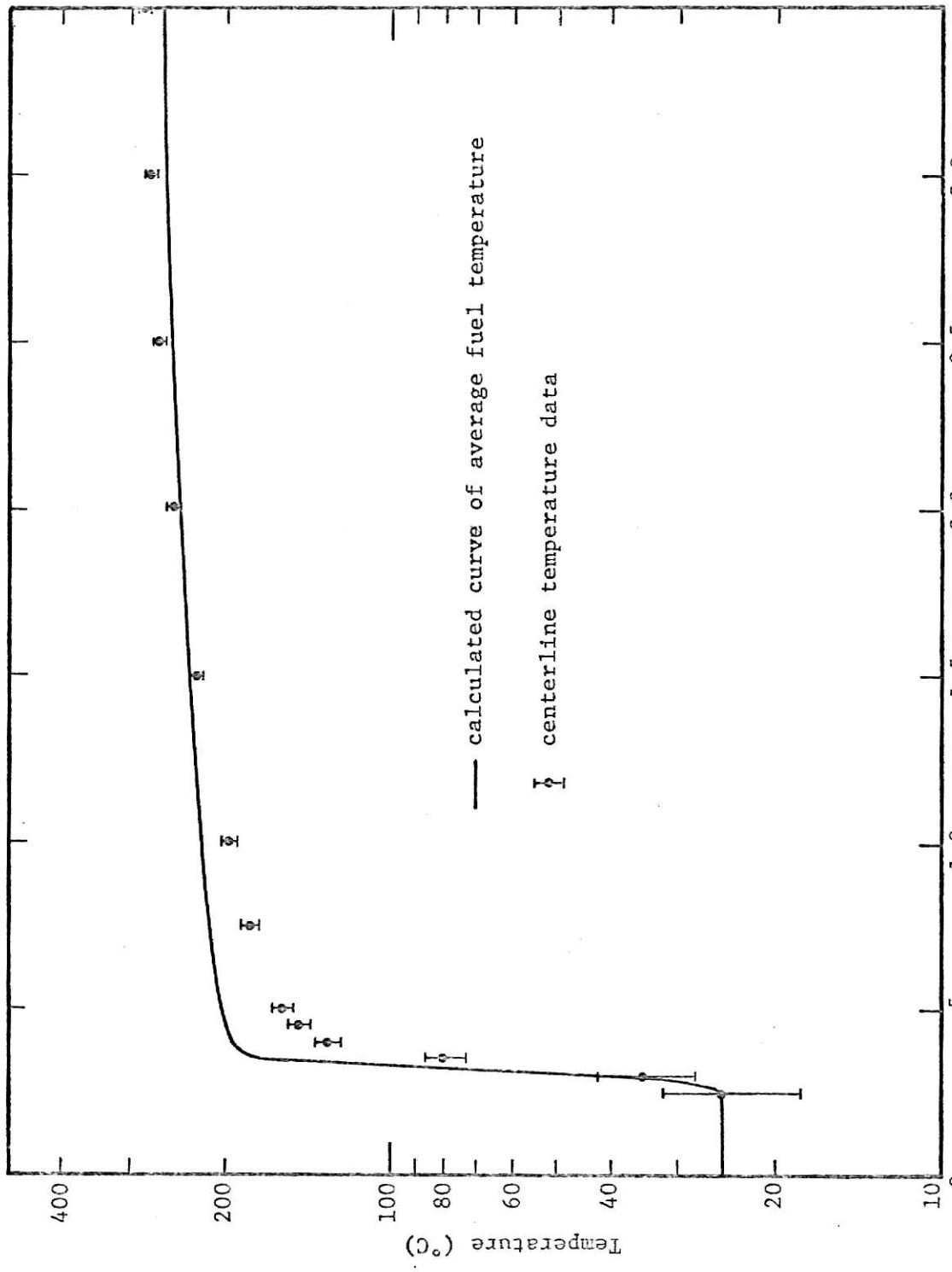

Figure 19. Transient temperature data and calculations for the $1.76 pulse.

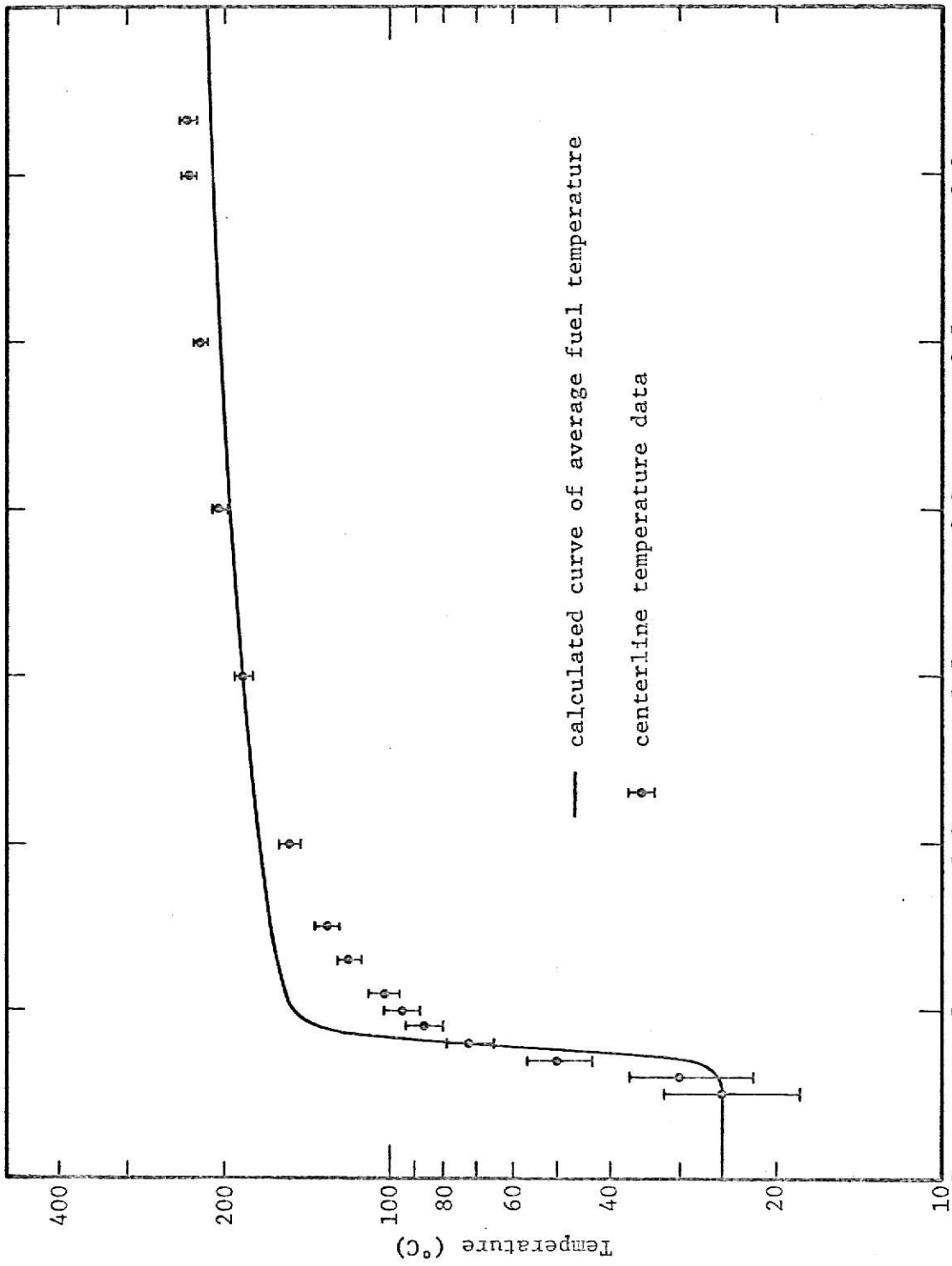

Figure 20. Transient temperature data and calculations for the $1.55 pulse.

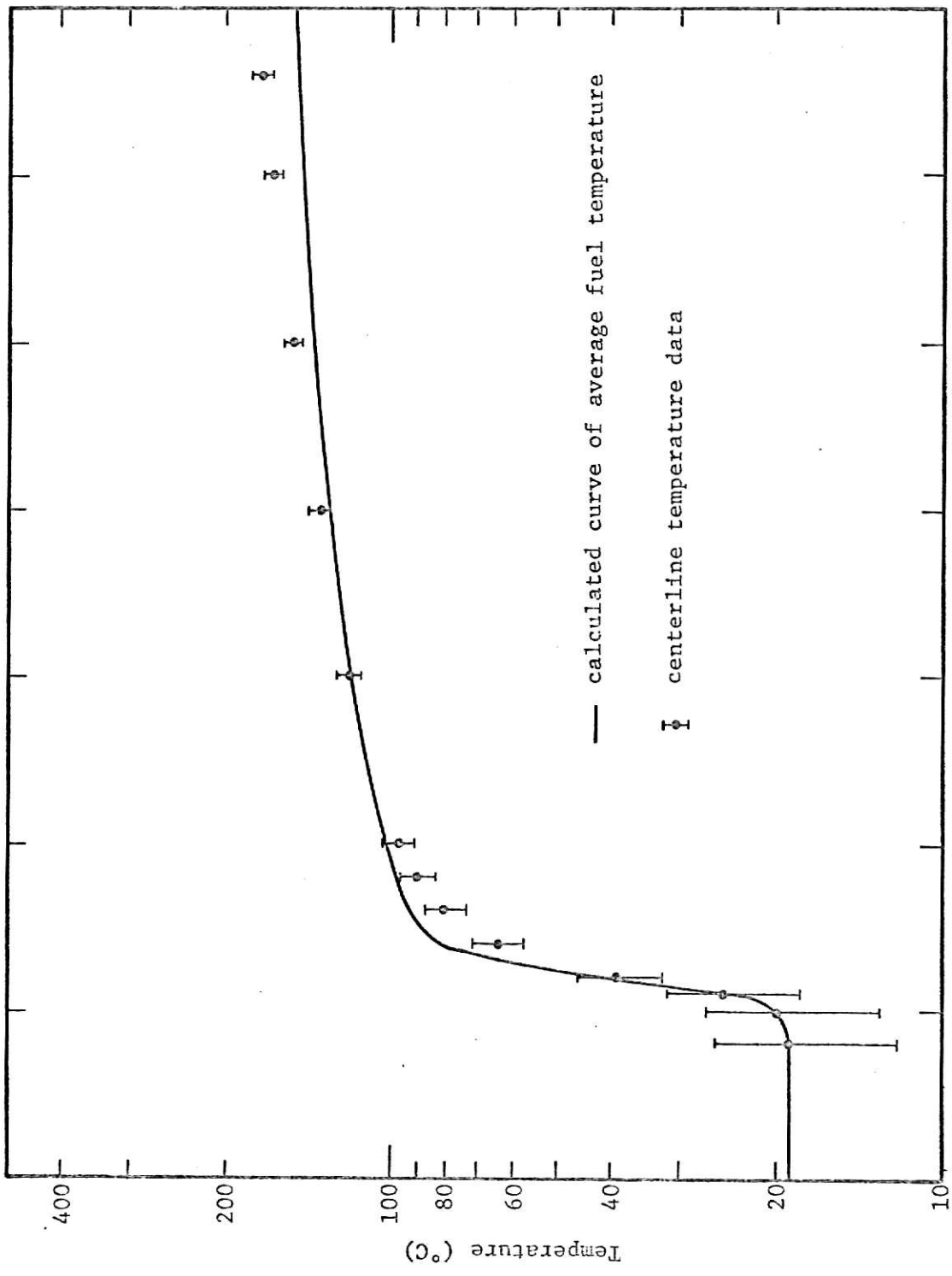

Figure 21. Transient temperature data and calculations for the $1.25 pulse.

6.0 SUGGESTIONS FOR FURTHER STUDY

It is suggested that the method of experimental determination of the flux distribution be extended to include the effects of control rods, graphite dummy elements, source, and the experimental facilities that are in the core region. This would require several different core loadings in order to move the particular discontinuity near a foil insertion hole. For example, moving the fuel-moderator element in F-9 to position F-6, the source in F-10 to F-9, and the graphite dummy in F-6 to position F-10 would provide a geometry to investigate the effect of the source element on the flux distribution in the fuel-moderator element in F-8 using foil insertion holes A and B. The extension of this type or a similar analysis to the other discontinuities in the core will eliminate the assumption of the same flux in all the elements of the same ring.

Another suggested improvement is a more accurate method of measuring the channel inlet and outlet water temperatures of a fuel element. The use of 3 thermocouples, one on each side of the triangular-shaped spacer, would provide a better estimate of the outlet water temperature. The inlet water temperature measurement could be improved by installing a thermocouple at the end of a tube which would be inserted into the nearest foil insertion hole to the fuel-moderator element.

A more sophisticated measurement of the pulse rod motion is required. The use of a slide wire or a rack and pinion gear coupled to a potentiometer would provide a more accurate technique for this measurement.

An instrumented fuel-moderator element with thermocouples at several different radial positions but at the same vertical level, would yield the

spatial distribution of the fuel temperature during steady state and pulsing operations. However, the cost of such an element might be prohibitive.

7.0 ACKNOWLEDGEMENT

The author expresses his gratitude to Dr. M. J. Robinson for his guidance and help throughout this investigation. Thanks are extended to the Department of Nuclear Engineering for providing the funds and equipment used in this work. Special thanks are given to Mr. R. W. Clack and Mr. J. McCleskey for their cooperation with regards to performing the experiments. I also wish to thank Dr. N. D. Eckhoff and Mr. G. P. Rathbun for their suggestions and particular contributions. A sincere expression of love and gratitude is extended to the author's wife who because of her sacrifices has made this work possible.

LITERATURE CITED

1. Schnurer, G. T.
"Role of a Research Reactor in Support of a Nuclear Power Program." TAB-134 (April 1967).

2. Graff, A. P., et al.
"TRIGA - A High Performance Steady Steady State/Pulsing Reactor." GA-7259 (Sept. 1966).

3. Graff, A. P., et al.
"Research Reactors - A Vital Tool for Nuclear Education and Research." GA-8189 (Sept. 1967).

4. TRIGA Training Manual. GAMD-1495 (1960).

5. Scalettar, R.
"The Fuchs-Nordheim Model with Variable Heat Capacity." Nuclear Science and Engineering, 16 (Letter to Ed., 1963).

6. West, G. B., et al.
"Kinetic Behavior of TRIGA Reactors." GA-7882 (1967).

7. Ash, Milton
Nuclear Reactor Kinetics, McGraw-Hill (1965).

8. Glasstone, S. and A. Sesonske
The Elements of Nuclear Reactor Theory, D. Van Nostrand (1963).

9. Technical Foundations of TRIGA. GA-471 (1958).

10. Keepin, G.
Physics of Nuclear Kinetics, Addison-Wesley (1965).

11. Hazards Summary Report, Engineering Experiment Station Special Report No. 7, Kansas State University, Manhattan, Kansas (1961).

12. Stone, R. and Sleeper, H.
"TRIGA Transient Experiments: Interim Report." GA-531 (1958).

13. Bonilla, C. F.
Nuclear Engineering, McGraw-Hill (1957).

14. Bouchey, G. D.
"Experimental Neutron Flux Measurements and Power Calibration in the Kansas State University TRIGA Mark II Nuclear Reactor," a Master's Thesis, Kansas State University (1967).

15. Dwork, J., et al.
"Self Shielding Factors for Infinitely Long Hollow Cylinders." KAPL-1262 (Jan. 1955).

16. Wyman, G. P., et al.
"Transient Temperature Measurements in Reactor Fuels," AEC Symposium Series 2, TID-7662 (1964).

17. Utilization Facility License No. R-88 for the Kansas State University TRIGA Mark II Reactor.

18. Eckhoff, N. D.
"Optimal Neutron Activation Analysis," a Ph.D. Dissertation, Kansas State University (1968).

19. Vigil, J. C.
"Solution of the Reactor Kinetics Equations by Analytic Continuation." Nuclear Science and Engineering, 29, 392-401 (1967).

20. Vigil, J. C.
"Solution of the Non Linear Reactor Kinetics Equations by Continuous Analytic Continuation," LA-3518 (1966).

21. Rohl, J., et al.
Radioisotopes Applications Engineering, D. Van Nostrand (1961).

22. Weaver, L. E.
Systems Analysis of Nuclear Reactor Dynamics, Rowman and Littlefield (1963).

23. Adler, F. T., et al.
"Semianalytical Methods for the Analysis of Reactor Transients," AEC Symposium Series 2, TID-7662 (1964).

APPENDIX A

Three computer programs were used to evaluate the data taken at steady state power levels. The code, AVGFLUX, which calculated the necessary neutron flux values, provided punched output on cards. This output was used as input into CLTEMP, the code which calculated the average radial temperatures in the fuel-moderator elements. Punched output on cards from CLTEMP provided the input to AVGTEMP, the code which determined the average fuel temperature of the core as a function of power.

AVGFLUX - The Computer Program for the Average Flux Calculations

This program calculates the vertical distribution of the average radial flux for a fuel-moderator element in each of the 5 rings as described in Section 4.3.1. It also calculates the average flux in the element from the equation

$$\bar{\phi}_k = \frac{1}{I} \sum_{i=1}^{I} \phi_{ik}$$

where $\bar{\phi}_k$ = average flux in the kth element,

ϕ_{ik} = average radial flux in the kth element at the ith level,

I = number of vertical levels.

The average flux in the element is necessary for the calculation of the average heat generation rate used in Section 4.1.4.

Comment cards present in the program aid in understanding the logic. The variables are defined in the Fortran listing and in the input data given below.

Input Data

Card 1: FORMAT (2I3, 4X, 3F10.0, 3E13.6)

NFLUX - number of flux measurements taken per foil insertion hole.

NHOLE - number of foil insertion holes used.

ELMTS - number of fuel elements in the core.

ZETA - disadvantage factor.

POWER - power in kilowatts.

FACT - conversion factor from meter current reading to neutron flux.

VFACT - conversion factor from current variance to neutron flux variance.

FDCF - flux depression correction factor for the miniature fission chamber.

Cards 2-16: FORMAT (8F10.0)

FLUX(I,J) - current data.

Card 17: FORMAT (8F10.0)

RING(J) - number of fuel elements in each ring.

Card 18: FORMAT (20A4)

P(I) - title card for output listing of the calculated flux values from the current data.

Cards 19-33: FORMAT (8F10.0)

VARF(I,J) - current variance data.

Card 34: FORMAT (20A4)

P(I) - title card for the output listing of the calculated flux variances from the current variance data.

The Fortran Listing for AVGFLUX

```
      DIMENSION FLUX(30,10),FAVG(10),AFF(30,10),RING(5),P(20),VARF(30
     1),AFVAR(10)
 1001 FORMAT(8F10.0)
 1003 FORMAT(8E10.3)
 1004 FORMAT(20A4)
 1006 FORMAT(1H ,8(E15.8,1X))
C
C********** NFLUX=NUMBER OF FLUX MEASUREMENTS TAKEN PER HOLE
C********** NHOLE=NUMBER OF FLUX MAPPING HOLES USED
C********** ELMTS=NUMBER OF FUEL ELEMENTS IN THE CORE
C********** ZETA=DISADVANTAGE FACTOR
C********** POWER EXPRESSED IN KILOWATTS
C********** FLUX(I,J)=FLUX MEASUREMENT AT ITH LEVEL IN JTH HOLE
C********** RING(J)=NUMBER OF FUEL ELEMENTS IN JTH RING
C********** VARF(I,J) IS THE VARIANCE OF FLUX(I,J)
C********** FACT IS THE CONVERSION FACTOR FOR THE FLUX
C********** VFACT IS THE CONVERSION FACTOR FOR THE VARIANCE
C********** FDCF IS THE FLUX DEPRESSION CORRECTION FACTOR
C
      READ(1,1000)NFLUX,NHOLE,ELMTS,ZETA,POWER,FACT,VFACT,FDCF
 1000 FORMAT(2I3,4X,3F10.0,3E13.6)
C
C********** J=1 IS THE FLUX DISTRIBUTION IN THE CENTRAL THIMBLE
C********** J=6 IS THE FLUX DISTRIBUTION AT THE PERIPHERY
C********** I=1 IS THE LOWEST POSITION
C
      DO 1 I=1,NFLUX
    1 READ(1,1001)(FLUX(I,J),J=1,NHOLE)
      READ(1,1001)(RING(J),J=1,5)
      READ(1,1004)(P(I),I=1,20)
      WRITE(3,1005)(P(I),I=1,20)
 1005 FORMAT(1H1,20X,20A4)
      DO 3 I=1,NFLUX
      DO 2 J=1,NHOLE
    2 FLUX(I,J)=FLUX(I,J)*FACT/FDCF
    3 WRITE(3,1006)(FLUX(I,J),J=1,NHOLE)
      DO 5 I=1,NFLUX
    5 READ(1,1001)(VARF(I,J),J=1,NHOLE)
      READ(1,1004)(P(I),I=1,20)
      WRITE(3,1013)(P(I),I=1,20)
 1013 FORMAT(1H-,20X,20A4)
      DO 6 I=1,NFLUX
      DO 7 J=1,NHOLE
    7 VARF(I,J)=VARF(I,J)*VFACT/(FDCF**2)
    6 WRITE(3,1006)(VARF(I,J),J=1,NHOLE)
      DO 8 I=1,NFLUX
      DO 8 J=1,NHOLE
      FLUX(I,J)=FLUX(I,J)/ POWER
    8 VARF(I,J)=VARF(I,J)/(POWER**2)
      READ(1,1004)(P(I),I=1,20)
```

```
      WRITE(3,1005)(P(I),I=1,20)
      DO9I=1,NFLUX
    9 WRITE(3,1006)(FLUX(I,J),J=1,NHOLE)
      READ(1,1004)(P(I),I=1,20)
      WRITE(3,1013)(P(I),I=1,20)
      DO4I=1,NFLUX
    4 WRITE(3,1006)(VARF(I,J),J=1,NHOLE)
C
C********** AVERAGE FLUX IN THE FUEL AT THE ITH LEVEL
C         VARF(I,J) IS THE VARIANCE OF AFF(I,J)
C         AFF(I,J) IS THE AVERAGE FLUX PER WATT IN THE JTH FUEL ELEMENT AT
C                ITH LEVEL
C
      NHR=NHOLE-1
      DO 10 I=1,NFLUX
      DO 10 J=1,NHR
      VARF(I,J)=(VARF(I,J+1)+VARF(I,J))/((2.*ZETA)**2)
   10 AFF(I,J)=(FLUX(I,J+1)+FLUX(I,J))/(2.*ZETA)
      WRITE(3,1002)
 1002 FORMAT(1H1,20X,37HAVERAGE FLUX IN FUEL AT THE ITH LEVEL/)
      DO 11 I=1,NFLUX
      WRITE(2,1100)(AFF(I,J),J=1,NHR)
   11 WRITE(3,1006)(AFF(I,J),J=1,NHR)
 1100 FORMAT(5E15.8)
      WRITE(3,1014)
 1014 FORMAT(1H-,20X,49HVARIANCE OF AVERAGE FLUX IN FUEL AT THE ITH LEVE
     1L/)
      DO 12 I=1,NFLUX
      WRITE(2,1100)(VARF(I,J),J=1,NHR)
   12 WRITE(3,1006)(VARF(I,J),J=1,NHR)
C
C********** AVERAGE FLUX IN THE JTH FUEL ELEMENT
C         FAVG(J) IS THE AVERAGE FLUX PER WATT IN THE KTH FUEL ELEMENT
C         AFVAR(J) IS THE VARIANCE OF FAVG(J)
C
      DO 21 J=1,NHR
      SUM =0.0
      VUM=0.0
      DO 20 I=1,NFLUX
      VUM=VUM+VARF(I,J)
   20 SUM=SUM+AFF(I,J)
      AFVAR(J)=VUM/(FLOAT(NFLUX)**2)
   21 FAVG(J)=SUM/(FLOAT(NFLUX))
      WRITE(3,1012)
 1012 FORMAT(1H-,20X,36HAVERAGE FLUX IN THE JTH FUEL ELEMENT/)
      WRITE(3,1006)(FAVG(J),J=1,NHR)
      WRITE(2,1100)(FAVG(J),J=1,NHR)
      WRITE(3,1017)
 1017 FORMAT(1H-,20X,48HVARIANCE OF AVERAGE FLUX IN THE JTH FUEL ELEMENT
     1/)
      WRITE(3,1006)(AFVAR(J),J=1,NHR)
      WRITE(2,1100)(AFVAR(J),J=1,NHR)
      CALLEXIT
      END
```

CLTEMP - The Computer Program for the Centerline and Average Radial Fuel Temperature Calculations

The program consists of the main program and the subroutine TRAP which is a numerical integration routine using the trapezoidal rule. The main program (CLTEMP) performs the calculations for the centerline temperatures and the average radial temperatures outlined in Sections 4.1.4 and 4.1.2 respectively. Comment cards present in the program aid in understanding the logic. Some of the variables used in the program are defined in the Fortran listing and others are defined in the input data given below. It should be noted that this program generates a significant amount of output, thus the user should specify 3 times the number of rings times the number of power sets in the control cards for the number of output pages.

Input Data

Card 1: FORMAT (8F10.0)

RO - radius of the fuel elements (cms).

C - cladding thickness (cms).

CLADK - thermal conductivity of the cladding (watts/cm °C).

AC - cross sectional area of the fuel (cm^2).

CP - specific heat at constant pressure for water.

PREC - fractional accuracy specified for film coefficient iteration.

Card 2: FORMAT (5E15.8)

A1, A2, A3, A4 - coefficients for the empirical equation of the fuel thermal conductivity.

G - conversion factor for neutron flux to power density.

Cards 3-17: FORMAT (5E15.8)

Cards 3-17: AFF(I,J) - average flux in the jth fuel element at the ith vertical position (punched output of AVGFLUX).

Cards 18-32: FORMAT (5E15.8)

VARF(I,J) - variances of AFF(I,J) (punched output of AVGFLUX).

Card 33: FORMAT (5E15.8)

FAVG(J) - average flux in a fuel element (punched output of AVGFLUX).

Card 34: FORMAT (8F10.0)

P - power in kilowatts.

Cards 35-37: FORMAT (8F10.0)

TM(I,J) - measured centerline temperatures at P kilowatts.

Card 38: FORMAT (8F10.0)

TWI(J) - measured inlet water temperatures at P kilowatts.

Card 34: FORMAT (8F10.0)

TWO(J) - measured outlet water temperatures at P kilowatts.

Cards 40-44: FORMAT (20A4)

O(I) - title for output results for this power data set.

Cards 34through 44 are repeated for each power data set.

The Fortran Listing for CLTEMP

```
      DIMENSION HGR(15),AFF(15,5),THFX(15),TWO(5),TM(15,5),FUELK(15),TA(
     115),PHFX(15),H(10),TS(15),TC(15),O(20),TWI(5),TF(15),PHFP(15),AHGR
     2(5),FAVG(5),TG(15),VHGR(15),VARF(15,5),VTHFX(15),VPHFX(15),VR(15)
      READ(1,1000)RO,C,CLADK,AC,CP,PREC
 1000 FORMAT(8F10.0)
      READ(1,1001)A1,A2,A3,A4,G
 1001 FORMAT(5E15.8)
      CLDR=ALOG((RO+C)/RO)/(2.*CLADK)
      DO1I=1,15
    1 READ(1,1001)(AFF(I,J),J=1,5)
      DO8I=1,15
    8 READ(1,1001)(VARF(I,J),J=1,5)
      READ(1,1001)(FAVG(J),J=1,5)
      B1=.2939025
      B2=.9488443E-03
      B3=-.2688496E-05
      B4=.2173816E-08
      B5=-.1669121E+09
      B6=.4090963E+07
      B7=.5700616E+05
      B8=.3952822E+02
      HAVG=.05
C
C        POWER IN KILOWATTS
C
    2 READ(1,1000)P
      IF(P.EQ.0.0)CALLEXIT
      WRITE(2,1001)P
      DO3I=7,9
    3 READ(1,1000)(TM(I,J),J=1,5)
      READ(1,1000)(TWI(J),J=1,5)
      READ(1,1000)(TWO(J),J=1,5)
      DO100J=1,5
      READ(1,1010)(O(I),I=1,20)
 1010 FORMAT(20A4)
      WRITE(3,1011)(O(I),I=1,20)
 1011 FORMAT(1H1,20X,20A4///)
C
C        J=1,2,3,4,5 CORESPONDS TO THE B,C,D,E,F RINGS RESPECTIVELY
C        I=1 IS THE LOWEST POSITION IN THE FUEL ELEMENT
C        HEAT GENERATION AND FLOW RATE CALCULATIONS
C
      DO10I=1,15
      HGR(I)=P*G*AFF(I,J)
      VHGR(I)=P*P*G*G*VARF(I,J)
   10 WRITE(3,1020)I,HGR(I),VHGR(I)
 1020 FORMAT(1H ,4HHGR(,I3,2H)=,E14.8,5X,E15.8)
      CALL TRAP(HGR,15,THFX,J,2.54)
      AHGR(J)=P*G*FAVG(J)
      FLOW=AC*THFX(J)/(CP*(TWO(J)-TWI(J)))
```

```
      WRITE(3,1002)FLOW,THFX(J),AHGR(J)
 1002 FORMAT(1H0,5HFLOW=,E12.6,2X,16HGRAMS PER SECOND,5X,5HTHFX=,E14.8,1
     14HWATTS PER SQCM,5X,5HAHGR=,E14.8,14HWATTS PER SQCM//)
      CALL TRAP(VHGR,15,VTHFX,J,2.54)
      VFLOW=((AC/(CP*(TWO(J)-TWI(J))))**2)*VTHFX(J)
      WRITE(3,1201)VFLOW,VTHFX(J)
C
C        FILM COEFFICIENT CALCULATIONS
C
      AFT=(TWI(J)+TWO(J))/2.
      ACT=AFT+RO*RO*AHGR(J)/(2.*(RO+C)*HAVG)
    4 DT=ACT-TWI(J)
      BFT=(ACT+AFT)/2.
      BFTF=1.8*BFT+32.
      GRPR=B5+B6*BFTF+B7*BFTF**2+B8*BFTF**3
      GRPR=GRPR*DT*1.8
      FLUK=B1+B2*BFTF+B3*BFTF**2+B4*BFTF**3
      X=1./3.
      HAVG=(.13*FLUK*GRPR**X)/2057.
    7 ECT=AFT+RO*RO*AHGR(J)/(2.*HAVG*(RO+C))
      WRITE(3,1200)BFT,AFT,ECT,HAVG
      IF(ABS(ECT-ACT)/ACT.LE.PREC)GOTO5
      ACT=ECT
      GOTO4
 1200 FORMAT(1H ,4HBFT=,F7.2,4X,4HAFT=,F7.2,4X,4HECT=,F7.2,4X,10HFILM CO
     1EF=,E15.8)
C
C        HEAT FLUX CALCULATIONS
C
    5 HHA=HAVG*(ECT-AFT)
      HAHGR=AHGR(J)*RO/2.
      DHA=ABS(HHA-HAHGR)*100./HAHGR
      THHA=HHA*416.
      HTHFX=THFX(J)*AC
      DTH=ABS(THHA-HTHFX)*100./HTHFX
      WRITE(3,1201)HHA,HAHGR,DHA,THHA,HTHFX,DTH
 1201 FORMAT(1H0,6(E15.8,5X)//)
      HUM=0.0
      VGAP=0.0
      DO20I=7,9
      TT=TM(I,J)
      WRITE(3,1006)I,TT
 1006 FORMAT(1H ,36HITERATION OF AVG FUEL TEMP AT LEVEL ,I2,3X,F7.2,3X,E
     114.8)
C
C        AVERAGE FUEL TEMPERATURE ITERATION
C
   11 FUELK(I)=A1*TT**3+A2*TT**2+A3*TT+A4
      TA(I)=TM(I,J)-HGR(I)*RO*RO/(8.*FUELK(I))
      WRITE(3,1006)I,TA(I),FUELK(I)
      IF((ABS(TT-TA(I)))/TT.LE.PREC)GOTO12
      TT=TA(I)
      GOTO11
```

```
C
C          CALCULATION OF GAP RESISTANCE
C
   12 CALL TRAP(HGR,I,PHFX,I,2.54)
      PHFP(I)=PHFX(I)
      Z=(TM(I,J)-TWI(J)-AC*PHFX(I)/(FLOW*CP))/(HGR(I)*RO*RO)
      H(I)=Z-(.25/FUELK(I)+CLDR+.5/(HAVG*(RO+C)))
      CALL TRAP(VHGR,I,VPHFX,I,2.54)
      TERM1=((AC/(FLOW*CP))**2)*(VPHFX(I)+VFLOW*(PHFP(I)/FLOW)**2)
      TERM2=VHGR(I)*(TM(I,J)-TWI(J)-AC*PHFP(I)/(FLOW*CP))**2
      VGAP=(1.25+TERM1+TERM2)/((HGR(I)*RO*RO)**2)+VGAP
   20 HUM=HUM+H(I)
      HA=HUM/3.
      VGAP=VGAP/9.
      WRITE(3,1003)H(7),H(8),H(9),HA,VGAP
 1003 FORMAT(1HO,5HR(7)=,E12.6,3X,5HR(8)=,E12.6,3X,5HR(9)=,E12.6,3X,5HRA
     1VG=,E12.6,2X,E14.8)
      WRITE(3,1004)
 1004 FORMAT(1H-,5HLEVEL,6X,4HTMAX,6X,4HTAVG,6X,4HTSUR,6X,4HTGAP,6X,5HTC
     1LAD,5X,6HTFLUID,9X,4HTVAR//)
C
C          CENTERLINE TEMPERATURE CALCULATIONS
C          TM(I,J) IS THE CENTERLINE TEMPERATURE
C          TS(I) IS THE FUEL SURFACE TEMPERATURE
C          TG(I) IS THE GAP TEMPERATURE
C          TC(I) IS THE CLAD TEMPERATURE
C          TF(I) IS THE FLUID TEMPERATURE
C
      DO25I=7,9
      TM(I,J)=TWI(J)+AC*PHFP(I)/(FLOW*CP)+HGR(I)*RO*RO*(.25/FUELK(I)+CLD
     1R+1./(2.*HAVG*(RO+C))+HA)
      TS(I)=TM(I,J)-HGR(I)*RO*RO/(4.*FUELK(I))
      TG(I)=TM(I,J)-HGR(I)*RO*RO*(.25/FUELK(I)+HA)
      TC(I)=TM(I,J)-HGR(I)*RO*RO*(1./(4.*FUELK(I))+CLDR+HA)
      TF(I)=TWI(J)+AC*PHFP(I)/(FLOW*CP)
      CALL TRAP(VHGR,I,VPHFX,I,2.54)
      TERM1=((AC/(FLOW*CP))**2)*(VPHFX(I)+VFLOW*(PHFP(I)/FLOW)**2)
      TERM2=(((.5/FUELK(I)+HA+CLDR+1./(HAVG*(RO+C)))*RO*RO/2.)**2)*VHGR(
     1I)
      VTMAX=.625+TERM1+TERM2+VGAP*(HGR(I)*RO*RO/2.)**2
      VR(I)=VTMAX+VHGR(I)*(RO*RO/(8.*FUELK(I)))**2
   25 WRITE(3,1005)I,TM(I,J),TA(I),TS(I),TG(I),TC(I),TF(I),VR(I)
 1005 FORMAT(1H ,1X,I3,5X,6(F7.2,3X),3X,E14.8)
      DO30I=10,15
      FUELK(I)=FUELK(I-1)
      CALL TRAP(HGR,I,PHFX,I,2.54)
      TM(I,J)=TWI(J)+AC*PHFX(I)/(FLOW*CP)+HGR(I)*RO*RO*(.25/FUELK(I)+CLD
     1R+1./(2.*HAVG*(RO+C))+HA)
      TA(I)=TM(I,J)-HGR(I)*RO*RO/(8.*FUELK(I))
      TS(I)=TM(I,J)-HGR(I)*RO*RO/(4.*FUELK(I))
      TG(I)=TM(I,J)-HGR(I)*RO*RO*(.25/FUELK(I)+HA)
      TC(I)=TM(I,J)-HGR(I)*RO*RO*(1./(4.*FUELK(I))+CLDR+HA)
      TF(I)=TWI(J)+AC*PHFX(I)/(FLOW*CP)
```

```
      CALL TRAP(VHGR,I,VPHFX,I,2.54)
      TERM1=((AC/(FLOW*CP))**2)*(VPHFX(I)+VFLOW*(PHFX(I)/FLOW)**2)
      TERM2=(((.5/FUELK(I)+HA+CLDR+1./(HAVG*(RO+C)))*RO*RO/2.)**2)*VHGR(
     1I)
      VTMAX=.625+TERM1+TERM2+VGAP*(HGR(I)*RO*RO/2.)**2
      VR(I)=VTMAX+VHGR(I)*(RO*RO/(8.*FUELK(I)))**2
      WRITE(3,1005)I,TM(I,J),TA(I),TS(I),TG(I),TC(I),TF(I),VR(I)
      FUELK(I)=A1*TA(I)**3+A2*TA(I)**2+A3*TA(I)+A4
      TM(I,J)=TWI(J)+AC*PHFX(I)/(FLOW*CP)+HGR(I)*RO*RO*(.25/FUELK(I)+CLD
     1R+1./(2.*HAVG*(RO+C))+HA)
      TA(I)=TM(I,J)-HGR(I)*RO*RO/(8.*FUELK(I))
      TS(I)=TM(I,J)-HGR(I)*RO*RO/(4.*FUELK(I))
      TG(I)=TM(I,J)-HGR(I)*RO*RO*(.25/FUELK(I)+HA)
      TC(I)=TM(I,J)-HGR(I)*RO*RO*(1./(4.*FUELK(I))+CLDR+HA)
      TF(I)=TWI(J)+AC*PHFX(I)/(FLOW*CP)
      CALL TRAP(VHGR,I,VPHFX,I,2.54)
      TERM1=((AC/(FLOW*CP))**2)*(VPHFX(I)+VFLOW*(PHFX(I)/FLOW)**2)
      TERM2=(((.5/FUELK(I)+HA+CLDR+1./(HAVG*(RO+C)))*RO*RO/2.)**2)*VHGR(
     1I)
      VTMAX=.625+TERM1+TERM2+VGAP*(HGR(I)*RO*RO/2.)**2
      VR(I)=VTMAX+VHGR(I)*(RO*RO/(8.*FUELK(I)))**2
      WRITE(3,1005)I,TM(I,J),TA(I),TS(I),TG(I),TC(I),TF(I),VR(I)
   30 FUELK(I)=A1*TA(I)**3+A2*TA(I)**2+A3*TA(I)+A4
      DO35M=1,6
      I=7-M
      FUELK(I)=FUELK(I+1)
      CALL TRAP(HGR,I,PHFX,I,2.54)
      TM(I,J)=TWI(J)+AC*PHFX(I)/(FLOW*CP)+HGR(I)*RO*RO*(.25/FUELK(I)+CLD
     1R+1./(2.*HAVG*(RO+C))+HA)
      TA(I)=TM(I,J)-HGR(I)*RO*RO/(8.*FUELK(I))
      TS(I)=TM(I,J)-HGR(I)*RO*RO/(4.*FUELK(I))
      TG(I)=TM(I,J)-HGR(I)*RO*RO*(.25/FUELK(I)+HA)
      TC(I)=TM(I,J)-HGR(I)*RO*RO*(1./(4.*FUELK(I))+CLDR+HA)
      TF(I)=TWI(J)+AC*PHFX(I)/(FLOW*CP)
      CALL TRAP(VHGR,I,VPHFX,I,2.54)
      TERM1=((AC/(FLOW*CP))**2)*(VPHFX(I)+VFLOW*(PHFX(I)/FLOW)**2)
      TERM2=(((.5/FUELK(I)+HA+CLDR+1./(HAVG*(RO+C)))*RO*RO/2.)**2)*VHGR(
     1I)
      VTMAX=.625+TERM1+TERM2+VGAP*(HGR(I)*RO*RO/2.)**2
      VR(I)=VTMAX+VHGR(I)*(RO*RO/(8.*FUELK(I)))**2
      WRITE(3,1005)I,TM(I,J),TA(I),TS(I),TG(I),TC(I),TF(I),VR(I)
      FUELK(I)=A1*TA(I)**3+A2*TA(I)**2+A3*TA(I)+A4
      TM(I,J)=TWI(J)+AC*PHFX(I)/(FLOW*CP)+HGR(I)*RO*RO*(.25/FUELK(I)+CLD
     1R+1./(2.*HAVG*(RO+C))+HA)
      TA(I)=TM(I,J)-HGR(I)*RO*RO/(8.*FUELK(I))
      TS(I)=TM(I,J)-HGR(I)*RO*RO/(4.*FUELK(I))
      TG(I)=TM(I,J)-HGR(I)*RO*RO*(.25/FUELK(I)+HA)
      TC(I)=TM(I,J)-HGR(I)*RO*RO*(1./(4.*FUELK(I))+CLDR+HA)
      TF(I)=TWI(J)+AC*PHFX(I)/(FLOW*CP)
      CALL TRAP(VHGR,I,VPHFX,I,2.54)
      TERM1=((AC/(FLOW*CP))**2)*(VPHFX(I)+VFLOW*(PHFX(I)/FLOW)**2)
      TERM2=(((.5/FUELK(I)+HA+CLDR+1./(HAVG*(RO+C)))*RO*RO/2.)**2)*VHGR(
     1I)
```

```
      VTMAX=.625+TERM1+TERM2+VGAP*(HGR(I)*RO*RO/2.)**2
      VR(I)=VTMAX+VHGR(I)*(RO*RO/(8.*FUELK(I)))**2
      WRITE(3,1005)I,TM(I,J),TA(I),TS(I),TG(I),TC(I),TF(I),VR(I)
   35 FUELK(I)=A1*TA(I)**3+A2*TA(I)**2+A3*TA(I)+A4
C
C         ADJUSTMENT OF CENTERLINE TEMPERATURE
C
      DO200I=1,15
  200 TM(I,J)=TM(I,J)+(25.-TWI(J))
      DO220I=1,15
      TT=TM(I,J)
      WRITE(3,1006)I,TT
  211 FUELK(I)=A1*TT**3+A2*TT**2+A3*TT+A4
      TA(I)=TM(I,J)-HGR(I)*RO*RO/(8.*FUELK(I))
      WRITE(3,1006)I,TA(I),FUELK(I)
      IF((ABS(TT-TA(I)))/TT.LE.PREC)GOTO212
      TT=TA(I)
      GOTO211
  212 CALL TRAP(HGR,I,PHFX,I,2.54)
      CONTINUE
      CALL TRAP(VHGR,I,VPHFX,I,2.54)
      TERM1=((AC/(FLOW*CP))**2)*(VPHFX(I)+VFLOW*(PHFX(I)/FLOW)**2)
      TERM2=(((.5/FUELK(I)+HA+CLDR+1./(HAVG*(RO+C)))*RO*RO/2.)**2)*VHGR(
     1I)
      VTMAX=.625+TERM1+TERM2+VGAP*(HGR(I)*RO*RO/2.)**2
      VR(I)=VTMAX+VHGR(I)*(RO*RO/(8.*FUELK(I)))**2
  220 WRITE(3,1205)I,TM(I,J),TA(I),VR(I)
 1205 FORMAT(1H ,1X,I3,5X,2(F7.2,3X),3X,E14.8)
      WRITE(2,1001)(TA(I),I=1,15)
      WRITE(2,1001)(VR(I),I=1,15)
  100 CONTINUE
      GOTO2
      END



      SUBROUTINE TRAP(Y,NPTS,T,J,DELTA)
      DIMENSIONY(15),T(15)
      IF(NPTS.LE.2)GOTO5
      DO2I=1,NPTS
    2 T(I)=0.0
      NPR=NPTS-1
      DO1M=2,NPR
    1 T(J)=T(J)+Y(M)
      T(J)=(T(J)+0.5*(Y(1)+Y(NPTS)))*DELTA
      RETURN
    5 IF(NPTS.EQ.2)GOTO10
      T(1)=Y(1)
      RETURN
   10 T(J)=.5*(Y(1)+Y(2))*DELTA
      RETURN
      END
```

AVGTEMP - The Computer Program for the Average Fuel Temperature Calculations

This program calculates the average temperature of the fuel in the core at a particular power and the value of the thermal conductance (Eq. (5)) corresponding to that power and temperature. Comment cards present in the program aid in understanding the logic. The variables are defined in the Fortran listing and in the input data given below.

Input Data

Card 1: FORMAT (4I3, F8.0, 2F10.0)

NFLUX - number of vertical temperatures per element.

NHR - number of rings.

NTLO - lowest vertical position of measured centerline temperature.

NTHI - highest vertical position of measured centerline temperature.

ELMTS - number of fuel elements in core.

TO - reactor tank water temperature.

VTO - variance of reactor tank water temperature.

Card 2: FORMAT (5E15.8)

RING(J) - number of elements per ring.

Card 3: FORMAT (5E15.8)

POWER - power in kilowatts (punched output of CLTEMP).

Cards 4-8: FORMAT (5E15.8)

TEMP(I,J) - average radial temperatures (punched output of CLTEMP).

Cards 9-13: FORMAT (5E15.8)

TVAR(I,J) - variance of average radial temperatures (punched output of CLTEMP).

Cards 3 through 13 are repeated for each power data set.

The Fortran Listing for AVGTEMP

```
      DIMENSION TEMP(15,5),TVAR(15,5),TAVG(5),VARAT(5),RING(5)
C
C           NTLO=LOWEST VERTICAL POSITION OF TEMPERATURE MEASUREMENT
C           NTHI=HIGHEST VERTICAL POSITION OF TEMPERATURE MEASUREMENT
C
      READ(1,1000)NFLUX,NHR,NTLO,NTHI,ELMTS,TO,VTO
 1000 FORMAT(4I3,F8.0,2F10.0)
      T1=1.0
      V1=0.0
 1001 FORMAT(5E15.8)
      READ(1,1001)(RING(J),J=1,NHR)
      WRITE(3,1008)
 1008 FORMAT(1H1,36X,30HTEMPERATURE DATA AND AVERAGING///)
C
C           POWER IN KILOWATTS
C
   39 READ(1,1001)POWER
      IF(POWER.EQ.0.0)CALL EXIT
C
C        TEMP(I,J)=AVERAGE RADIAL TEMP AT THE ITH LEVEL IN THE JTH ROD
C        TVAR(I,J)=THE VARIANCE OF TEMP(I,J)
C        J=1,2,3,4,5 CORRESPOND TO THE B,C,D,E,F RINGS RESPECTIVELY
C        I=1 IS THE LOWEST VERTICAL LEVEL
C
      DO2J=1,5
    2 READ(1,1001)(TEMP(I,J),I=1,15)
      DO 4 I=NTLO,NTHI
    4 WRITE(3,1009)(TEMP(I,J),J=1,NHR)
 1009 FORMAT(1H ,4HDATA,6X,6(E15.8,2X))
      DO9J=1,5
    9 READ(1,1001)(TVAR(I,J),I=1,15)
      DO 99 I=NTLO,NTHI
   99 WRITE(3,1015)(TVAR(I,J),J=1,NHR)
 1015 FORMAT(1H ,8HVARIANCE,2X,6(E15.8,2X))
C
C        TAVG(J)=AVERAGE TEMPERATURE OF THE JTH FUEL ELEMENT
C        VARAT(J)=THE VARIANCE OF TAVG(J)
C
      DO 31 J=1,NHR
      SUM=0.0
      VUM=0.0
      DO 30 I=NTLO,NTHI
      VUM=VUM+TVAR(I,J)
   30 SUM=SUM+TEMP(I,J)
      VARAT(J)=VUM/(FLOAT(NFLUX)**2)
   31 TAVG(J)=SUM/(FLOAT(NFLUX))
      WRITE(3,1010)(TAVG(J),J=1,NHR)
 1010 FORMAT(1H0,16HAVG TEMP PER ROD,5X,6(E15.8,2X))
      WRITE(3,1016)(VARAT(J),J=1,NHR)
 1016 FORMAT(1H ,8HVARIANCE,13X,6(E15.8,2X))
```

```
C
C            AVERAGE FUEL TEMPERATURE OF THE CORE
C
      SUM=0.0
      TUM=0.0
      DO 50 J=1,5
      TUM=TUM+VARAT(J)*(RING(J)**2)
   50 SUM=SUM+TAVG(J)*RING(J)
      TBAR=SUM/ELMTS
      VBAR=TUM/(ELMTS**2)
      TRP=POWER/(TBAR-TO)
      VPOW=(.03*POWER)**2
      VTRP=VPOW/((TBAR-TO)**2)+POWER**2*(VBAR+VTO)/((TBAR-TO)**4)
      WRITE(3,1011)POWER ,TBAR,VBAR,TRP,VTRP
 1011 FORMAT(1HO,6HPOWER=,F10.3,5X,18HAVERAGE FUEL TEMP=,E15.8,5X,9HVARI
     1ANCE=,E15.8,5X,4HTRP=,E15.8,5X,4HVAR=,E15.8///)
      WRITE(2,1101)TBAR,T1,VBAR,V1,TRP,VTRP
 1101 FORMAT(6E12.6)
      GO TO 39
      END
```

APPENDIX B

TRIGA Flow Parameters and Temperature Distribution

The following results were calculated and used in the determination of the centerline temperatures of a fuel-moderator element.

Figure B-1 presents the mass flow rates per ring as a function of reactor power. Two obvious conclusions can be made from the data: first, the mass flow rate is proportional to the power, and second, the flow rate is proportional to the number of fuel-moderator elements per ring. The B and F rings have the same number of elements but B has a greater flow rate because more power is generated in a B-ring element than in an F-ring element, and also the cooling holes in the lower grid plate (Fig. B-2) surround the B-ring but offer no inlet directly to the F-ring.

The average water temperature rise as a function of power is shown in Fig. B-2. The power is calculated from the equation

$$P = \dot{m}_T \, c_p \, \overline{\Delta T} \, ,$$

where $\dot{m}_T$ is the total core flow rate at some power P obtained from Fig. B-1, and is plotted vs. measured power in Fig. B-3.

The behavior of the calculated film coefficients (Eq. (14)) with the measured reactor power is presented in Fig. B-4. As might be expected, the film coefficient is proportional to power. The difference between the average cladding temperature and the average water temperature in the channel surrounding the fuel-moderator element, i.e., $\bar{T}_c - \bar{T}_w$, is shown in Fig. B-5 as a function of the measured power. The reactor power can be calculated from Figs. B-4 and B-5 and the equation

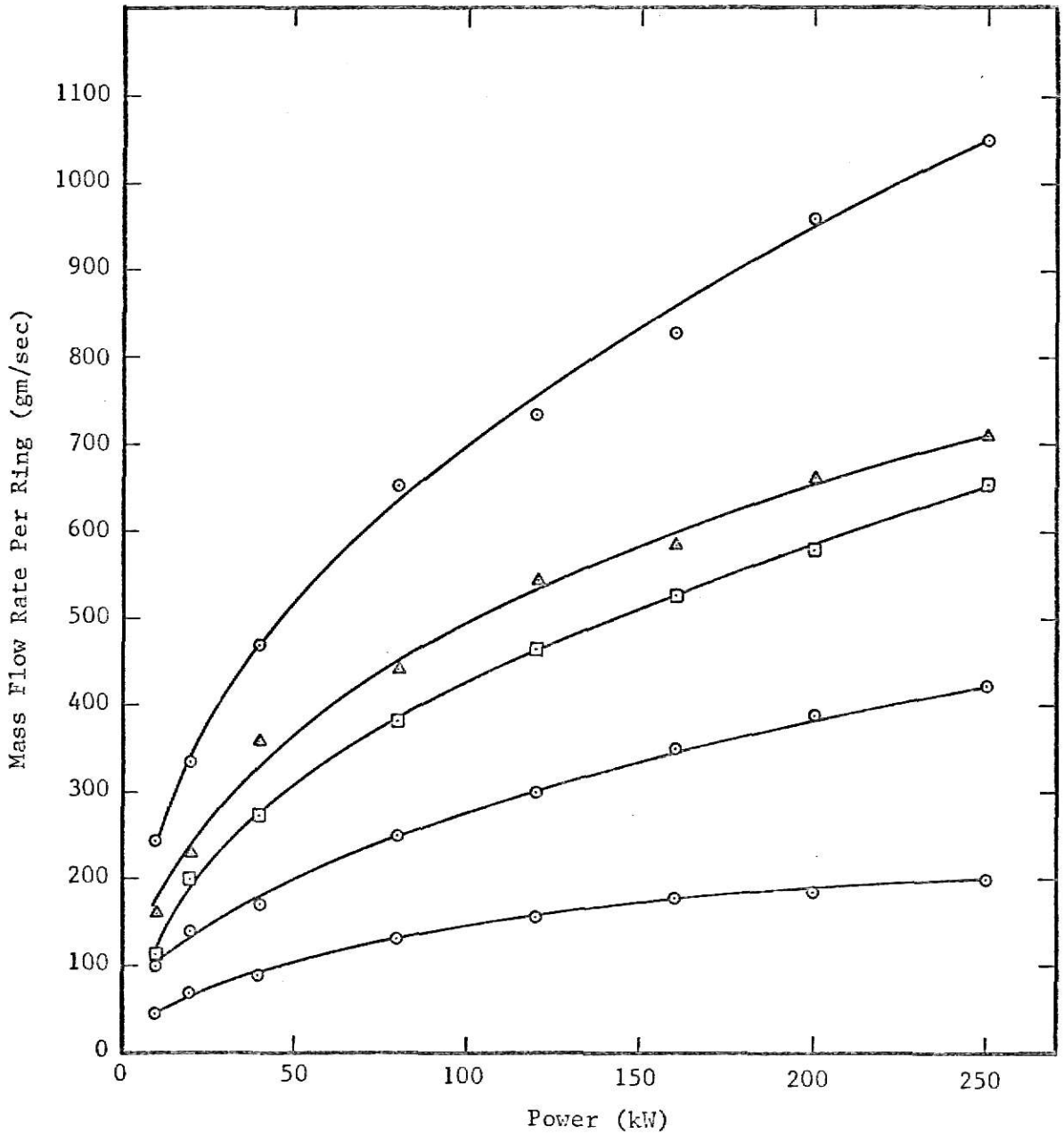

Figure B-1. Mass flow rate per ring as a function of reactor power.

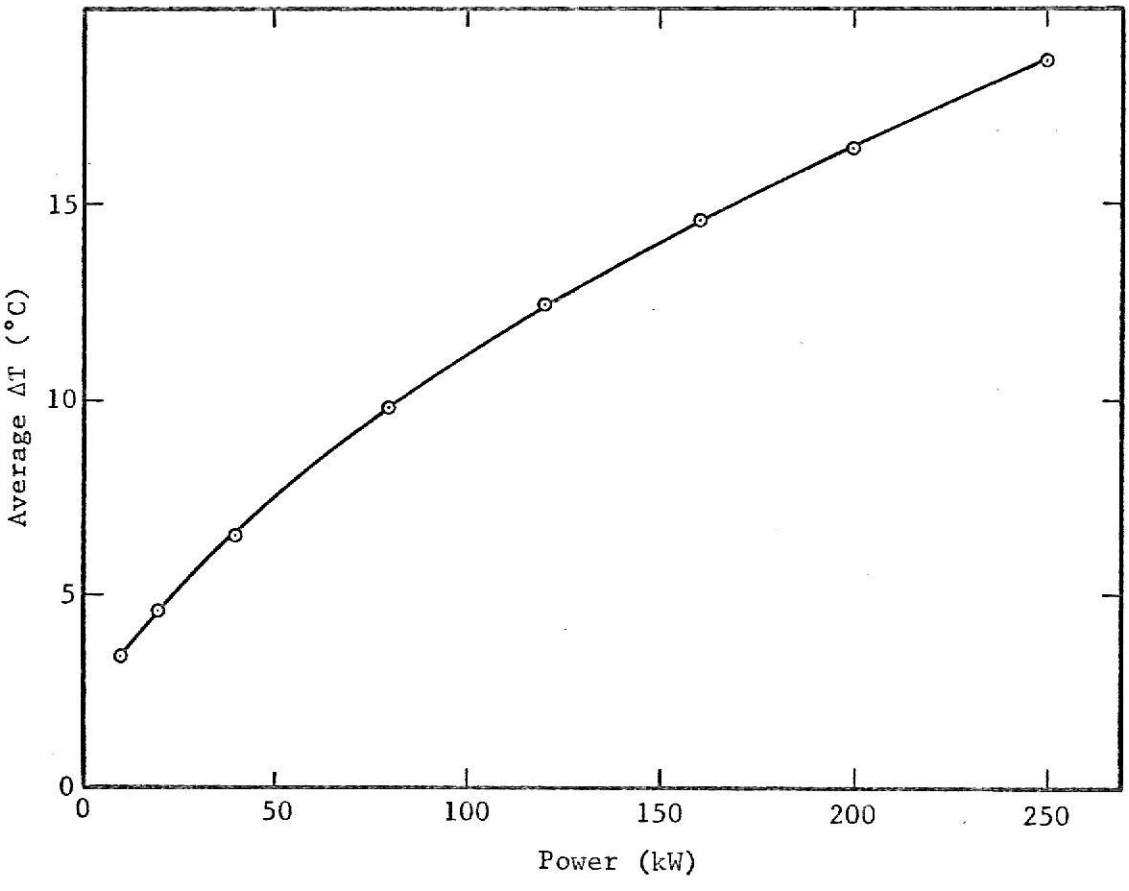

Figure B-2. Average water temperature rise as a function of reactor power.

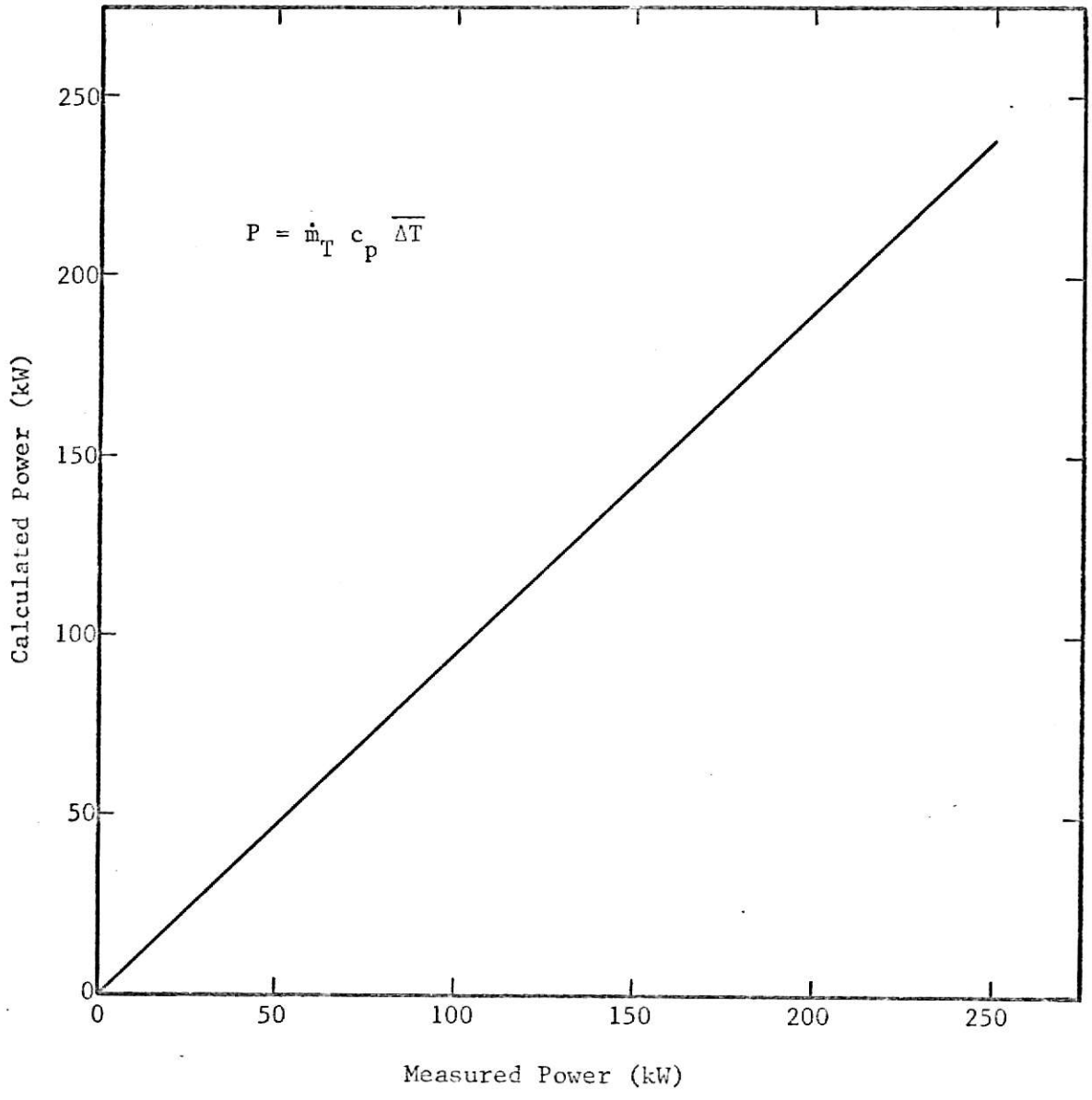

Figure B-3. Comparison of the calculated power with the measured power.

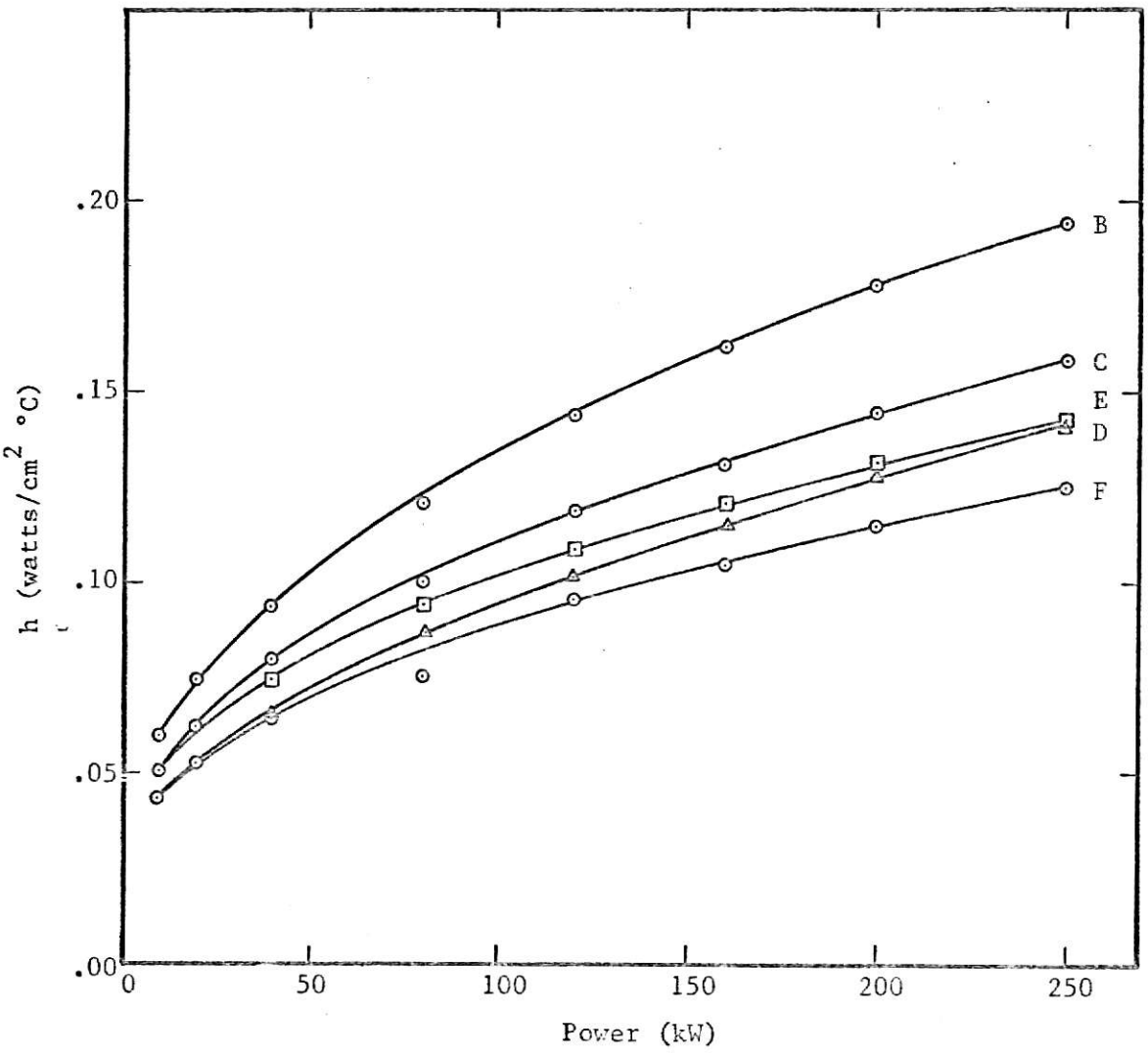

Figure B-4. Film coefficients as functions of reactor power.

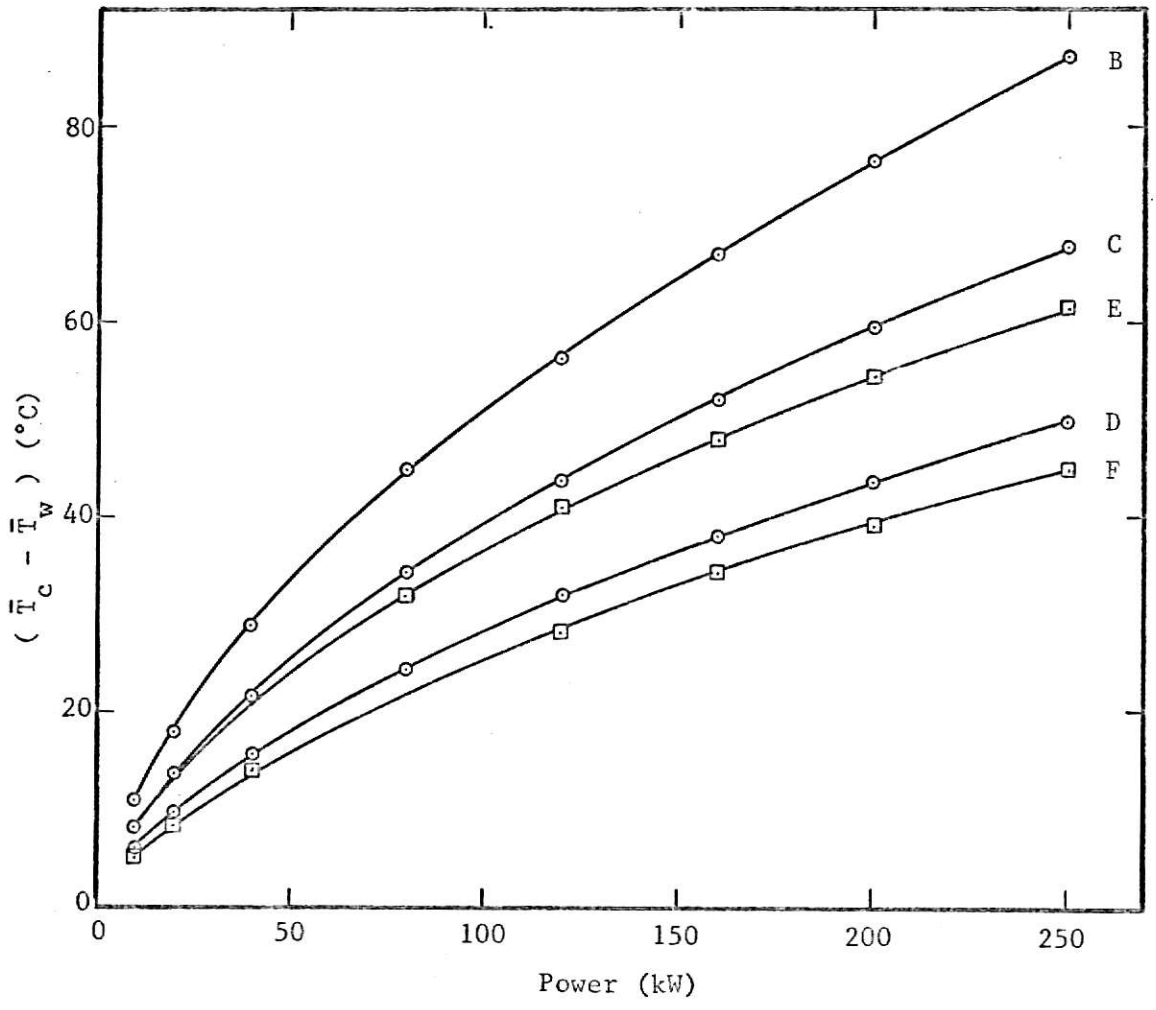

Figure E-5. Average cladding and average water temperature difference.

$$P = A_s \sum_{k=1}^{5} m_k h_k (\bar{T}_c - \bar{T}_w)_k ,$$

where A_s = outside surface area of the fueled length of the fuel-moderator element,

m_k = number of fuel elements per ring,

h_k = film coefficient of an element in the kth ring.

This calculated power is plotted vs. measured power in Fig. B-6.

The core radial temperature distribution is presented in Fig. B-7 with power as a parameter. Up to 200 kilowatts the gradient of the distribution is as expected, i.e., the maximum temperature is in the innermost ring. At 250 kilowatts, however, the maximum temperature shifts to the C-ring, but because of license restrictions, 250 kilowatts is the maximum steady state power level, so no further data could be taken to substantiate this trend.

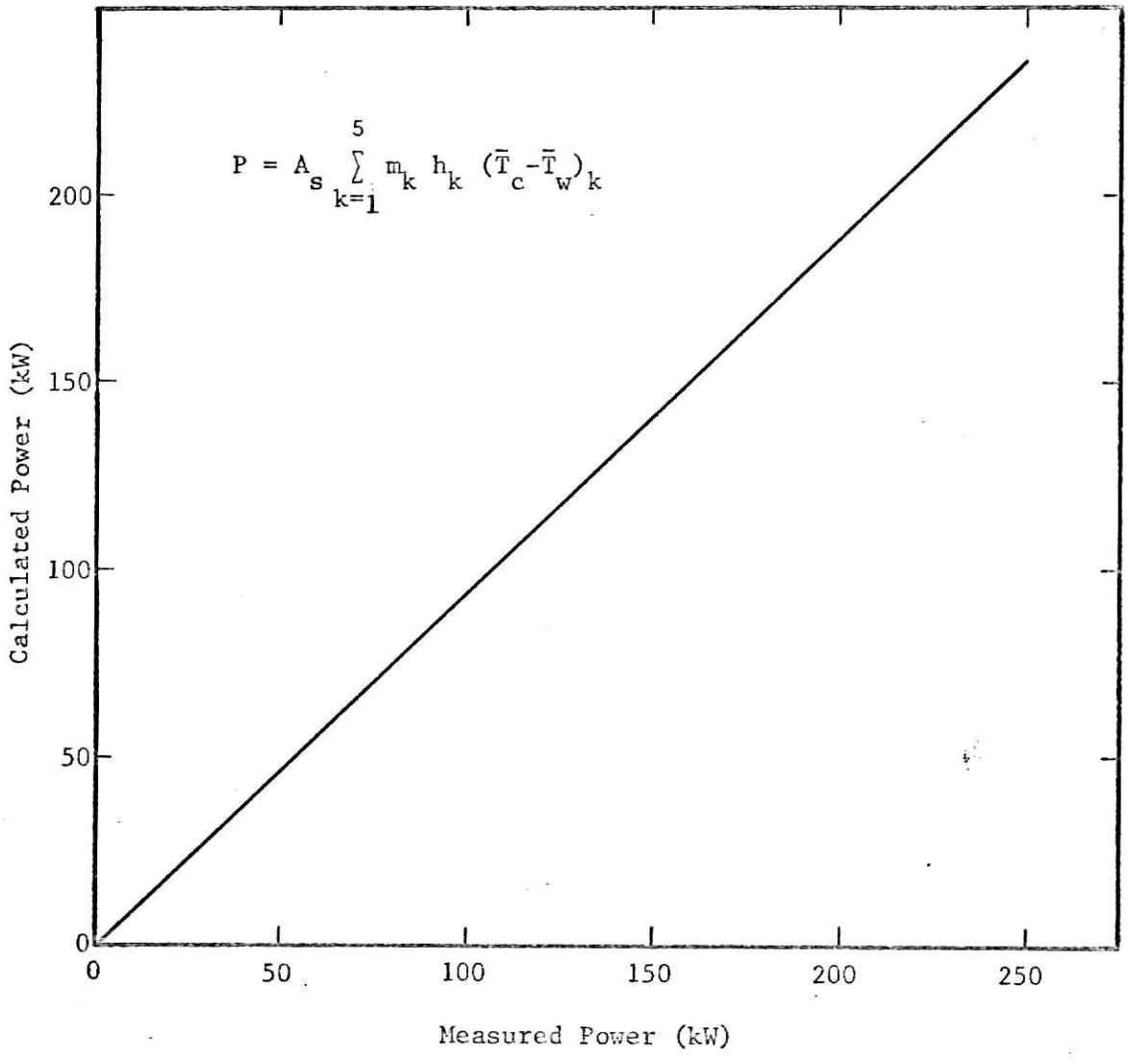

Figure B-6. Comparison of the calculated power with the measured power.

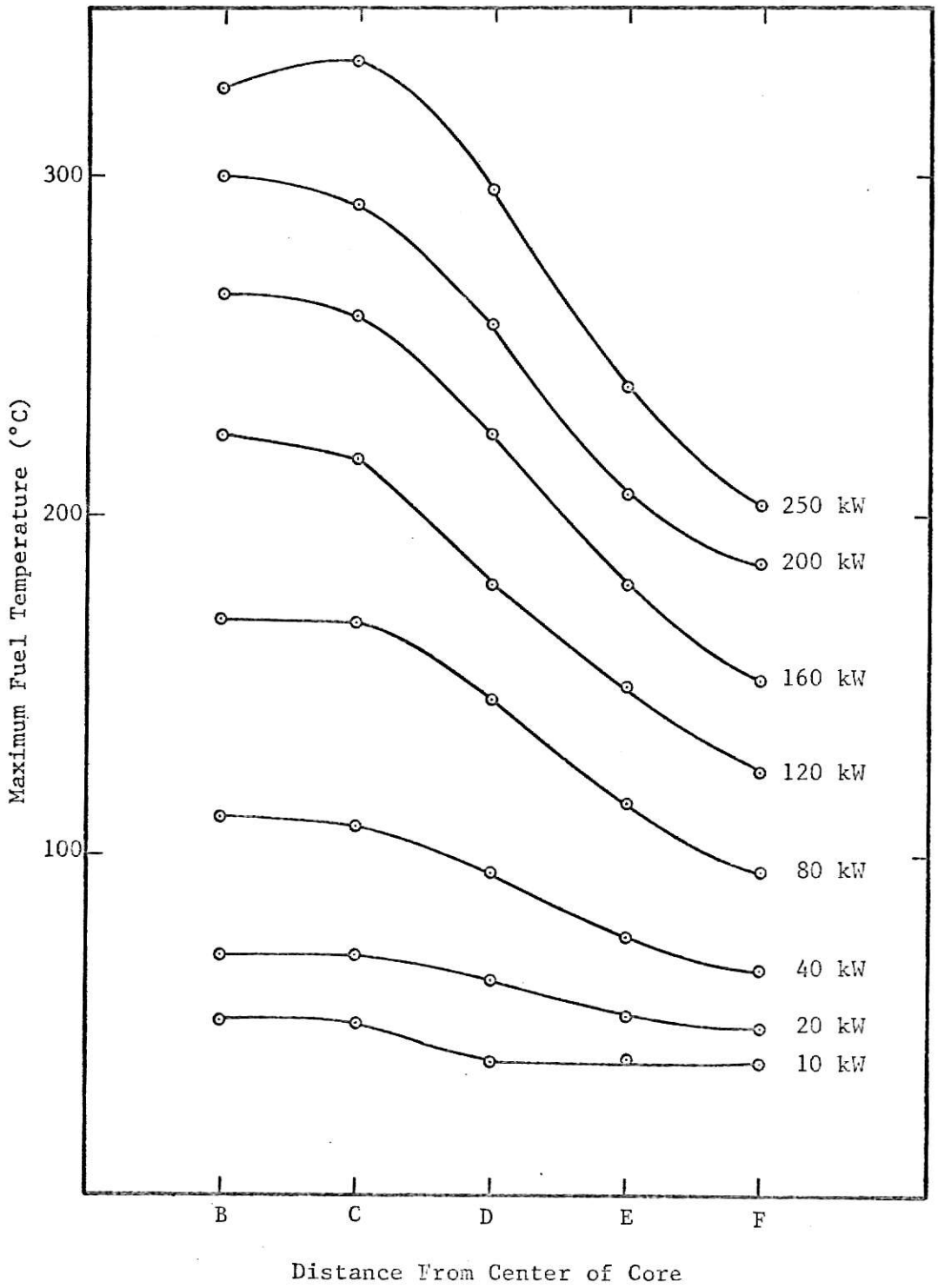

Figure B-7. Core radial temperature distribution.

APPENDIX C

Weighted Least Squares Analysis (18)

In order to fit the calculated values of the core thermal conductance as a function of temperature and yet propagate the errors, the following technique was used.

Gauss Markoff Theorem:

If the general linear hypothesis model of full rank, i.e., if

$$\underline{Y} = \underline{X}\,\underline{B} + \underline{e}$$

is such that the following two conditions on the error vector are met,

1. $E[e] = 0$,
2. $V[e] = \sigma^2 \underline{I}$,

the best minimum-variance linear unbiased estimate of $\underline{B}$ is given by least squares.

The above theorem states that minimum variance, unbiased estimators result from the least squares technique if the errors have a mathematical expectation of zero and have variances which are homoscedastic in form, i.e., the variance-covariance matrix of the errors is equal to a constant times an identity matrix (18).

Consider the parameters, K_i and T_i, where K_i is a core thermal conductance value corresponding to an average fuel temperature T_i. The data are to be fit to the equation

$$\underline{K} = \underline{T}\,\underline{B} + \underline{e} \qquad \text{(C.1)}$$

or

$$\begin{vmatrix} K_1 \\ K_2 \\ \cdot \\ \cdot \\ \cdot \\ K_n \end{vmatrix} = \begin{vmatrix} T_{11} & 1 \\ T_{21} & 1 \\ \cdot & \cdot \\ \cdot & \cdot \\ \cdot & \cdot \\ T_{n1} & 1 \end{vmatrix} \begin{vmatrix} B_1 \\ B_2 \end{vmatrix} + \begin{vmatrix} e_1 \\ e_2 \\ \cdot \\ \cdot \\ \cdot \\ e_n \end{vmatrix} .$$

Equation (C.1) has the statistical properties of $E[e] = 0$ and $V[e] = \sigma^2 \underline{V}$ where $\underline{V}$ is a (nxn) variance-covariance matrix, i.e., the diagonal elements are variances and the off-diagonal elements are covariances. It is necessary to transform the above heteroscedastic variances to the homoscedastic form.

Let

$$\underline{\tilde{S}}\ \underline{S} = \underline{S}^2 = \underline{V} ,$$

where $\underline{S}$ is a unique non-singular symmetric matrix.

Let

$$\underline{S}^{-1}\ \underline{e} = \underline{f} ,$$

where $E[\underline{f}] = 0$ and

$$\begin{aligned} V[\underline{f}] &= E[\underline{f}\ \underline{\tilde{f}}] = E[\underline{S}^{-1}\ \underline{e}\ \underline{\tilde{e}}\ \underline{S}^{-1}] \\ &= \underline{S}^{-1}\ E[\underline{e}\ \underline{\tilde{e}}]\underline{S}^{-1} \\ &= \underline{S}^{-1}\ \sigma^2\ \underline{V}\ \underline{S}^{-1} \\ &= \sigma^2\ \underline{S}^{-1}\ \underline{S}^2\ \underline{S}^{-1} \\ &= \sigma^2\ \underline{I} . \end{aligned}$$

Thus the transformation to the homoscedastic form of variances has been accomplished, the Gauss Markoff theorem has been satisfied, and minimum variance unbiased estimators for $\underline{B}$ will be obtained.

The following procedure is used to find the minimum variance unbiased estimator of $\underline{B}$. Premultiply Eq. (C.1) by S^{-1}, i.e.,

$$\underline{S}^{-1}\ \underline{K} = \underline{S}^{-1}\ \underline{T}\ \underline{B} + \underline{S}^{-1}\ \underline{e} . \qquad \text{(C.2)}$$

Apply normal least squares, in particular,

$$\underline{S}^{-1}\ \underline{T}\ \underline{B} = \underline{S}^{-1}\ \underline{K}$$

$$\tilde{\underline{T}}\ \underline{S}^{-1}\ \underline{S}^{-1}\ \underline{T}\ \underline{B} = \tilde{\underline{T}}\ \underline{S}^{-1}\ \underline{S}^{-1}\ \underline{K}\ ,$$

$$\underline{B} = \underline{D}\ \tilde{\underline{T}}\ \underline{V}^{-1}\ \underline{K}\ , \tag{C.3}$$

where

$$\underline{D} = (\tilde{\underline{T}}\ \underline{V}^{-1}\ \underline{T})^{-1}\ . \tag{C.4}$$

For convenience define a weighting matrix $\underline{W}$ as

$$\underline{W} = \underline{V}^{-1}\ ,$$

thus

$$\underline{b} = \underline{D}\ \tilde{\underline{T}}\ \underline{W}\ \underline{K} \tag{C.5}$$

where the vector $\underline{b}$ is the minimum variance unbiased estimator of $\underline{B}$. The ith element of $\underline{b}$ is

$$b_i = \sum_{j=1}^{2} D_{ij} \sum_{\ell=1}^{n} T_{\ell j} \sum_{k=1}^{n} W_{\ell k}\ K_k\ . \tag{C.6}$$

Assume the covariances are zero, i.e., the errors are statistically independent, thus all $W_{\ell k} = 0$ and all $W_{kk} \neq 0$, then

$$b_i = \sum_{j=1}^{2} D_{ij} \sum_{k=1}^{n} T_{kj}\ W_{kk}\ K_k\ ,$$

or

$$b_i = \sum_{k=1}^{n} W_{kk}\ K_k\ U_{ik}\ , \tag{C.7}$$

where for convenience,

$$U_{ik} = \sum_{j=1}^{2} D_{ij}\ T_{kj}\ . \tag{C.8}$$

The variance of b_i is

$$\sigma^2(b_i) = \sum_{k=1}^{n} \left[(W_{kk}\, U_{ik})^2\, \sigma^2\,(K_k) + \sum_{j=1}^{2} (W_{kk}\, K_k\, D_{ij})^2\, \sigma^2\,(T_{kj}) \right] .$$

Consider the first term,

$$\sum_{k=1}^{n} W_{kk}\, U_{ik}^2 = \sum_{k=1}^{n} W_{kk}\, U_{ik}\, [D_{i1}\, T_{k1} + D_{i2}\, T_{k2}]$$

$$= D_{i1} \sum_{k=1}^{n} W_{kk}\, U_{ik}\, T_{k1} + D_{i2} \sum_{k=1}^{n} W_{kk}\, U_{ik}\, T_{k2} .$$

In general

$$D_{i\ell} \sum_{k=1}^{n} W_{kk}\, U_{ik}\, T_{k\ell} = D_{i\ell} \sum_{k=1}^{n} W_{kk}\, T_{k\ell}\, [D_{i1}\, T_{k1} + D_{i2}\, T_{k2}]$$

$$= D_{i\ell} \left[D_{i1} \sum_{k=1}^{n} T_{k1}\, W_{kk}\, T_{k\ell} + D_{i2} \sum_{k=1}^{n} T_{k2}\, W_{kk}\, T_{k\ell} \right] .$$

If $\ell = i$, then

$$D_{ii} \sum_{k=1}^{n} W_{kk}\, U_{ik}\, T_{ki} = D_{ii} \left[D_{i1} \sum_{k=1}^{n} T_{k1}\, W_{kk}\, T_{ki} + D_{i2} \sum_{k=1}^{n} T_{k2}\, W_{kk}\, T_{ki} \right]. \quad (C.9)$$

From Eq. (C.4)

$$\underline{D}(\tilde{\underline{T}}\, \underline{W}\, \underline{T}) = \underline{I} \quad (C.10)$$

or

$$\begin{vmatrix} D_{11} & D_{12} \\ D_{21} & D_{22} \end{vmatrix} \begin{vmatrix} T_{11} & T_{21} & \cdots & T_{n1} \\ 1 & 1 & \cdots & 1 \end{vmatrix} \begin{vmatrix} W_{11} & & & \\ & W_{22} & & \\ & & \ddots & \\ & & & W_{nn} \end{vmatrix} \begin{vmatrix} T_{11} & 1 \\ T_{21} & 1 \\ \vdots & \vdots \\ T_{n1} & 1 \end{vmatrix} = \begin{vmatrix} 1 & 0 \\ 0 & 1 \end{vmatrix}$$

or

$$\begin{vmatrix} D_{11}(T_{11}W_{11}T_{11} + \ldots + T_{n1}W_{nn}T_{n1}) + D_{12}(W_{11}T_{11} + \ldots + W_{nn}T_{n1}) & D_{11}(T_{11}W_{11} + \ldots + T_{n1}W_{nn}) + D_{12}(W_{11} + \ldots + W_{nn}) \\ D_{21}(T_{11}W_{11}T_{11} + \ldots + T_{n1}W_{nn}T_{n1}) + D_{22}(W_{11}T_{11} + \ldots + W_{nn}T_{n1}) & D_{21}(T_{11}W_{11} + \ldots + T_{n1}W_{nn}) + D_{22}(W_{11} + \ldots + W_{nn}) \end{vmatrix} = \begin{vmatrix} 1 & 0 \\ 0 & 1 \end{vmatrix}$$

In general then for row 1 multiplication,

$$D_{11} \sum_{k=1}^{n} T_{k1} W_{kk} T_{k1} + D_{12} \sum_{k=1}^{n} W_{kk} T_{k1} = 1, \tag{C.11}$$

$$D_{11} \sum_{k=1}^{n} T_{k1} W_{kk} + D_{12} \sum_{k=1}^{n} W_{kk} = 0 \tag{C.12}$$

Comparison of Eqs. (C.9), (C.11), and (C.12), shows that the term in the brackets of Eq.(C.9) is unity because $T_{k2} = 1$. For row 2 multiplication,

$$D_{21} \sum_{k=1}^{n} T_{k1} W_{kk} T_{k1} + D_{22} \sum_{k=1}^{n} W_{kk} T_{k1} = 0, \tag{C.13}$$

$$D_{21} \sum_{k=1}^{n} T_{k1} W_{kk} + D_{22} \sum_{k=1}^{n} W_{kk} = 1. \tag{C.14}$$

Comparison of Eqs. (C.9), (C.13), and (C.14) shows again that the bracket is unity. Also, for both cases, if $\ell \neq i$, the bracket is zero. Thus the variance of the estimator b_i is

$$\sigma^2(b_i) = \sum_{k=1}^{n} D_{ii} W_{kk} \sigma^2(K_k) + \sum_{j=1}^{2} (W_{kk} K_k D_{ij})^2 \sigma^2 (T_{kj}) . \tag{C.15}$$

To generate the weighting matrix $\underline{W} = \underline{V}^{-1}$, an estimate of the variance matrix $\underline{e}$ is made. From Eq. (C.1),

$$\sigma^2(e_i) = \sigma^2(K_i) + \sum_{j=1}^{2} [B_j^2\ \sigma^2(T_{ij}) + T_{ij}^2\ \sigma^2(B_j)] \qquad (C.16)$$

which follows from the standard propagation of errors technique (21). Thus the above equation and Eqs. (C.4), (C.7), and (C.15) will be used in the following iterative scheme to determine the estimators b_i.

1. Neglect the 2nd terms of Eq. (C.16) and calculate $\sigma_1^2(e_i)$.
2. Calculate $\underline{D}$ from Eq. (C.4) using $\underline{W} = \underline{V}^{-1} = 1/\underline{\sigma_1^2(e)}$.
3. Calculate the estimator vector $\underline{b}$ from Eq. (C.7).
4. Calculate $\sigma^2(b_i)$ from Eq. (C.15).
5. Calculate $\sigma_2^2(e_i)$ from Eq. (C.16) using $\underline{B} = \underline{b}$.
6. Repeat steps 2, 3, 4, and 5 until the difference between the (n-1)st and the nth estimate of the vector $\underline{b}$ is less than or equal to 1%.

The analysis is similar for the reactivity temperature coefficient. The curves of average fuel temperature and reactivity loss as functions of power level (Figs. 9 and 11), provide a parametric relation between reactivity loss and average fuel temperature. If the fuel temperature is corrected for the average water temperature increase across the core as described in Section 4.3.3, the equation takes the form

$$\Delta\rho_i = \alpha_1\ T_i + \alpha_2$$

where $\Delta\rho_i$ is the ith reactivity loss corresponding to T_i, the ith average fuel temperature corrected for the water temperature increase across the core. The reactivity temperature coefficient is α_1 and α_2 is the intercept which is negligibly small.

LINFIT - The Computer Code for the Weighted Least Squares Analysis

This code was used to fit the data of core thermal conductance vs. average fuel temperature (Fig. 10) and the data of reactivity loss vs. average fuel temperature rise (Fig. 12) as described above. Comment cards in the program will aid in understanding the logic. The variables are defined in the Fortran listing and in the input data given below.

Input Data

Card 1: FORMAT (I3,F10.0)

NDATA - number of data points

EPSLN - fractional error to terminate iteration.

Card 2: FORMAT (6E12.6)

X(I,J) - independent variable.

XVAR(I,J) - variance of independent variable

Y(I) - dependent variable.

YVAR(I) - variance of dependent variable.

The card 2 input is repeated for each data point. This input is provided by punched output on cards from AVGTEMP.

The Fortran Listing for LINFIT .

```
      DIMENSION X(50,2),Y(50),YVAR(50),XVAR(50,2),W(50,50),C(2,2),BVAR(2
     1),B(2)
C
C********** X IS THE INDEPENDENT VARIABLE
C********** XVAR IS THE VARIANCE OF THE INDEPENDENT VARIABLE
C**********  Y IS THE DEPENDENT VARIABLE
C**********  YVAR IS THE VARIANCE OF THE DEPENDENT VARIABLE
C********** NDATA IS THE NUMBER OF DATA POINTS
C********** EPSLN IS THE FRACTIONAL TERMINATION ERROR
C
  100 READ(1,1000)NDATA,EPSLN
      IF(NDATA.EQ.0)CALLEXIT
 1000 FORMAT(I3,F10.0)
      DO 1 I=1,NDATA
    1 READ(1,1001)(X(I,J),J=1,2),(XVAR(I,J),J=1,2),Y(I),YVAR(I)
 1001 FORMAT(6E12.6)
 1101 FORMAT(1H ,2(E15.8,5X))
      WRITE(3,1002)
 1002 FORMAT(1H1,17X,6HX-DATA,32X,10HX-VARIANCE,22X,6HY-DATA,12X,10HY-VA
     1RIANCE//)
      DO 2 I=1,NDATA
    2 WRITE(3,1003)(X(I,J),J=1,2),(XVAR(I,J),J=1,2),Y(I),YVAR(I)
 1003 FORMAT(/6(E15.8,5X))
      MF=0
      WRITE(3,1004)
 1004 FORMAT(1HL,8X,5HSLOPE,13X,8HVARIANCE,10X,9HINTERCEPT,12X,8HVARIANC
     1E,8X,16HFRAC SLOPE ERROR,2X,20HFRAC INTERCEPT ERROR//)
C
C********** FORM THE WEIGHTING MATRIX, W(I,J)
C
      DO 19 I=1,NDATA
   19 W(I,I)=1./YVAR(I)
      GO TO 39
   20 CONTINUE
      DO 38 I=1,NDATA
      SUM=0.0
      DO 35 J=1,2
   35 SUM=SUM+XVAR(I,J)*B(J)**2+BVAR(J)*X(I,J)**2
   38 W(I,I)=1./(YVAR(I)+SUM)
   39 L=1
      M=1
C
C********** FORM THE D MATRIX DESIGNATED AS C(I,J)
C
      DO 49 I=1,2
      DO 49 J=1,2
      C(I,J)=0.0
      DO 49 K=1,NDATA
   49 C(I,J)=C(I,J)+X(K,I)*W(K,K)*X(K,J)
```

```
C
C********** INVERT THE C MATRIX
C
      D=C(1,1)*C(2,2)-C(1,2)*C(2,1)
      TERM=C(1,1)
      C(1,1)=C(2,2)/D
      C(1,2)=-C(1,2)/D
      C(2,1)=-C(2,1)/D
      C(2,2)=TERM/D
C
C********** CALCULATE THE ESTIMATORS,B(J)
C
      DO 58 I=1,2
      B(I)=0.0
      DO 58 J=1,2
      SUM=0.0
      DO 57 K=1,NDATA
   57 SUM=SUM+X(K,J)*W(K,K)*Y(K)
   58 B(I)=B(I)+C(I,J)*SUM
C
C********** CALCULATE THE ERROR OF THE LINEAR FIT
C
      DO 69 I=1,2
      SUM=0.0
      DO68K=1,NDATA
      DO 68 J=1,2
   68 SUM=SUM+XVAR(K,J)*(W(K,K)*Y(K)*C(I,J))**2
   69 BVAR(I)=SUM+C(I,I)
      WRITE(3,1005)(B(I),BVAR(I),I=1,2)
 1005 FORMAT(/4(E15.8,5X))
      IF(MF.GT.0)GO TO70
      SLOPE=B(1)
      CEPT=B(2)
      MF=1
      GO TO 20
C
C********** TERMINATION CRITERION
C
   70 SERROR=(B(1)-SLOPE)/SLOPE
      CERROR=(B(2)-CEPT)/CEPT
      IF(ABS(SERROR).LE.EPSLN) L=0
      IF(ABS(CERROR).LE.EPSLN) M=0
      WRITE(3,1006)SERROR,CERROR
 1006 FORMAT(1H+,80X,2(E15.8,5X))
      LM=L+M
      IF(LM.EQ.0)GOTO100
      SLOPE=B(1)
      CEPT=B(2)
      GO TO 20
      END
```

APPENDIX D

Solution of the Transient Equations by Analytic Continuation

The procedure for the solution of the transient equations (Eqs. (1), (2), (4), (5)) by analytic continuation is a specialization to functions of a real variable of a method known as continuous analytic continuation (19). In this method the dependent variables are expanded in Taylor series over time intervals in which they are analytic.

In general, denoting the dependent variable at time t_j as $y_i(t_j)$, then

$$y_i(t_{j+1}) \cong \sum_{k=0}^{K} y_i^{(k)}(t_j)(t_{j+1}-t_j)^k/k! \tag{D.1}$$

where the superscript k denotes the order of the derivative and K the order of the expansion.

In the exact expansion of Eq. (D.1), there is a remainder after the (K+1)st term. In particular

$$R_i(t_{j+1}) = y_i^{(K+1)}(\eta)(t_{j+1}-t_j)^{K+1}/(K+1)! \tag{D.2}$$

where $t_j \leq \eta \leq t_{j+1}$

and $$y_i^{(K+1)}(\eta) = [y_i^{(K)}(t_{j+1}) - y_i^{(K)}(t_j)]/(t_{j+1}-t_j) \ . \tag{D.3}$$

Note that the time step, $t_{j+1}-t_j$, is present in Eq. (D.2). This time step can be obtained by requiring the fractional truncation error for each expansion to be equal to or less than a specified truncation error criterion ε, i.e.,

$$\left| \frac{R_i(t_{j+1})}{y_i(t_{j+1})} \right| \leq \varepsilon \tag{D.4}$$

Substituting Eq. (D.2) into Eq. (D.4) leads to

$$(t_{j+1}-t_j)_i = \left[\frac{(K+1)!\ \varepsilon\ |y_i(t_{j+1})|}{|y_i^{(K+1)}(\eta)|} \right]^{(K+1)^{-1}} \tag{D.5}$$

which is the largest time step for the y_i dependent variable. For a fixed K and ε, the time step is proportional to the ratio

$$|y_i(t_{j+1})|/|y_i^{(K+1)}(\eta)| \ .$$

Thus the time step automatically expands or contracts, depending on the behavior of the function, in order to maintain a constant fractional truncation error (19).

A common time step must be used for all the transient equation variables that are expanded in Taylor series, and necessarily it must be computed from the variable which yields the smallest time step. If this variable is designated y_m, then the common time step is

$$t_{j+1} - t_j = \left[\frac{(K+1)!\ \varepsilon\ |y_m(t_{j+1})|}{|y_m^{(K+1)}(\eta)|} \right]^{(K+1)^{-1}} \tag{D.6}$$

Because of the presence of the time step in $y_m(t_{j+1})$ and $y_m^{(K+1)}(\eta)$, an iterative procedure is used as follows:

1) A tentative time step is computed from

$$(t_{j+1}-t_j)_t = \left[\frac{(K+1)!\ \varepsilon\ |y_m(t_j)|}{|y_m^{(K+1)}(t_j)|} \right]^{(K+1)^{-1}} \tag{D.7}$$

2) Then values of $y_m(t_{j+1})$ and its derivatives are calculated using the tentative time step.

3) A new time step is calculated from Eq. (D.6) using $y_m^{(K+1)}(\eta)$ calculated from Eq. (D.3).

4) If the new time step is larger than its tentative time step (which means that the tentative time step gives a smaller truncation error than required or smaller by a prescribed factor), the calculations proceed to the next time step. If the improved time step is smaller, then it becomes the tentative time step and 2, 3, and 4 are repeated.

Steps 1 through 4 are repeated for each variable and the smallest time step is used. Note that to use Eq. (D.6) only values of

$$y_m(t_j),\ y_m'(t_j),\ \ldots,\ y_m^{(K+1)}(t_j)$$

must be known to extend the solution to time t_{j+1}.

In the neighborhood of times τ_1, τ_2, and τ_3, Eq. (4) can no longer be expanded in a Taylor series because of the discontinuities introduced by the step functions. Thus it is necessary to require that the time step be such that the solution is not attempted at times which fall within some finite time interval around these discontinuities.

The Computer Program for the Transient Calculations

The program consists of the main program and three subroutines. Subroutine DERIV calculates the derivatives of the dependent variables, subroutine TIME calculates the time step, subroutine FACT calculates factorials, and the main program calculates the dependent variables besides providing for input and output. The program can be easily followed from the flow sheet presented in Fig. D-1. The variables

used in the program are defined in the Fortran listing and the input data given below.

Input Data

Card 1: FORMAT (6I3)

JMAX - number of time steps the program is to calculate before termination.

Card 2: FORMAT (6E13.6)

DECAY(I) - precursors decay constant, maximum of six.

Card 3: FORMAT (6E13.6)

B(I) - delayed fractions of precursors, maximum of six.

Card 4: FORMAT (8F10.0)

D(1,1) - neutron density at time zero.

TEMP(1,1) - average fuel temperature at time zero.

R(1,1) - reactivity insertion at time zero.

T(10,1) - time zero.

ERROR - truncation error, see Vigil (19,20).

H - conversion factor from neutron density to power in watts.

CONE - slope of average fuel heat capacity.

CTWO - intercept of average fuel heat capacity.

Card 5: FORMAT (8F10.0)

BETA - effective delayed neutron fraction.

PLIFE - prompt neutron lifetime.

A - ramp reactivity insertion rate (rod going up).

ALFA - constant reactivity temperature coefficient.

OUT - the time the pulse rod reaches its uppermost position.

RONE - slope of core unit conductance.

RTWO - intercept of core unit conductance.

G - ramp reactivity insertion rate (rod going down).

Card 6: FORMAT (8F10.0)

DROP - the time the pulse rod leaves its uppermost position.

DOWN - the time the pulse rod reaches its lowest position.

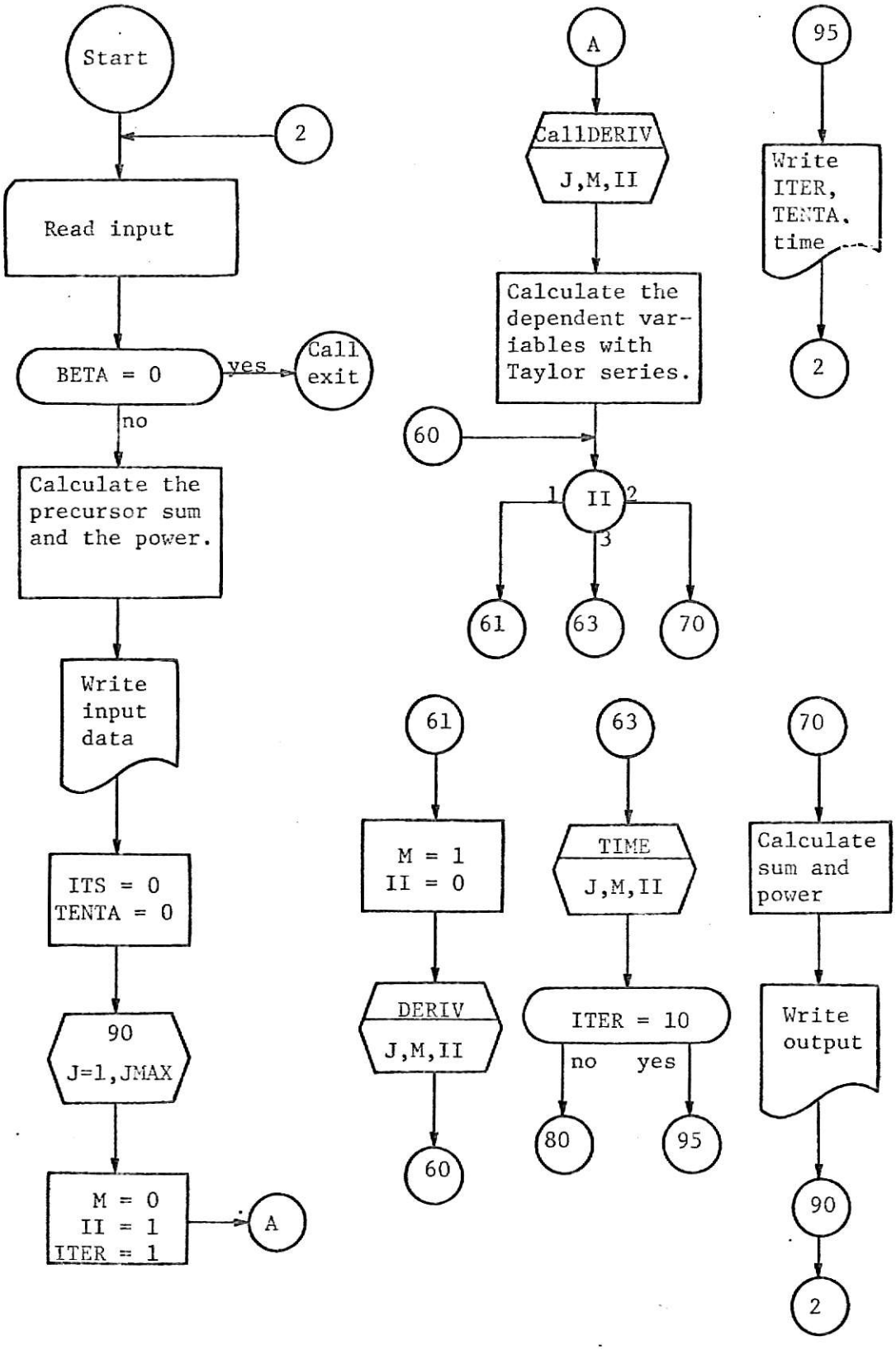

Figure D-1. Flow sheet.

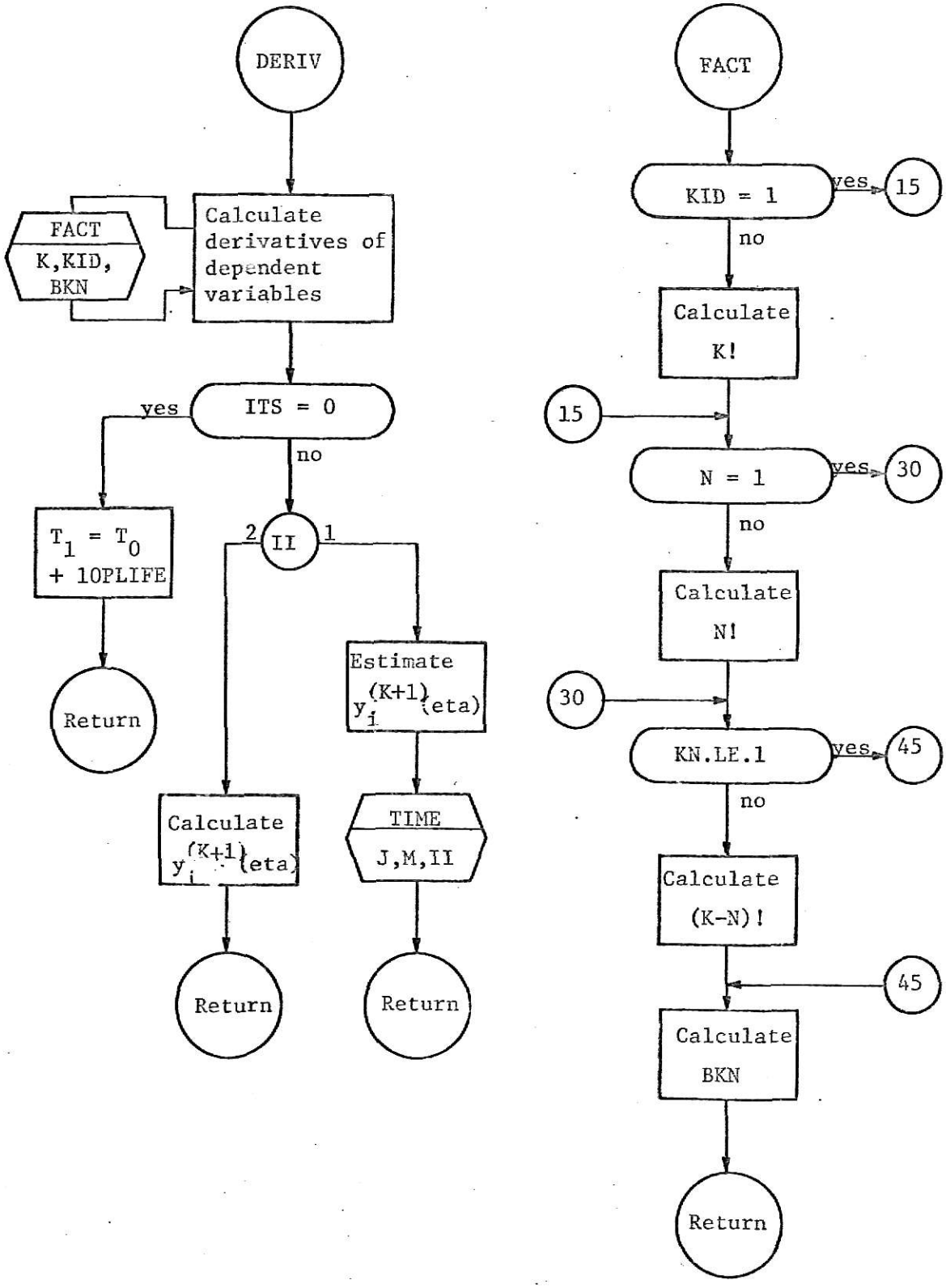

Figure D-1. (continued)

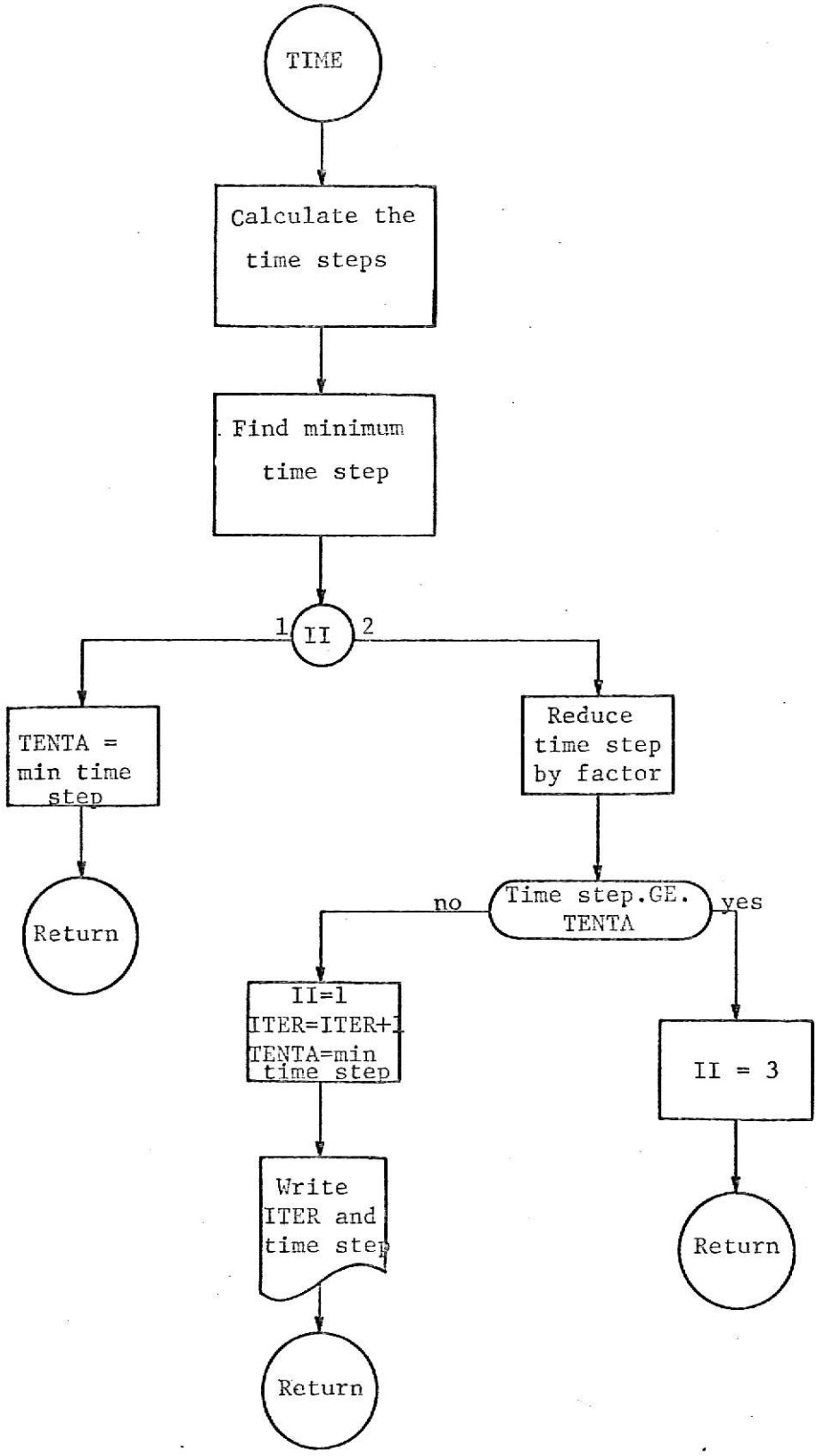

Figure D-1. (continued)

The Fortran Listing for the Transient Calculations

```
      DIMENSION D(6,500),C(6,6,500),TEMP(6,500),R(6,500),T(10,500),CETA(
     16),DECAY(6),B(6)
      COMMON D,C,TEMP,R,T,DETA,CETA,TMPETA,RETA,ERROR,ITER,STEP,DECAY,BE
     1TA,PLIFE,B,A,ALFA,OUT,ITS,TENTA,H,CONE,CTWO,RONE,RTWO,DROP,DOWN,G
 1000 FORMAT(8F10.0)
 1001 FORMAT(6I3)
 1002 FORMAT(1H1)
 1003 FORMAT(1H1,2X,9HTIME(SEC),10X,12HNEUT DENSITY,4X,17HPRECURSOR DENS
     1ITY,5X,12HFUEL TEMP(C),5X,18HREACTIVITY(DELTAK),6X,12HPOWER(WATTS)
     2)
 1004 FORMAT(6(E15.8,5X))
 1005 FORMAT(6E13.6)
 1010 FORMAT(10X,63H***** TEN ITERATIONS FOR TENTATIVE TIME STEP HAVE BE
     1EN EXECUTED )
 1020 FORMAT(1H1,15HBETA EFFECTIVE=,F7.4,12H   GEN TIME=,F9.6,3HSEC,8H
     1 RAMP=,F9.6,13H   TEMP COEF=,F9.6,19H   RAMP STOPPED AT=,F9.6)
 1030 FORMAT(5X,5HGROUP,I3,18H   DECAY CONSTANT=,F8.4,20H   DELAYED FRAC
     1TION=,F8.5)
C
C         D IS NEUTRON DENSITY
C         C IS PRECURSOR DENSITY
C         TEMP IS THE AVERAGE FUEL TEMPERATURE
C         R IS THE REACTIVITY
C         T IS THE TIME
C         ERROR IS THE FRACTIONAL TRUNCATION ERROR OF THE TAYLOR SERIES
C         BETA IS THE EFFECTIVE DELAYED NEUTRON FRACTION
C         PLIFE IS THE NEUTRON GENERATION TIME
C         A IS THE RAMP INSERTION RATE
C         ALFA IS THE PROMPT TEMPERATURE COEFFICIENT
C         OUT IS THE TIME OF THE COMPLETION OF THE RAMP
C         DECAY(I) IS THE DECAY CONSTANT OF THE ITH PRECURSOR
C         B(I) IS THE DELAYED FRACTION OF THE ITH PRECURSOR
C         H IS THE CONVERSION FACTOR FROM NEUTRON DENSITY TO WATTS
C         CONE IS THE SLOPE OF THE HEAT CAPACITY CURVE
C         CTWO IS THE INTERCEPT OF THE HEAT CAPACITY CURVE
C         RONE ISTHE SLOPE OF THE THERMAL UNIT CONDUCTANCE  CURVE
C         RTWO IS THE INTERCEPT OF THE THERMAL UNIT CONDUCTANCE CURVE
C         G IS THE RAMP INSERTION RATE (ROD GOING DOWN)
C         DROP IS THE TIME THE ROD LEAVES ITS UPPERMOST POSITION
C         DOWN IS THE TIME THE ROD REACHES ITS BOTTOM MOST POSITION
C
      READ(1,1001)JMAX
      READ(1,1005)(DECAY(I),I=1,6)
      READ(1,1005)(B(I),I=1,6)
    2 READ(1,1000)D(1,1),TEMP(1,1),R(1,1),T(10,1),ERROR,H,CONE,CTWO
      READ(1,1000)BETA,PLIFE,A,ALFA,OUT,RONE,RTWO,G
      READ(1,1000)DROP,DOWN
      IF(BETA.EQ.0.)CALL EXIT
      WRITE(3,1020)BETA,PLIFE,A,ALFA,OUT
      DO 1 I=1,6
```

```
    1 WRITE(3,1030)I,DECAY(I),B(I)
      DO 10 I=1,6
   10 C(I,1,1)=B(I)*D(1,1)/(PLIFE*DECAY(I))
      SUM=0.0
      DO 11 I=1,6
   11 SUM=SUM+C(I,1,1)
      POWER=   H*D(1,1)
      WRITE(3,1003)
      WRITE(3,1004)T(10,1),D(1,1),SUM,TEMP(1,1),R(1,1),POWER
      DO 12 I=1,9
   12 T(I,1)=T(10,1)
      ITS=0
      TENTA=T(10,1)
C
C        START THE TRANSIENT
C
      DO 90 J=1,JMAX
      M=0
      II=1
      ITER=1
      CALL DERIV(J,M,II)
   80 CONTINUE
C
C******** CALCULATE THE DEPENDENT VARIABLES USING TAYLOR SERIES
C
      STEP=T(10,J+1)-T(10,J)
      D(1,J+1)=D(1,J)+D(2,J)*STEP+D(3,J)*STEP**2/2.+D(4,J)*STEP**3/6.+D(
     15,J)*STEP**4/24.
      DO 82 I=1,6
   82 C(I,1,J+1)=C(I,1,J)+C(I,2,J)*STEP+C(I,3,J)*STEP**2/2.+C(I,4,J)*STE
     1P**3/6.+C(I,5,J)*STEP**4/24.
      TEMP(1,J+1)=TEMP(1,J)+TEMP(2,J)*STEP+TEMP(3,J)*STEP**2/2.+TEMP(4,J
     1)*STEP**3/6.+TEMP(5,J)*STEP**4/24.
      R(1,J+1)=R(1,J)+R(2,J)*STEP+R(3,J)*STEP**2/2.+R(4,J)*STEP**3/6.+R(
     15,J)*STEP**4/24.
   60 CONTINUE
      GO TO (61,63,70),II
   61 M=1
      II=2
      CALL DERIV(J,M,II)
  555 CONTINUE
      GO TO 60
   63 CALL TIME(J,M,II)
  666 CONTINUE
      IF(ITER.EQ.10)GO TO 95
      GO TO 80
C
C******** WRITE OUTPUT
C
   70 SUM=0.0
      DO 50 I=1,6
   50 SUM=SUM+C(I,1,J+1)
      POWER=   H*D(1,J+1)
```

```
   90 WRITE(3,1004)T(10,J+1),D(1,J+1),SUM,TEMP(1,J+1),R(1,J+1),POWER
      GO TO 91
   95 WRITE(3,1010)
   91 CONTINUE
      GO TO 2
      END



      SUBROUTINE DERIV(J,M,II)
      DIMENSION D(6,500),C(6,5,500),TEMP(6,500),R(6,500),T(10,500),CETA(
     16),DECAY(6),B(6)
      COMMON D,C,TEMP,R,T,DETA,CETA,IMPETA,RETA,ERROR,ITER,STEP,DECAY,BE
     1TA,PLIFE,B,A,ALFA,OUT,ITS,TENTA,H,CONE,CTWO,RONE,RTWO,DROP,DOWN,G
      RATE=A
C
C        DERIVATIVES
C
      DO 100 K=1,5
      USF1=0.0
      CSUM=0.0
      DO 103 I=1,6
  103 CSUM=CSUM+DECAY(I)*C(I,K,J+M)
      DSUM=0.0
      IF(K.EQ.1)GO TO 104
      KID=K-1
      DO 102 N=1,KID
      CALL FACT(N,KID,BKN)
  102 DSUM=DSUM+BKN*R(N+1,J+M)*D(K-N,J+M)
  104 D(K+1,J+M)=((R(1,J+M)-BETA)*D(K,J+M)+DSUM)/PLIFE+CSUM
      DO 110 I=1,6
  110 C(I,K+1,J+M) =B(I)*D(K,J+M)/PLIFE-DECAY(I)*C(I,K,J+M)
      CAP=CONE*(TEMP(1,J+M)-TEMP(1,1))+CTWO
      RELAX=RONE*TEMP(1,J+M)+RTWO
      KRD=K-1
      IF(KRD.EQ.0)RKTH=RELAX
      IF(KRD.EQ.1)RKTH=RONE
      IF(KRD.GE.2)RKTH=0.0
      IF(KRD.GE.1)USF1=1.0
      FT=H*D(K,J+M)-RKTH*(TEMP(1,J+M)-TEMP(1,1))-(RELAX+CONE*FLOAT(KRD))
     1*TEMP(K,J+M)*USF1
      IF(KRD.LE.2) GO TO 118
      ST=FLOAT(KRD)*RONE*TEMP(KRD,J+M)
      GO TO 119
  118 ST=0.0
  119 TEMP(K+1,J+M)=(FT+ST)/CAP
      IF((T(10,J+M).GE.OUT).AND.(T(10,J+M).LT.DROP))A=0.0
      IF((T(10,J+M).GE.DROP).AND.(T(10,J+M).LT.DOWN))A=-G
      IF(T(10,J+M).GE.DOWN)A=0.0
      IF(K.GE.3) A=0.
  100 R(K+1,J+M)=A+ALFA*TEMP(K+1,J+M)
      A=RATE
```

```
      IF(ITS.EQ.0)GO TO 999
      GO TO (120,130),II
  120 CONTINUE
      DO 121 I=1,6
  121 CETA(I)=C(I,6,J)
      DETA=D(6,J)
      TMPETA=TEMP(6,J)
      RETA=R(6,J)
      CALL TIME(J,M,II)
  555 CONTINUE
C
C        RETURN TO STATEMENT NUMBER 80 IN MAIN PROGRAM
C
      RETURN
  130 DETA=(D(5,J+M)-D(5,J))/STEP
      DO 135 I=1,6
  135 CETA(I)=(C(I,5,J+M)-C(I,5,J))/STEP
      TMPETA=(TEMP(5,J+M)-TEMP(5,J))/STEP
      RETA=(R(5,J+M)-R(5,J))/STEP
C
C        RETURN TO STATEMENT NUMBER 555 IN MAIN PROGRAM
C
      RETURN
  999 T(10,J+1)=T(10,J)+10.*PLIFE
      ITS=1
C
C        RETURN TO STATEMENT NUMBER 80 IN MAIN PROGRAM
C
      RETURN
      END



      SUBROUTINE TIME(J,M,II)
      DIMENSION D(6,500),C(6,6,500),TEMP(6,500),R(6,500),T(10,500),CETA(
     16),DECAY(6),B(6)
      COMMON D,C,TEMP,R,T,DETA,CETA,TMPETA,RETA,ERROR,ITER,STEP,DECAY,BE
     1TA,PLIFE,B,A,ALFA,OUT,ITS,TENTA,H,CONE,CTWO,RONE,RTWO,DROP,DOWN,G
 1000 FORMAT(1H ,10H**********,5X,I3,5X,2(E15.8,5X))
 1030 FORMAT(1H ,10H**********,5HLMIN=,I3)
      LMAX=9
      IF(R(1,J+M).EQ.0.0) LMAX=8
      P=.2
      IF(LMAX.NE.9)GO TO 30
C
C        TIME STEP CALCULATION
C
      T(9,J+1)=T(9,J)+(ERROR*720.*ABS(R(1,J+M))/(ABS(RETA)))**P
   30 T(8,J+1)=T(8,J)+(ERROR*720.*ABS(TEMP(1,J+M))/(ABS(TMPETA)))**P
      T(1,J+1)=T(1,J)+(ERROR*720.*ABS(D(1,J+M))/(ABS(DETA)))**P
      DO 31 I=2,7
      K=I-1
   31 T(I,J+1)=T(I,J)+(ERROR*720.*ABS(C(K,1,J+M))/(ABS(CETA(K))))**P
```

```
C
C         MINIMUM TIME STEP
C
      DUMMY=100.
      DO 15 L=1,LMAX
      IF(T(L,J+1).LT.DUMMY)GO TO 10
      GO TO 15
   10 LMIN=L
      DUMMY=T(L,J+1)
   15 CONTINUE
      IF(DUMMY.EQ.OUT) DUMMY=DUMMY-10.*PLIFE
      IF(DUMMY.EQ.DROP)DUMMY=DUMMY-10.*PLIFE
      IF(DUMMY.EQ.DOWN)DUMMY=DUMMY-10.*PLIFE
      T(10,J+1)=DUMMY
      WRITE(3,1030)LMIN
      GO TO (300,400),II
  300 TENTA=T(10,J+1)
C
C         RETURN TO STATEMENT NUMBER 555 IN SUBROUTINE DERIV
C
      RETURN
  400 CONTINUE
      PREST=TENTA/1.1
      IF(T(10,J+1).GE.PREST)GO TO 500
      II=1
      ITER=ITER+1
      WRITE(3,1000)ITER,T(10,J+1),TENTA
      TENTA=T(10,J+1)
C
C         RETURN TO STATEMENT NUMBER 666 IN MAIN PROGRAM
C
      RETURN
  500 II=3
C
C         RETURN TO STATEMENT NUMBER 666 IN MAIN PROGRAM
C
      RETURN
      END
```

```
      SUBROUTINE FACT(N,KID,BKN)
C
C        K FACTORIAL
C
      IF(KID.EQ.1)GO TO 15
      FK=FLOAT(KID)
      KIDR=KID-1
      DO 10 L=1,KIDR
      F=FLOAT(KID)-FLOAT(L)
   10 FK=F*FK
      GO TO 16
   15 FK=1.0
   16 CONTINUE
C
C        N FACTORIAL
C
      IF(N.EQ.1)GO TO 30
      FN=FLOAT(N)
      NUT=N-1
      DO 20 L=1,NUT
      F=FLOAT(N)-FLOAT(L)
   20 FN=F*FN
      GO TO 31
   30 FN=1.0
   31 CONTINUE
C
C        (K-N) FACTORIAL
C
      KN=KID-N
      IF(KN.LE.1)GO TO 45
      FKN=FLOAT(KN)
      KNOT=KN-1
      DO 40 L=1,KNOT
      F=FLOAT(KN)-FLOAT(L)
   40 FKN=F*FKN
      GO TO 46
   45 FKN=1.0
   46 BKN=FK/(FN*FKN)
      RETURN
      END
```

APPENDIX E

Average Fuel Heat Capacity

West, et.al. (6) suggests the use of the empirical equations of enthalphy for uranium metal and zirconium hydride for the calculation of the fuel heat capacity. In particular,

$$(H-H_{25})_{ZrH_x} = \{0.03488\ T^2 + [34.446 + 14.807(x-1.65)]T - 882.95 - 370.18(x-1.65)\}\text{joules/mole} \quad \text{(E.1)}$$

and

$$(H-H_{25})_u = [0.6483(10^{-4})T^2 + 0.1087\ T - 2.758]\text{joules/gm} \quad \text{(E.2)}$$

where $(H-H_{25})$ = change in enthalphy from 25°C,

T = temperature in °C,

x = hydrogen to zirconium ratio which is 1 for the KSU TRIGA Mark II (11).

There are an average of 37 grams of U^{235} per fuel-moderator element (11), and since each element is 8% by weight uranium enriched 20% in U^{235}, there are 2125 grams of ZrH in a fuel-moderator mixture of 2310 grams. Thus the number of moles of ZrH per element is 23. Multiplying Eq. (E.1) by 23 moles and Eq. (E.2) by 37 grams, the change in enthalphy for the element becomes

$$(H-H_{25}) = (0.815\ T^2 + 590\ T + 14{,}290)\text{watt sec.}$$

The heat capacity is then

$$C = \frac{\partial H}{\partial T} = 1.63(T-25) + 590\ \frac{\text{watt secs}}{°\text{C element}}\ .$$

Since there are 63 fuel-moderator elements in the core, the total average fuel heat capacity becomes

$$C = 103(T-25) + 37,200 \frac{\text{watt secs}}{^{\circ}C} ,$$

where T is the average fuel temperature of the core.

APPENDIX F

Thermocouple Temperature Measurement Corrections

The thermocouple used for obtaining the fuel temperature data during the transient does not have an immediate response to the rapidly changing temperature of its environment. The thermocouple is embedded in the center of the instrumented fuel-moderator element and has a time constant associated with the finite time required for the heat generated in the fuel to transfer to it. This time constant (0.29 seconds) is greater than the largest pulse width at half of maximum (0.13 seconds). Thus the following procedure was adopted to correct the measured data for this effect.

Consider the thermocouple to be characterized by the following electrical circuit:

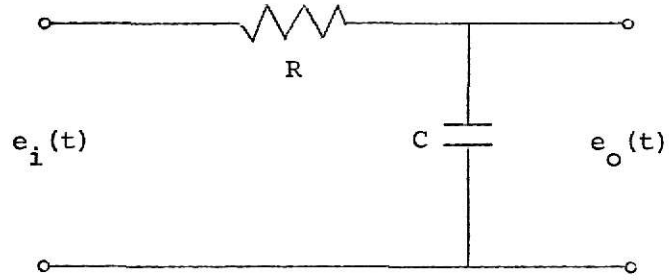

By Kirchoff's voltage law,

$$e_i(t) = R\, i(t) + \frac{1}{c}\int_0^t i(t)\, dt \,, \tag{F.1}$$

and the output voltage can be expressed as

$$e_0(t) = \frac{1}{c}\int_0^t i(t)\, dt \,. \tag{F.2}$$

The Laplace transforms of Eqs. (F.1) and (F.2) are

$$E_i(s) = RI(s) + \frac{1}{Cs} I(s) \ , \tag{F.3}$$

and

$$E_0(s) = \frac{1}{Cs} I(s) \ . \tag{F.4}$$

Substitution of Eq. (F.4) into Eq. (F.3) yields

$$E_0(s) = \frac{E_i(s)}{\tau(s+1/\tau)} \tag{F.5}$$

where $\tau = RC$ and is known as the time constant of the system. The corresponding solution of Eq. (F.5) in the time domain can be obtained using the convolution integral (22). In particular,

$$e_0(t) = \frac{1}{\tau} \int_0^t dt' \, e_i(t') \, e^{-\left(\frac{t-t'}{\tau}\right)} \ . \tag{F.6}$$

The corresponding form of Eq. (F.6) for the thermocouple behavior is

$$T_T(t) = \frac{1}{\tau} \int_0^t dt' \, T_a(t') \, e^{-\frac{t-t'}{\tau}} \tag{F.7}$$

where $T_T(t)$ = the measured fuel temperature at time t with the thermocouple,

$T_a(t)$ = the actual fuel temperature at time t.

From a given set of transient temperature data, a trial and error procedure was used with Eq. (F.7) to determine the actual fuel temperature. The value of the time constant was 0.29 seconds, which was experimentally determined by Wyman, et.al. (16) for TRIGA instrumented fuel elements.

Figure F-1 presents the measured data and the corrected data for the $1.55 reactivity insertion.

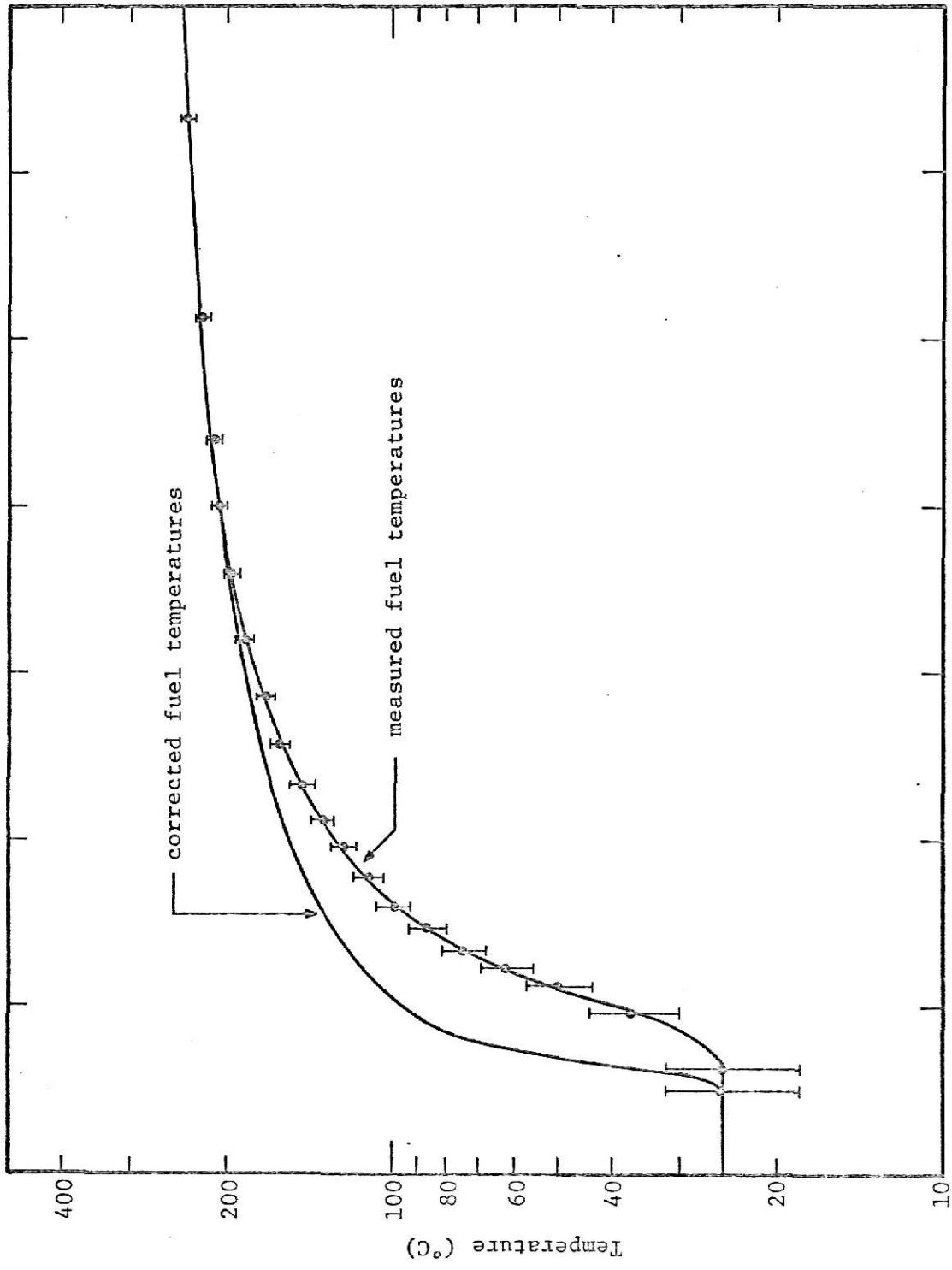

Figure F-1. Measured and corrected fuel temperatures of the $1.55 pulse.

AN ANALYSIS OF THE PULSING CHARACTERISTICS OF THE KANSAS STATE UNIVERSITY TRIGA MARK II NUCLEAR REACTOR

by

JERRY W. STAUDER

B.S., Kansas State University, 1967

AN ABSTRACT OF A MASTER'S THESIS

submitted in partial fulfillment of the

requirements for the degree

MASTER OF SCIENCE

Department of Nuclear Engineering

KANSAS STATE UNIVERSITY

Manhattan, Kansas

1969

ABSTRACT

Reactors with pulsing capability, such as the TRIGA, provide a tool for research and education in areas ranging from activation analysis to the support of power reactor programs. A necessary requirement, to be able to utilize and understand the behavior of the reactor during the pulsed mode of operation is to have an analytical model to predict the response of the reactor.

The purpose of this work was to develop and test such a model. The basic approach was to combine the space independent reactor kinetic equations with a space independent thermal model through the reactivity temperature coefficient. The thermal model describes the average fuel temperature of the core and was based on a total average fuel heat capacity and a core thermal conductance between the fuel and the reactor tank bulk water. The reactivity temperature coefficient was assumed constant and was, along with the thermal unit conductance, experimentally determined from data taken at steady state power levels below 250 kilowatts.

The data were obtained with a movable instrumented fuel-moderator element that was placed in various regions of the reactor. Since the fuel temperatures could be measured only in the axial middle of the element, estimates of the fuel temperatures at other axial locations were made through the use of a heat balance between the fuel and the incoming water to the reactor core. This calculation required knowledge of the volumetric heat generation rate in the fuel which was obtained by measuring the axial neutron flux distribution with a miniature fission chamber.

The transient model calculations were compared with actual transient data and were found to give a satisfactory description of the reactor power.